



Høgskulen på Vestlandet

ING5002 - Master Thesis

ING5002-MOPPG-2023-HØST-FLOWassign

Predefinert informasjon

Startdato:	01-12-2023 12:00 CET	Termin:	2023 HØST
Sluttdato:	20-12-2023 14:00 CET	Vurderingsform:	Norsk 6-trinns skala (A-F)
Eksamensform:	Masteroppgave		
Flowkode:	203 ING5002 1 MOPPG 2023 HØST		
Intern sensor:	(Anonymisert)		

Deltaker

Kandidatnr.:	104
---------------------	-----

Informasjon fra deltaker

Antall ord *:	28988
----------------------	-------

Egenerklæring *: Ja

Jeg bekrefter at jeg har Ja registrert oppgavetittelen på norsk og engelsk i StudentWeb og vet at denne vil stå på vitnemålet mitt *:

Jeg godkjenner autalen om publisering av masteroppgaven min *

Ja

Er masteroppgaven skrevet som del av et større forskningsprosjekt ved HVL? *

Nei

Er masteroppgaven skrevet ved bedrift/uirksomhet i næringsliv eller offentlig sektor? *

Nei

**FLAME PROPAGATION BETWEEN BATTERY CELLS –
EFFECT OF DISTANCE**



Okeke Obinna Nelson

WESTERN NORWAY UNIVERSITY OF APPLIED SCIENCES

Master Thesis in Fire Safety Engineering


Haugesund
January 2024



Western Norway
University of
Applied Sciences

**FLAME PROPAGATION BETWEEN BATTERY CELLS –
EFFECT OF DISTANCE**

Master thesis in Fire Safety Engineering

Author: Okeke Obinna Nelson	Author sign. 
Thesis submitted: Spring 2024	Open thesis
Tutor: Bjarne Christian Hagen Einar Arthur Kolstad	
Keywords: Thermal Runaway, flame propagation, safety vent, alkaline battery, Li-ion battery, cell, short- circuit, SOC, cell spacing, module, experiment/scenarios.	Number of pages: 82 + Appendix: 10 Haugesund, 3 rd January 2024 Place/Date/year
This thesis is a part of the master's program in Fire Safety Engineering at Western Norway University of Applied Sciences. The author(s) is responsible for the methods used, the results that are presented, the conclusion and the assessments done in the thesis.	

Preface

This master's thesis is conducted as a partial fulfilment of the requirement for the degree of Master in Fire Safety Engineering at the Western Norway University of Applied Sciences (HVL), Haugesund. The master's degree is taught at the Department of Safety, Chemistry and Biomedical Laboratory Sciences, campus Haugesund. This study is credited with 60 ETC points.

The idea of this work was from my supervisors, where investigation on propagation on batteries such as Li-ion with higher energy density is applied on different 3 x 3 configuration scenarios (0 cm, 0.5 cm and 1 cm) to witness flame propagation. This can be associated with e-automotives such as scooters, e-bikes, EVs, etc. Many cell arrangements in a case make up a module or pack to power this equipment, and the capacity may also vary. Failure of any cell can lead to thermal runaway and spread to other cells escalating the risk and consequence.

It was challenging to carry out experiment in adverse weather conditions during winter but due to the passion to contribute positively towards the ongoing energy transition and safety of lives, property and environment made me do it and i am glad i did.

Acknowledgments

I want to use this medium to give a special thanks to my supervisors, Bjarne Christian Hagen, and Einar Arthur Kolstad, for their relentless commitment, encouragement, valuable impact and guidance toward the success of this project.

In addition, I want to especially thank my wife for her sacrifices for taking good care of my little daughter while I am away from home. Also, I want to thank my mother, siblings, in-laws, for their kind wishes and encouragement to make this a success.

I will not fail to thank Anita Katharina Meyer for her support during the experimental work and Dheeraj Dilip Karyaparambil Ph.D. Candidate (HVL), for always being willing to make input and Xiaoquin Hu (Vicky) for her assistant when I initially started this project and finally to the rest of the HVL staffs who have assisted one way or the other.

Abstract

Lithium-ion (Li-ion) batteries have been widely used for battery energy storage systems [1]. Batteries are important due to their vast applications, ranging from consumer electronics to electric vehicles, bikes, scooters, hoverboards, etc. [2]. Batteries are also used as energy storage units for renewable sources such as wind and solar energy [3]. In certain situations, manufacturers are not solely worried about the onset of thermal runaway in a single cell, but also about the potential spread it might cause to adjacent cells in close proximity [4].

Commercial alkaline and Li-ion batteries were exposed to a controlled butane flame to investigate the propagation with the effect of distance (0 cm, 0.5 cm and 1 cm) between the cells in the module. This study includes six scenarios with a total of 13 experiments conducted for both single cell experiments which shows the behaviour of these cells and 3X3 configuration which is used to determine propagation and was conducted in the winter in the Western Part of Norway. The ambient temperature ranged from -3 to 8 °C with a highly windy condition when the experiment was conducted.

The result of the study resulted in propagation in only one cell in a 3 X 3 configuration with 0 cm spacing. Thus, more cell spacing reduces the likelihood and impact of propagation and damage in another cell. TR behaviours were experienced in 5 different ways which can pose a high risk of contributing to propagation such as diffused flame with or without explosion, and jet flame, which can lead to propagation beyond the 0 cm scenario.

From this study, a recommendation of 0.5 cm (5 mm) spacing should be implemented for modules using an 18650 Li-ion battery under similar temperate conditions observed in this work. Due to various behaviour displayed during TR for reaction with flames or fire, can go further to transfer heat in a close cell and elevate their temperature to exceed the thermal limit which can result in propagation and can have severe consequences in a more confined space. Though the spacing recommendation can impact the weight of the module case, safety is more of a concern.

Sammendrag

Table of contents

Preface.....	I
Acknowledgments.....	II
Abstract	III
Sammendrag	IV
Table of contents.....	V
Table of Figures	VIII
List of Tables.....	X
Definitions	XI
1. Introduction.....	1
1.1 Background.....	1
2.2 Problem statement.....	2
2.3 Limitation.....	2
2. Theory and Literature Review	3
2.1 Principal design of batteries.....	3
2.2 Battery chemistry and classifications	4
2.2.1 Alkaline battery	5
2.2.2 Lithium-ion (Li-ion) battery	5
2.3 Charging and discharging Principle of Li-ion battery.....	10
2.4 Types of Li-ion Batteries	10
2.5 Thermal runaway in batteries	12
2.5.1 Increase in Temperature	13
2.5.2 Internal Pressure Increases	14
2.5.3 Cell Venting/ Gas Ignition	14
2.6 Fire and damage to battery.....	16
2.7 Abuse methods to induce Failure.....	16
2.7.1 Electrical abuse.....	16
2.7.2 Mechanical Abuse	18
2.7.3 Thermal Abuse.....	19
2.8 Thermal runaway propagation in multiple cells.....	21
2.8.1 Heat Transfer in Battery	24
2.8.2 Battery and Safety	24

2.8.3	Safety standards and codes for battery	26
2.8.4	Battery management system (BMS).....	27
3	Experimental set-up and procedures	30
3.1	Purpose and Scenarios	30
3.2	Battery types.....	30
3.3	Set-up	31
3.3.1	Single cell (scenario 1 and 2)	31
3.3.2	3 x 3 Cell Configuration	33
3.3.3	Location of ignition source	35
3.3.4	Test compartment	35
3.4	Procedures.....	35
3.4.1	Single cell procedure	35
3.4.2	3 x 3 Configuration (0 cm, 0.5 cm, and 1 cm) procedure	36
3.5	Safety considerations before the experiment.....	36
4	Results	38
4.1	Single cell	39
4.1.1	Alkaline single cell.....	40
4.1.2	Li-ion single cell with thermal runaway.....	40
4.1.3	Li-ion single-cell experiment with no thermal runaway reaction.....	43
4.2	3X3 cell configuration.....	44
4.2.1	3 X 3 alkaline configuration, no spacing.....	45
4.2.2	3X3 Li-ion configuration, 0 cm (no spacing)	46
4.2.3	Li-ion 3x3 configuration, 0.5 cm spacing.	50
4.2.4	Li-ion 3x3 configuration, 1 cm spacing.	54
4.2	Thermal runaway behaviours.....	57
4.3	Thermal runaway and temperature	60
4.4	Thermal runaway and mass loss	61
5.	Discussion	63
5.1	Different effects of battery behaviours on fire and heat.....	63
5.2	Effect of distance between cells on thermal runaway propagation	64
5.3	Different behaviours during thermal runaway.....	69
5.4	Safety concerns, prevention, and control.	72
6	Conclusion	76

7	Further work.....	77
8	References.....	78
9.	Appendix.....	A
	Appendix A	A
	Alkaline single cell experiment, Scenario (1-2 and 1-3)	A
	Appendix B	C
	Li-ion Single cell experiment, Scenario (2-6)	C
	Appendix C.....	E
	Li-ion 3 x 3 cell configurations 1cm spacing. Scenario (6-13).....	E
	Appendix D	H
	Li-ion 3x3 cell configuration 0.5cm spacing experiment 2. Scenario (5-11).....	H
	Appendix E.....	I

Table of Figures

Figure 2.1: Schematic of the fundamental structure of lithium-ion battery cells [10].	3
Figure 2.2: Overview of battery categories and their types.	4
Figure 2.3: shows the comparison of the different rechargeable battery technologies in terms of volumetric and gravimetric energy density [12]. Updated volumetric and gravimetric energy densities with novel technologies [20].	6
Figure 2.4: shows the photos of the four types of Li-ion cells, A [28] BCD [21].	11
Figure 2.5: (a) safety vent activates due to internal pressure build-up, (b) schematic of thermal runaway (c) Aftermath thermal runaway [31] [22].	13
Figure 2.6: Abuse conditions resulting in thermal runaway [9]	17
Figure 2.7: Difference between battery cell, module, and pack [15]	22
Figure 2.8: Tab configuration of battery pack: (A) branched style (M-type) (B) snake-like style(S-type) [9].	23
Figure 2.9: Electrode voltages for several material combination with lithium. LTO: lithium titanate (Li ₄ TiO ₁₂) [14]	26
Figure 3.1: (a) shows the AA Alkaline cell placed in the hole in a reversed way with the anode exposed to the butane flame (b) shows the 18650 Li-ion placed in the hole in a normal way.	31
Figure 3.2: Schematic of the set-up of single cells experiment.	32
Figure 3.3: Li-ion 0.5 cm spacing apart with hole diameter in an insulating board.	34
Figure 3.4: The photo shows one of the experiments with 3 x 3 configuration and 1 cm spacing.	35
Figure 4.1: shows a typical graphical representation of an alkaline single cell experiment (a) shows the temperature variation with time (b) mass vs time.	39
Figure 4.2: shows a typical graphical representation of the mass and temperature of a Li-ion single cell experiment (a) shows the temperature variation with time and (b) mass vs time.	41
Figure 4.3: The heating process of Li-ion single cell (experiment 2). (a) the safety vent valve activation (b) Activation of TR with rapid sparks (c) explosion with flying debris and slight gas emission afterward (d) Aftermath of TR, protrusion of the inner foil-like material from the cell.	42
Figure 4.4: The heating process of Li-ion single cell (experiment 1). (a) beginning of cell heating (b) the safety vent valve activation with a flash of flame (c) end of cell heating with a small flame seen on the cell and no further reaction (TR) occurred.	43
Figure 4.5: Li-ion single cell (experiment 1). (a) Temperature variation with time (b) mass vs time.	44
Figure 4.6: Schematic representation of both Alkaline and Li-ion 3X3 configurations, 0 cm spacing and location of each cell having the same corresponding thermocouple attached to it, applicable to all 3X3 configuration scenarios.	45
Figure 4.7: Alkaline 3x3 configuration, 0 cm (no spacing). (a) temperature as a function of time (b) mass as a function of time.	45
Figure 4.8: The heating process of Li-ion 3x3 configuration with no spacing (experiment 1). (a) beginning of igniting cell 1 (b) pressure build-up in cell activates safety vent valve in cell 1 with increased flame due to vented gas (c) initiation point of TR on cell 1 with sparks (d) TR ejected gas and fire engulfed cell 1 and partly on cell 2 and 4 (e) cell 2 safety vent valve activated during the TR process on cell 1 and increased flame (f) cell 4 safety vent valve activates during the heating process and emitted gases sustained flame (g) butane burner removed at 120 s and small diffused flame spotted on cell 2 (h) Cell 2 slight internal pressure release increased flame (i) flame and heat propagation on cell 2 through conduction, and	

radiation triggered Thermal runaway on cell 2 with flare and spark (j) excessive whitish gas/smoke ejection from cell 2, extinguished flame (k) heat propagation activated cell 3 safety vent valve..... 47

Figure 4.9: Results of Li-ion 3x3 cell configuration with no spacing (experiment 1). (a) Temperature variation with time (b) mass vs time for Li-ion cell. 48

Figure 4.10: Schematic representation of cells on Li-ion 3x3 configuration, 0.5 cm spacing. 50

Figure 4.11: The heating process of li-ion cell 3x3 configuration, 0.5 cm spacing (experiment 1). (a) initiation of butane torch burner to cell 1(b) safety vent valve cell 1 activates with wind effect on ignited gas (c) initiation of TR on cell 1 (d) visible smoke emission during TR (e) safety vent activates (f) safety vent activates with increased flame (h) butane torch burner removed at 120 s and flame decays drastically with little flame spotted on cell 1 (i) current situation of cells after the experimental abuse with cell 1 fully burnt..... 51

Figure 4.12: Li-ion 3x3 configuration, 0.5 cm spacing (experiment 1). (a) Temperature variation with time (b) mass loss with time 52

Figure 4.13: Li-ion 3x3 configuration 0.5cm spacing (experiment 2). Temperature variation with time, indicating the points of occurrence of events..... 53

Figure 4.14: Location of cell and thermocouple..... 54

Figure 4.15: shows a timeline of several events in Li-ion 3x3 cell configuration 1cm spacing, experiment 1 (a) An initial burning process on cell 1 and cell 5 partly affected by the flame and radiation (b) cell 1 safety vent activation with gas ignition on cell 1 (c) initiation of TR with sparks/flare on cell 1 (d) rapid gas ejection with little sparks on cell 1 (e) jet fire ejection from cell 1 touching the roof of the compartment (f) cell 5 safety vent activation with ignition (g) reduction of the flame on cell 5 after removing heat source (h) cooling of the cells. 55

Figure 4.16: Li-ion 3x3 cell configuration 1cm spacing, experiment 1 (a) temperature variation with time (b) mass loss vs time..... 56

Figure 4.17: (a) Activation of TR with rapid sparks (b) explosion with flying debris and slight gas emission afterward. Also seen in Figure 4.3 b and c. 58

Figure 4.18: TR propagation on cell 2 initiates with flare and sparks (i) excessive whitish gas/smoke ejection from cell 2, extinguished flame. Also seen in Figure 4.8 i and j. 58

Figure 4.19: Li-ion single cell experiment 3. (a) Initiation of TR with flare/sparks with whitish gas emission (b) explosion accompanied by a flame jet touched the ceiling. See appendix. 59

Figure 4.20: Li-ion 3x3 configuration 1cm spacing (experiment 2). (a) flare with sparks (b) explosion with flying debris accompanied by gas emission with radiation flame engulfed cell 1 59

Figure 4.21: Li-ion 3x3 configuration 0.5 cm spacing (experiment 2). (a) initiation of TR with flare /sparks (b) Diffused flame engulfed cell with gas/smoke ejected during TR without explosion 60

Figure 4.22: Temperature variation with time for all cells with TR in all experiments conducted. 61

Figure 5.1: Schematic representation of some experiments from previous and present studies..... 67

Figure 5.2: Different behaviours experienced during TR, are presented from Figure 4.17b to Figure 4.21b. 70

List of Tables

Table 2.1: shows the physical and chemical properties of the four (4) most used rechargeable batteries [9].	5
Table 2.2: Typical components of Li-ion batteries and their compositions [9].	7
Table 2.3: Shows the summary of Electrolyte properties desired for various lithium-ion batteries and their comparison based on the state of matter [21].	9
Table 2.4: Permissible Temperature Limits for various batteries [26].	12
Table 2.5: shows the vented gas characterization [30].	15
Table 2.6: shows standard methods simulating Li-ion battery internal short circuit [10].	19
Table 2.7: The fire behaviors of cylindrical 18650 lithium-ion batteries (cathode and graphite anode) under discharge conditions [9].	21
Table 2.8: Comparison of different types of battery management system (BMS) [9].	28
Table 3.1: shows information about the commercial batteries used for the experiment.	31
Table 4.1: Summary of all experiments conducted. Indicating experiment with TR reaction with an explosion resulted in a low peak temperature and high mass loss of the cell and TR reaction without explosion resulted in a high temperature and low mass loss.	38
Table 4.2: Summary of Li-ion 3x3 configuration, 0 cm spacing, experiment 1.	49
Table 4.3: Summary of Li-ion 3x3 configuration, 0.5 cm spacing, experiment 1.	53
Table 4.4: Summary of Li-ion 3x3 configuration 0.5 cm spacing, experiment 2.	54
Table 4.5: Summary of Li-ion 3x3 configuration 1 cm spacing, experiment 1.	57

Definitions

TR	Thermal runaway	CO ₂	Carbon dioxide
Li-ion	Lithium-ion	NO	Nitrogen dioxide
SOC	State of Charge	SO ₂	Sulfur dioxide
SEI	Solid electrolyte Interface	COHb	Carboxyhaemoglobin
Ni-Cd	Nickel cadmium	CH ₄	Methane
NMH	Nickel metal hydride	C ₂ H ₄	Ethylene
LMO	Lithium manganese oxide	POF ₃	Phosphoryl fluoride
LCO	Lithium cobalt oxide	C ₂ H ₆	Ethane
LTO	Lithium titanate oxide	HCl	Hydrogen chloride
ECPs	Electronic conducting polymers	C ₇ H ₈	Toulene
LFP	Lithium iron phosphate	C ₆ H ₆	Benzene
HF	Hydrogen Sulfide	CH ₄ O	Methanol
H ₂	Hydrogen	FR	Fire retardant
CO	Carbon monoxide	ARC	Accelerating rate calorimetry.
ACS	Air cooling system	PCM-CS	Phase change material cooling system
LCS	Liquid cooling system	FCS	Forced cooling system.
DMC	Dimethyl carbonate	DEC	Diethyl carbonate
EC	Ethylene carbonate	T	Temperature of the boundary of the battery
C_p	Specific heat capacity	σ	Stefan-Boltzmann constant
$\frac{dT}{d\tau}$	Temperature rise rate	q_{rad}	Heat radiation
q_r	Self-heat generation rate	h	Conduction coefficient
q_{Conv}	Heat convection	T_s	Surface temperature of the heater
ε	Emissivity	s	Seconds

1. Introduction

1.1 Background

In recent years there has been significant development and commercialization of battery energy storage systems. Lithium-ion (Li-ion) batteries have been widely used as a means of battery energy storage systems [1]. Batteries are important due to their vast applications, ranging from consumer electronics to electric vehicles, bikes, scooters, hoverboards, etc [2]. Batteries are also used as energy storage units for renewable sources such as wind and solar energy [3]. However, all batteries have potential risks of short circuits leading to thermal runaway, therefore, battery manufacturers are forced to meet safety standards [5].

Lithium-ion batteries contain flammable materials, which can create hazards when battery cells become jeopardized and enter thermal runaway [1]. There are many requirements for the battery depending on the use such as low weight, small volume, low cost, long-life time including the safety of the battery [6]. Due to the high-density storage in batteries such as Li-ion batteries, any form of abuse such as thermal, electrical, and mechanical abuse can trigger spontaneous self-heating reactions or thermal runaway. Thermal runaway can lead to fire and explosion [7], resulting in casualties lead to casualties and property damage [8]. In certain situations, manufacturers are not solely worried about the onset of thermal runaway in a single cell, but also about the potential spread it might cause to adjacent cells in close proximity [4].

Fire is the most prioritized safety concern with the wide range of demands in energy storage all over the world. There is pressure on manufacturing companies to produce high-density, efficient, and long-cycle life batteries but there is less taught on the safety risk associated with fire due to new battery composition chemical composition, high level of stored energy, and flammability of most electrolytes [9]. The fire behaviours of lithium-ion batteries are affected by environmental conditions such as temperature. One fundamental source of concern is that a large battery system will use more number of cells, which means that the probability of cell failure within the battery system will increase. Another concern is that the consequences for example a fire may be much larger when using a large battery pack than for a small battery, simply because it consists of many more cells [6]. The combustion properties depend on the state of charge (SOC), while heat release rate (HRR), toxic gas concentration, and smoke yield (combustion properties) are associated with battery type and composition [8].

2.2 Problem statement

This study aims to explore the spread of flames and fire within batteries with 3 x 3 configurations under various spacing scenarios. One of the cells within the 3 x 3 configuration will be subjected to thermal abuse using a butane gas torch to cause failure in the cell. Subsequently, the propagation will be observed i.e., thermal energy released from exothermic reaction occurring in one cell transfers to adjacent cells. In addition, the two types of battery cells (alkaline, AA cells and 18650 Li-ion cells) will be examined to see how they react and affect the propagation process.

The following research questions will be investigated:

- How does the battery fail?
- How does spacing between battery cells affect propagation?
- At what temperature range a cell is likely to attain TR?

2.3 Limitation

This project was initiated by an industrial partner that would supply Li-ion batteries. Unfortunately, the industry partner chose to withdraw from the project at a critical time.

Without the industry partner, both types and numbers of batteries are significantly reduced, severely affecting the outcome of the thesis, due to limited funding and support from the previous partner, therefore the number of tests and scenarios are reduced accordingly.

2. Theory and Literature Review

This chapter will present the important aspects of batteries such as battery chemistry, ways failure can be induced, previous research on propagation, and hazards.

2.1 Principal design of batteries

A battery is made up of;

- Cathode
 - Anode
- } Electrodes
- Electrolyte
 - Separator and
 - Two current collectors (copper and Aluminium)

Figure 2.1 shows the structure of a battery. The cathode and anode store and release charges, and the electrolyte carries positively charged lithium ions from the anode to the cathode and vice versa through the pore space in the separator. The movement of the lithium ions creates free electrons in the anode, which creates a charge at the positive current collector (aluminium). The current then flows from the current collector through a device being powered to the negative collector (Copper). All the components of a battery need each other to function efficiently without malfunctioning. However, malfunction in any of these components will affect the battery negatively [10].

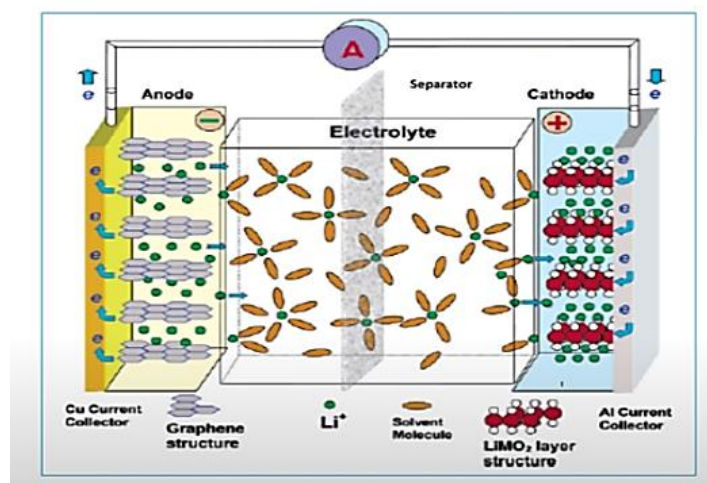


Figure 2.1 Schematic of the fundamental structure of lithium-ion battery cells [10].

2.2 Battery chemistry and classifications

A cell is a single unit that converts chemical energy into electrical energy. Cells are typically lighter and more compact than batteries. On the other hand, a battery is a collection of electrochemical cells connected in series or parallel. Batteries provide power for a longer duration, making them suitable for tasks that require extended energy, while cells are used for shorter tasks like operating clocks, lamps, or remote-control devices. Cells are generally more affordable than batteries [11].

The battery is made of two electrodes (a positive and a negative) separated by an electrolyte with the battery voltage being the difference in the potential build-up between the two electrodes [12] as seen in Figure 2.1. The battery is divided into two main classifications: Primary and secondary battery. A primary battery is designed to be used once and disposed of it cannot be recharged e.g., alkaline batteries and others as seen in Figure 2.2. Due to the electrochemical reaction that takes place inside of them being irreversible, primary batteries cannot be charged.

Secondary batteries are designed to have their chemical reaction reversed by applying electric current to the cell, it can be charged and discharged multiple times. An overview of battery categories and their types is seen in Figure 2.2. The secondary types of batteries commenced with the lead acid batteries. The lead acid battery is cost-effective and environmentally friendly, with approximately 90% can be recycled [13]. One demerit is the low energy density which cannot be improved because of the low theoretical value [14]. Nickel-cadmium (Ni-cd) battery provides slightly higher density and longer cycle lifetime than lead acid batteries, but the battery cost is much higher.

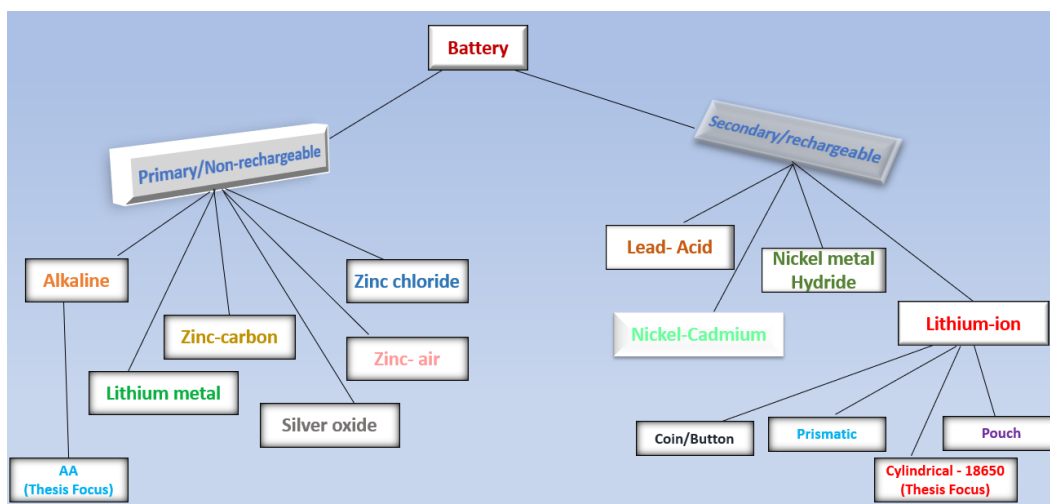


Figure 2.2 Overview of battery categories and their types.

The Nickel-metal hydride was further developed to improve nickel-cadmium batteries without toxic cadmium while having the same advantages as nickel-cadmium batteries [14]. The nickel metal hydride can be interchanged with nickel-cadmium batteries still maintaining the same cell voltage, discharge curves, and charge curves as nickel-cadmium batteries [14]. Nickel metal hydride has achieved almost double the energy density of nickel-cadmium batteries mainly for the high-power densities [14]. However, their low or high temperature performance is poor causing fast degradation of the battery in addition to the material cost [14]. The energy density is important in the technological aspect which came about with Lithium-ion batteries [15]. Table 2.1 shows the more properties and these rechargeable batteries.

2.2.1 Alkaline battery

Primary batteries such as alkaline batteries are a common type of disposable battery that uses manganese dioxide (MnO_2) as the positive electrode (cathode), zinc powder as the negative electrode (anode) and most electrolytes used are potassium hydroxide which is less volatile, and flammable compared to the electrolytes used in lithium-ion batteries [16]. They are widely used in various everyday devices like remote controls, toys, flashlights, clocks, and portable electronic devices due to their reliable performance and availability in different sizes (e.g., AA, AAA, C, D, 9V) [16]. Alkaline batteries are cost-effective and suitable for devices with moderate power requirements and intermittent use. However, they are not rechargeable and need to be disposed of properly once depleted.

Table 2.1 shows the physical and chemical properties of the four (4) most used rechargeable batteries [9].

Battery type	Negative Electrode	Positive Electrode	Electrolyte	Voltage (V)	Cycle life
Lithium-ion	Graphite	$LiCoO_2$	$LiPF_6$ (nonaqueous)	3.7	>1000
Lead-acid	Pb	PbO_2	H_2SO_4	2.1	<500
Ni-Cd	Cd	$NiOOH$	KOH (nonaqueous)	1.2	2000
NMH	Intermetallic	$NiOOH$	KOH (nonaqueous)	1.2	500-1000

2.2.2 Lithium-ion (Li-ion) battery

Lithium metal is number three in the periodic table, making it the lightest metal. In addition, lithium with -3.04 V as the most negative electrode potential [17]. The lithium-ion battery was originally developed in the 1970s by Stanley Whittingham, and in 1980, John Goodenough enhanced the performance by altering the cathode composition using lithium cobalt oxide [18]. In 1985, the first commercial Li-ion battery was produced by Akira Yoshino using petrol coke(carbon) as the anode material [18].

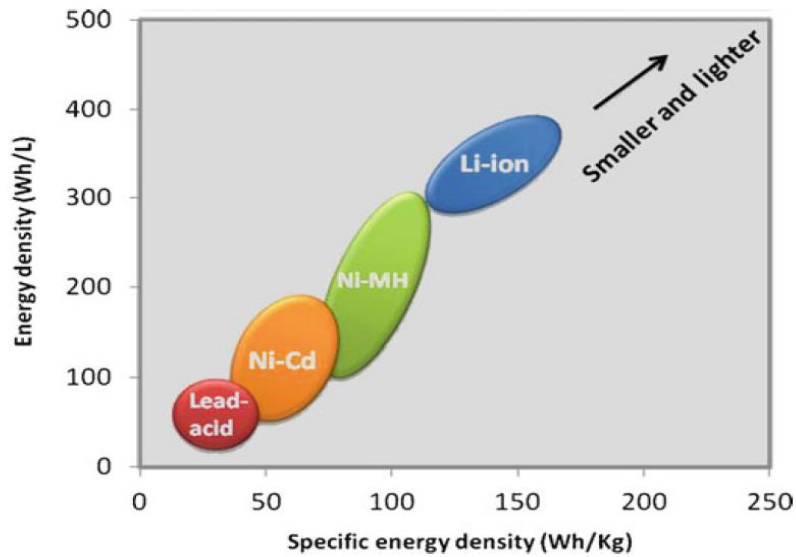


Figure 2.3 shows the comparison of the different rechargeable battery technologies in terms of volumetric and gravimetric energy density [12]. Updated volumetric and gravimetric energy densities with novel technologies [20].

The lithium-ion battery has the highest energy and excellent cycle stability with power density which has made it most preferred. It has a high voltage, no memory, little self-discharge [10], and is used in a very a range of communication, vehicles, and power tool devices.

In addition, they are being speedily introduced in large systems and are found in kWh to MWh energy capacity applications used in e.g., electrified vehicles, ships, and stationary grid storage plants [19]. The comparison in volumetric and gravimetric energy density in rechargeable batteries is seen in Figure 2.3. However, their capacity has increased up to the present time with different novel technologies i.e. sodium-ion and potassium-ion batteries [20]. Battery 2030+ road map aims to enhance quality, reliability, cycle lifetime and improved safety [21].

Lithium-ion (Li-ion) battery components

The Li-ion battery materials have evolved to help improve its life cycle, efficiency, and high energy density as seen in Table 2.2.

Table 2.2 Typical components of Li-ion batteries and their compositions [9]

Component	Common Composition
Anode	Graphitic carbons, hard carbons, synthetic graphite, lithium titanate oxide(LTO),tin-based alloys, and silicon-based alloys.
Cathode	Lithium manganese oxide (LMO), Lithium cobalt oxide (LCO), Lithium Nickel cobalt (NCA), Lithium nickel manganese cobalt oxide (NMC), Lithium iron phosphate (LFP), Electronic conducting polymers(ECPs).
Electrolyte	Lithium salts (mostly LiPF ₆) in organic solvents such as Ethylene carbonate(EC), diethyl carbonate (DEC), dimethyl carbonate (DMC), propylene carbonate(PC), gamma-butyrolactone (GBL), and room temperature ionic liquids (RTILs).
Separator	Polypropylene, Polyethylene, Cellulosic, Nonwoven fabrics, Ceramic
Current Collector	Copper for the anode. Aluminium for cathode

Anode(negative) and cathode (positive) - electrodes

The electrode consists of the anode and cathode. The most important parameters when analyzing the performance of Li-ion battery are the energy density and capacity [9].

The anode which represents the negative electrode is an important component with a key role in the operation of the battery. The anode in the Li-ion cell is typically made from a material that can intercalate or host lithium ions during the charging process [9]. The common compositions of the anode are seen in Table 2.2. The most common anode material is some form of carbon, usually graphite, in powder form, combined with binder material. The carbon can vary significantly in the source of the graphite (natural or synthetic), purity, particle size, particle size distribution, particle shapes, particle porosity, crystalline phase of carbon, degree of compaction, etc [15]. Graphite is the most widely used anode material due to its stability, high electrical conductivity, and ability to host lithium ions. However, the challenge of the intercalation of this material is the limited capacity to store Li-ion, thereby affecting the energy density of the battery [9]. Self-heating in Li-ion graphite anodes in the present electrolyte initiates at a temperature range of 70 °C – 90 °C [22], this can vary for different material compositions. Silicon is also used at the anode of Li-ion batteries with challenges in degradation but there is research for a self-healing mechanism to help regenerate the battery [21].

Anode materials like silicon, can store more lithium ions, potentially increasing the battery's energy capacity. However, silicon anodes also face challenges related to expansion and contraction during charging and discharging cycles.

The cathode is another critical component of a lithium-ion battery, working in conjunction with the anode to facilitate the flow of lithium ions and generate electrical energy. The cathode is where the Li- ions are received during the discharge phase of the battery operation. During discharging, lithium ions flow from the anode to the cathode through the electrolyte [10].

Various compositions used for the cathode are seen in Table 2.2. The most common cathode material in lithium-ion cells is lithium cobalt dioxide (LCO) because of its high energy density and good voltage stability [15]. The material used in the cathode of a battery can differ significantly based on its source, how pure it is, the size and characteristics of its particles, any coatings applied to the particles, the addition of other elements, the ratios in which different components are mixed, how tight it is packed, and its level of crystalline structure [15]. These factors can vary and have a big impact on the performance of the electrode.

For the safety of various positive electrode materials, results indicate that the cathode materials start reacting with the electrolyte in an exothermic (heat-releasing) manner at different temperatures, which range from approximately 130 – 250 °C [15].

Electrolyte

The main function of an electrolyte in a Li-ion battery is to safely transport the lithium-ions between the two electrodes, while the electrolyte is as thin as possible [23]. The electrolyte found in lithium-ion cells usually consists of a mixture of organic carbonates like ethylene carbonate or diethyl carbonate. This electrolyte contains dissolved Li-ions provided by a lithium salt, typically lithium hexafluorophosphate (LiPF₆). A small number of different additives to enhance the cell's performance, including its resistance to overcharging, cycle life, calendar life, and stability [15]. Lithium-ion electrolytes are of three types: liquid, solid and gel electrolyte. Regardless of the state, in summary, electrolyte properties for different lithium batteries are summarized in [23], based on the author's knowledge. However, electrolytes contain flammable materials which may also differ in their chemistry. Research is ongoing to improve electrolytes to ensure safety. [15]

Table 2.3 shows the summary of Electrolyte properties desired for various lithium-ion batteries and their comparison based on the state of matter [23].

Electrolyte Properties	Liquid	Solids	Gel
Fundamental Properties			
Ionic conductivity	High >10 ⁻³ Scm ⁻¹	Low >10 ⁻⁴ Scm ⁻¹	Medium >10 ⁻⁴ Scm ⁻¹
Contact/interfacial Properties	Good	Poor	Medium
Electrochemical stability	Poor	Good	Poor
Thermal stability	Poor	Good	Poor
Dimension stability	Poor	Good	Medium
Safety	Poor	Good	Medium
Additional properties required by a specific battery			
Resistance to forming or dissolving by-products (e.g., polysulfides for Li-S)	Low	High	Medium
Ability to dissolve oxygen	Good	Poor	Medium

Separator

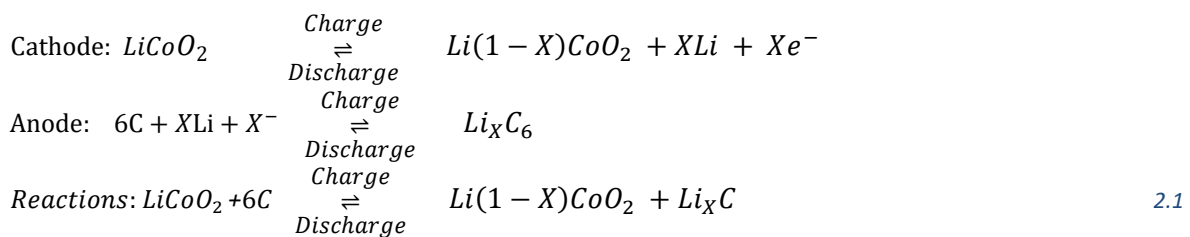
The separator helps to prevent direct contact between the anode and cathode while allowing Lithium-ions to flow through the electrolyte from the anode to the cathode and vice-versa. Lithium-ion cell separators most commonly are porous polyethylene, polypropylene, or composite polyethylene/polypropylene films [15]. These films are typically on the order of 20 μm thick, although thinner (approximately 10 μm) and thicker films can be found (approximately 40 μm). One of the challenges with the separator is the films are softened and this causes the pores of the separator to be closed at a temperature ranging from 130- 150 °C [15]. Another study said decomposition will occur depending on the type of separator composition (for polypropylene is 130 °C, for polyethylene is 170 °C and for ceramic coated separator is 200 –260 °C) [24]. The charge or discharge process is stopped by resisting the transport of Li-ions between the anode and cathode. This type of separator is referred to as the shutdown separator [15]. Several compositions of separators are seen in Table 2.2. Reducing the thickness of the separator will increase the capacity of a cell when constrained by dimensions. However, a thinner separator weakens the defense against internal short circuits which may result in fires and explosions [5].

Current collectors

The role of the current collector is to distribute current evenly throughout the cell to the active material, to provide mechanical support for the active material, and to provide a point of mechanical connection to leads that transfer current into the cell. The most common current collectors are thin foils or binders of copper used for the anode and aluminium used for the cathode. Due to the level of reliability and safety involved for the copper current collector to increase its oxidation and dissolve copper ions into the electrolyte at a very low voltage (approximately 1V for the cell) [15]. During several recharges, these dissolved copper ions plate as copper metal towards the negative surfaces reducing their permeability and making the cell prone to lithium plating.

2.3 Charging and discharging Principle of Li-ion battery

When charging the battery, the Lithium-ions move from the cathode materials, spread around the electrolyte, and move through the separator pores where it intercalates into the anode material [10]. In addition, electrons move in the opposite direction via the circuits to maintain electro-neutrality. When discharging, the lithium ions move from the anode back to the cathode [10]. The equation summarizes the working principle of a typical Lithium-ion battery using LCO (cathode)/graphite(anode) for the charge and discharge reaction as seen in equation 2.1:



The back-and-forth movement of the lithium-ion during charging and discharging produces some amount of heat [25]. The emitted heat is normal for the battery, however, if the heat has no sufficient venting during the charge and discharge state, the battery will become very hot which could compromise the battery safety [26].

2.4 Types of Li-ion Batteries

The four types of Li-ion cells i.e. cylindrical cell, Prismatic cell, Pouch cell and coin cell are seen in Figure 2.4. it includes both high and low-capacity cells. Due to the high resistance of cylindrical cells, its low cell capacity is used in most of the applications. The cell case is hard, and it can withstand high pressure [14].

The case is typically made from materials like stainless steel, nickel-plated steel, or other metals that provide durability, strength, and heat dissipation capabilities. The cylindrical cell has both small and large types with advancements in the battery cell design. Li-ion cylindrical cell is seen to be the used laptop computer batteries, electric bicycles, electric scooters, electric vehicles, commercial aircraft auxiliary power units (APUs), satellites, military applications, and energy storage and grid either in multi-cell arrangements or battery packs [15]. The most common type of lithium-ion cylindrical cell is 18650, 21700, and 26650 [15]. The 18650 denotes the diameter and length of the cell i.e., 18 mm diameter and 65 mm length [15].

Prismatic cells offer substantial capacity, reducing the need for a large number of battery packs to achieve the required capacity, and enhancing overall system stability [27]. These cells feature a robust, welded hard case that can withstand high pressure. However, higher cell capacity increases safety risks, particularly due to poor heat venting, which can affect cooling and cell components. Both prismatic and cylindrical cells are prone to high-pressure build-up, with built-in safety vents, but extreme pressures from malfunctions can lead to cell case explosions [19]. Prismatic cells come in small and large types in capacity.

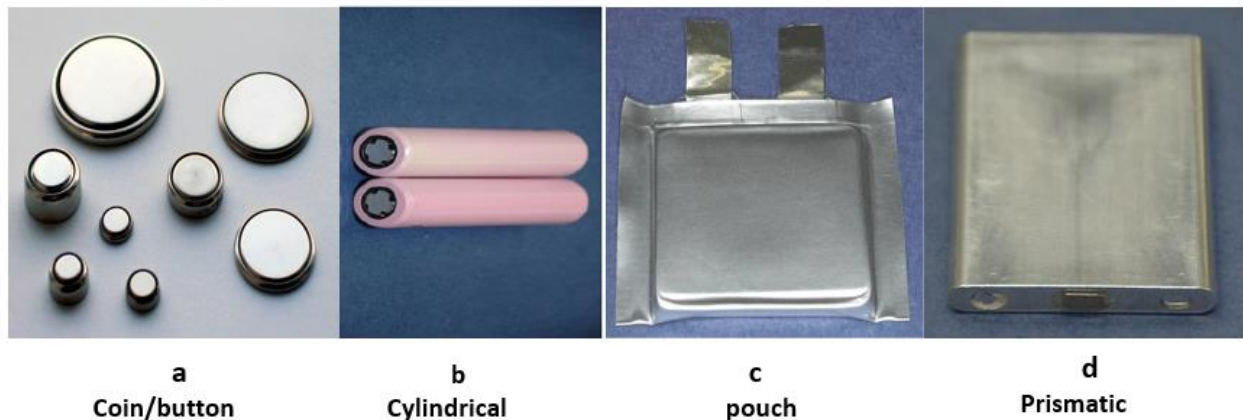


Figure 2.4 shows the photos of the four types of Li-ion cells, AB [28] CD [15]

Soft-pouch cells are also known as pouch, polymer, or Li-Po cells. The electrode is covered with a foil. The pouch is a polyamide aluminium-polypropylene compound, which is closed by a heating-sealing process [13]. The pouch cell is flexible in matching a specific shape. A common issue with soft pouch cells is that they can corrode when polarized leading to cell leakage and swelling [15].

A coin cell or button cell is a small single cell battery with a cylindrical look. it can be seen in small (button) and big sizes (coin cell) as seen in Figure 2.4a, and its diameter ranges from 5-25 mm wide and 1-6 mm high. The cathode is located at the bottom, and it is made with insulated stainless steel. The anode is at

the top and it is made up of made of zinc or lithium [28]. They have a low self-discharge feature even if the device is not in use for a long time. They are used to power small portable electronics.

2.5 Thermal runaway in batteries

Battery temperature varies and extreme temperatures (cold or heat) reduce charge acceptance, and the temperature needs to be within the normal range before charging [29]. Current and voltage have a temperature impact on batteries. High current use and limited voltage can result in fast charging, fast charging increases cell temperature and cell degradation. If the cell temperature is not monitored and brought under control, then the risk of thermal runaway increases [13].

There are acceptable temperature limits for all batteries. For Li-ion batteries, it is not safe to charge at a low temperature (see Table 2.4) because the rate of diffusion decreases on the anode side. When charging, the internal cell impedance causes an increase in temperature that compensates for the cold temperature, this happens to all batteries and ends up increasing charging time.

Table 2.4 Permissible Temperature Limits for various batteries [29]

BATTERY TYPE	CHARGE TEMPERATURE	DISCHARGE TEMPERATURE	CHARGE ADVISORY
Lead acid	-20 °C to 50 °C (-4 °F to 122 °F)	-20 °C to 50 °C (-4 °F to 122 °F)	Charge at 0.3 or less below freezing. Low V-threshold by 3m V/°C when hot.
NiCad, NiMH	0 °C to 45 °C (32 °F to 113 °F)	-20 °C to 65 °C (-4 °F to 149 °F)	Charge at 0.1 C between -18 °C and 0 °C. Charge at 0.3 C between 0 °C and 5 °C. The charge at 0.1 C between 45 °C is 70 °C. Charge acceptance at 60 °C is 45 %.
Li-ion	0 °C to 45 °C (32 °F to 140 °F)	-20 °C to 60 °C (-4 °F to 140 °F)	No charge is permitted below freezing. Good charge/discharge performance at higher temperatures but shorter life.

Thermal runaway may occur with all types of batteries, which is because of rapid self-heating of the cell with an increase in temperature followed by strong venting (smoke and gas release), cell case rupture/explosion, gas explosion and fire [6]. The process of thermal runaway to fire is caused by heat generation, accumulation, and propagation [30]. In most cases, thermal runaway occurs in Li-ion batteries after the safety vent (see Figure 2.5a) is activated and gases are emitted. Due to the rise in temperature and pressure build-up which is caused by decomposition and exothermic chemical reactions such as the

solid electrolyte interface (SEI) decomposition, electrolyte and electrode reactions, and melting separator inside the battery, release heat and gases. Schematic of the self-heating reaction of the battery is seen in Figure 2.5b). The result of a thermal runaway reaction in a Li-ion cell is shown in Figure 2.5c).

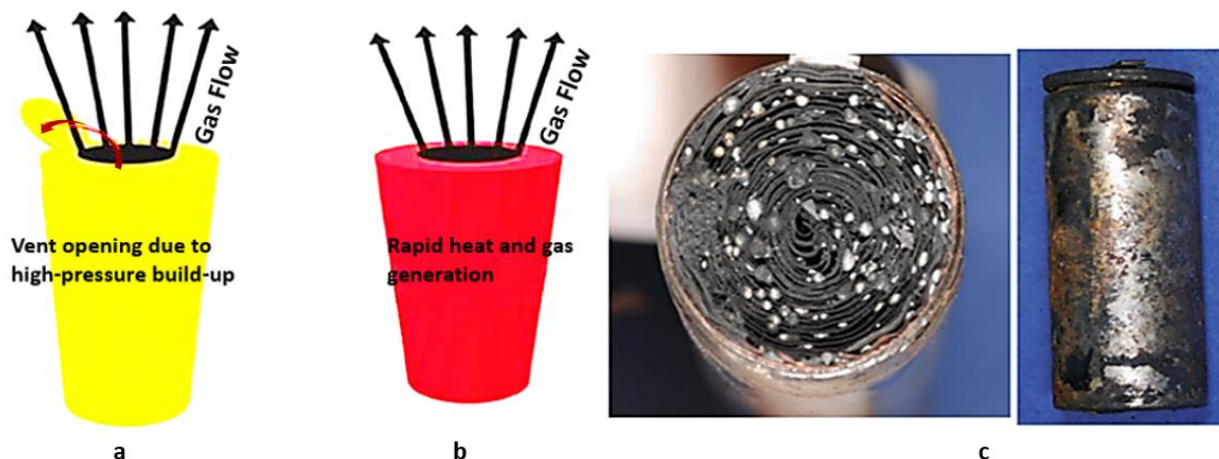


Figure 2.5 (a) safety vent activates due to internal pressure build-up, (b) schematic of thermal runaway (c) Aftermath thermal runaway [31] [22].

The mechanism that catalyzes thermal runaway comprises mechanical, electrical, and thermal abuse [31] and this can spread from one battery to the entire battery pack. The more energy stored in a cell determines the outcome when it experiences a thermal runaway reaction. For instance, Li-ion batteries possess high energy density compared to other cell chemistries, and their cells contain a flammable electrolyte [22]. If a cell reaches this temperature in an adiabatic (no heat is lost) environment, it will eventually self-heat to the point where thermal runaway is initiated. For a typical 100 % state of charge (SOC) 18650 cylindrical Li-ion cell that has attained self-heat temperature, it is likely for thermal runaway to occur after two days [22].

The severity of thermal runaway events depends on the following factors: the SOC of the cell, the ambient environmental temperature, the cell chemistry i.e., the electrochemical design of the cell and the mechanical design of the cell (electrolyte volume, cell size, etc.) [22]. A previous study by Ouyang et al, [32] reported that higher SOC also increases the thermal hazards of batteries and its consequences. Events that may occur before thermal runaway are:

2.5.1 Increase in Temperature

Temperature increases in the cell above 60 °C cause an oxidation reaction of electrolytes, which can further increase the cell temperature rapidly. Cathode material will also decompose and react with the electrolyte to form the SEI (solid electrolyte interface) [24]. At 120 – 250 °C the reaction between the

anode material and electrolyte occurs forming a new SEI layer and previous studies indicate decomposition in Li-ion graphite anodes with electrolyte initiates at a temperature range of 70 – 90 °C [22]. After the safety vent valve activates at 80 – 150 °C and the temperature keeps increasing, the separator will reduce in size and melt when the separator reaches the melting point depending on the type (for polypropylene is 130 °C, for polyethylene is 170 °C and for ceramic coated separator is 200 –260 °C) [24]. The temperature at this point is called short circuit temperature, due to the internal short circuit releasing electrical energy at an extremely high rate. At this point, TR cannot be stopped through external cooling due to rapid temperature increments. Lopez et al. [4], also summarized various side reactions that can take place in the cell components at different temperatures and heat release rates before thermal runaway. RISE [33], also revealed different side reactions that can occur within the cell components at varying temperatures.

When internal temperature increases, it can also result in melting separator and decomposition, which can affect the aluminium current collector at 660 °C [22].

2.5.2 Internal Pressure Increases

The internal pressure of the cell rises gradually as the temperature increases, this is caused by the heated electrolytes which will both vaporize and decompose, this could affect the cathode material thereby ejecting gases. During this process swelling is obvious for cells like prismatic and pouch cells but cylindrical cells design, the opening of the safety vent is obvious to relieve pressure in the cell [22]. However, if the cylindrical cell is sufficiently heated using an external source, the case wall will weaken creating a passage through the cell top or base.

2.5.3 Cell Venting/ Gas Ignition

As battery temperature and pressure increase, different gases and vapors are released because of the safety vent present in almost all lithium-ion batteries. So, it is important to investigate the gases released during the venting process. Previous studies have shown gas venting or ejection during high temperatures [31]. Hard case cells like cylindrical batteries will have internal pressure build-up before the pressure relief activates and venting occurs. depending on the mechanical design of the type of cell involved, the release of pressure may end up ejecting the cell content [22]. This is dependent on environmental conditions around the cell or battery pack. The vented gases may ignite and during thermal runaway, the cell case may rupture, or there may be a gas explosion and fire. These may further result in cell propagation in battery modules or packs.

However, these gases are not self-ignited. Sufficient oxygen must be available to sustain the combustion of hydrocarbons and there must be an ignition source present to ignite the vented gases. A hot cell may be an ignition source on the vented gas or a hot metal depending on the available ignition source considering the fire triangle is complete i.e., ignition source (heat), oxygen and combustible material (fuel). Ignition of vented gases from 18650 cylindrical Li-ion cells and higher are predominant.

Yuan et al. [34] experimented to investigate the thermal runaway effects of cylindrical Li-ion batteries with multiple chemistries using an accelerating rate calorimeter (ARC) test. The samples of the ejected gases were taken and analyzed using gas chromatography (GC). It was identified the major gases that were present, in the battery chemistry used were; Lithium iron phosphate (LFP), Lithium titanate (LTO) and lithium nickel manganese cobalt (NMC). The summary of the gases vented is seen in Table 2.5.

Table 2.5 shows the vented gas characterization [34]

Type	H ₂ (%)	CO (%)	CO ₂ (%)	CH ₄ (%)	C ₂ H ₂ (%)	C ₂ H ₄ (%)	C ₂ H ₆ (%)
LFP	23.34	4.50	25.39	5.90	0.08	3.26	1.29
LTO	8.41	5.30	37.60	1.23	0.0008	1.38	0.40
NMC 1	12.39	30.30	13.22	10.50	0.0026	0.10	0.16
NMC 2	12.54	28.06	19.91	12.90	0.0027	0.16	0.21

Ohsaki et al. [35], studied LCO prismatic batteries with a graphite anode. Several gases were ejected and the increase in temperature resulted in more volume of gases ejected. The result indicated that when the temperature of the battery exceeds 60 °C results in a rapid increase in exothermic reaction within the electrolyte which eventually increases the overall temperature rapidly, it was concluded that the thermal runaway occurred due to the forceful reaction between the overcharged anode and the electrolyte solvent at high temperature which occurred because of the exothermic reaction between the cathode and electrolyte. During thermal runaway, various combustion behaviours are observed, such as;

Jet Flames

Chen et al. [7] in their research of fire hazards of Li-ion batteries observed high speed jet flame combustion during TR. According to RISE [36], it stated that *“A battery fire can be violent, there can be jet flames coming out of the battery, burning battery cells being thrown out, the fire can lead to the emission of hot sparks, burning liquid and large quantities of toxic and flammable gases, which in turn can ignite in an explosion-like fire.”* Zhong et al. [37], observed a jet flame occurrence in one of the experiments on 3 x 3 configurations with 0 cm spacing, resulting in the propagation to adjacent cells.

Diffusion Flame

Kim et al. [8], observed a diffusion flame in the initial combustion stage during TR for 0 %, 50 %, and 100 % SOC in their experiment investigating the fire characteristics and heat release rate of Li-ion batteries.

2.6 Fire and damage to battery

The electrolyte in Li-ion batteries is flammable, contributing to the fire risk. Additionally, Li-ion battery cells possess high voltage, further increasing the fire hazard. The key difference between traditional alkaline and Li-ion batteries lies in their electrolytes. Li-ion batteries use a flammable electrolyte, whereas alkaline batteries use a conventional water-based electrolyte [38].

The separator, a component in the anode of a Li-ion battery, can generate a significant amount of heat. This heat can sustain a fire in the battery even without the presence of external air [38]. If the temperature rises beyond a specific threshold due to various factors, it triggers undesired internal reactions. This, in turn, leads to further heat release as the separator becomes damaged, causing the materials within the battery to break down. Consequently, the battery temperature can rapidly increase to 600 °C within seconds. Furthermore, some gases are released and increase the pressure inside the Li-ion battery, which causes fire and explosion permanently damaging the battery. According to an investigation by FFI and other research institutions [38], some cells can self-heat after repeated charge/discharging cycles.

With the high rate of using Li-ion batteries in many applications, there have been several records of incidents in different applications of this battery regardless of the manufacturers, therefore, the cell fire cannot be ignored.

2.7 Abuse methods to induce Failure.

An internal short circuit is the main cause of thermal runaway reaction when the separator is jeopardized and/or there is dendrite formation. A battery can be abused in the following ways: electrical, mechanical and thermal Abuse as seen in Figure 2.6 according to regulatory standards.

2.7.1 Electrical abuse

There are several ways in which Li-ion batteries can be abused electrically resulting in a battery thermal runaway reaction.

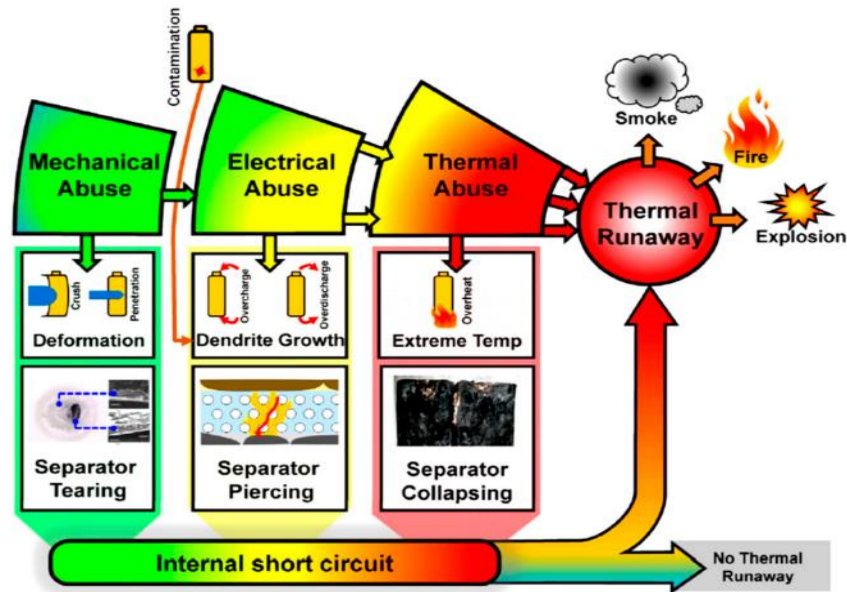


Figure 2.6 Abuse conditions resulting in thermal runaway [9]

Overcharging

Overcharging of Li-ion batteries can cause significant degradation of the anode and cathode. On the anode, it can lead to lithium plating (this are lithium metal deposits on the anode surface that have not inserted themselves into the anode material) instead of intercalation of lithium i.e., the insertion of lithium-ion from the cathode to the anode and vice-versa during the charging and discharging process [22]. The plated lithium reacts with electrolyte and forms dendrites that penetrate barriers between the cathode and anode and jeopardize the thermal stability of the cell, which leads to an internal short circuit and may further result in thermal runaway reaction, fire and explosion. The reaction in both the anode and the cathode as well as the lithium dendrite can result in the cell exceeding its thermal limits and the more severe the overcharge, the more potential for thermal runaway to occur [39]. Severe overcharge is not common with consumer electronics devices due to the overcharge protection mechanism within the battery pack such as the battery management system (BMS) but if it fails can be severe. Also, Larsson Fredrik and Mellander Bengt-Erik [40] experimented on an overcharge abuse test.

Over-discharge

Over-discharging a lithium cell to 0 V will not lead to a thermal runaway reaction [22]. However, such over-discharge can cause the electrode and current collectors to be damaged internally. It can also cause lithium plating when the cell is recharged (especially if the cell is discharged repeatedly) and can finally lead to

thermal runaway. Most consumer electronics have their set point for a specific voltage limit for their lithium-ion battery pack to prevent over-discharge.

External short circuit

This involves a high rate of discharge or charging which results in resistive heating within the cell to the point of high resistance. This type of internal heating affects the cell's thermal stability limit. As the capacity of a cell increases the likelihood of internal impedance heating leading to thermal runaway also increases. High-capacity cells convert more electrical energy to internal heat [22]. There are also available UN and UL testing standards are provided for such testing.

Previous studies by Larsson Fredrick and Mellander Bengt-Erik [40] are seen to use external short circuit methods to heat a cell to failure. Similarly, Lopez et al, [4] conducted an experiment on thermal runaway and propagation in Li-ion battery modules. They employed the external short circuit method, utilizing a flexible electrical connector and applied much power to heat the cell to failure.

2.7.2 Mechanical Abuse

Mechanical abuse of the battery can cause the current collectors and separators between the cathode and anode of the battery to break. This can lead to an internal short circuit, generating substantial heat and potentially triggering thermal runaway. With the rising number of electric vehicles, scenarios like severe collisions impacting the battery pack, causing crushing or penetration by external objects, can result in such damage [31]. Mechanical abuse can have critical consequences, either causing sudden failure or impacting the battery's efficiency, leading to a weakness that might result in internal cell faults over time. Both UN and UL consumer electronics standards stipulate a minimum requirement for batteries to undergo mechanical abuse tests at full charge (100% SOC) [22]. These tests assess the battery's ability to withstand flat plate crush and focused crush perpendicular to their electrode surfaces. [22]. Some battery manufacturers are subjected to conduct tests for their products even with nail penetration as it is mandatory as stated in UL 1642. Other mechanical abuse test in the UL 1642 standard includes vibration test and shock. Mechanical impact, such as crushing or penetration, is more likely to cause thermal runaway if it occurs at the edges of the electrodes rather than perpendicular to the surface of the electrode [22]. A summary of the test methods and relevant standards is seen in Table 2.6.

Table 2.6 shows standard methods simulating Li-ion battery internal short circuits [10].

TEST METHODS	STANDARD NUMBER
Nail Penetration	GB 31485-2015, UL 2580:2016
Heavy Impact	UN 38.3: 2016, UL 2580:2016
Crush	IEC 62133: 2012, UL 2580: 2016
Forced Internal short circuit	JIS C8714:2007

Lamb et al, from one of the experiments conducted, used a nail penetration type of test method to cause failure in cells [41].

2.7.3 Thermal Abuse

Thermal abuse leads to elevated internal and external temperatures that can cause the separator between the anode and cathode to melt, leading to an internal short circuit. This rapid increase in temperature may result in thermal runaway. Several abuse test methods conducted in previous studies, such as Larsson et al. [42] [6], involved subjecting cells to external heating to assess cell thermal stability using a ramp -up test with an Oven [43], heating rods [30], external fire heating using propane burner [42]. Ouyang et al. [32] and Zhong et al. [37] used an electrical heater with the shape 18650 cylindrical. Chen et al. [30] from their experiment used an electrically heated rod to cause failure in cells around it. Chen et al. [7], used an electrical heater to assess the fire hazards of 18650 cylindrical Li-ion batteries at different atmospheric pressure.

Zhao et al, [44] also conducted an accelerating rate calorimetry (ARC) test using 18650 cylindrical Li-ion batteries by using different states of charge (SOC) and cycling times to study the thermal runaway hazards. The ramp heating method uses an electrical heater to study thermal runaway hazards.

Flammable and other harmful or toxic gases Li-ion batteries.

As temperature increases in a battery with internal pressure build-up, the safety vent activates by releasing several gases that are ejected before and during thermal runaway which leads to fire and explosion. The electrolyte becomes the combustible material, the by-product of the burning reaction generates flammable gases.

Previous studies by Fredrik Larsson [6], detected Phosphoryl fluoride (POF₃) and hydrogen Fluoride (HF) and he stated that these gases are toxic threats and are high risk considering the amount of the gases released during the experiment. HF exists as a colourless gas or fume when ejected from the battery cell

as a liquid content and harmful to humans. It is easily absorbed in the skin and body tissues, which can damage cells. HF gas production from a cell is roughly estimated at 200 mg of HF/Wh [6].

According to the Centre for Disease Control (CDC), breathing HF can damage the lung tissue, and cause inflammation (swelling) and fluid accumulation in the lungs possibly leading to death from inconsistent heartbeat or fluid build-up in the lungs. The severity of HF depends on the amount, route, length of time of exposure, as well as the age and initial medical condition of the exposed person. There can be immediate signs and symptoms of exposure such as eyes, nose and respiratory tract irritation. Long-term health issues can cause lung disease. Therefore, the HF gas exposure hazard can be significant and should be analyzed carefully.

Ouyang et al [45] stated presence of CO, H₂ and SO₂ gases may be emitted. Golubkov et al. [46] detected that CO₂, H₂O, CO and C₂H₄ gases are emitted at a temperature of 80 – 120 °C. Chen et al, [30] detected carbon dioxide (CO₂) carbon monoxide (CO) ejection. Riebère et al. [47], investigated fire induced hazards of Li-ion batteries using fire calorimetry and analyzed the toxicity. The toxic gases discovered were HF, CO, NO, SO₂ and HCl. RISE [33] stated that the gases that can be present during degassing of Li-ion batteries are carbon monoxide (CO), methane (CH₄), ethane (C₂H₆), ethylene (C₂H₄), benzene (C₆H₆), toluene (C₇H₈), ethanol (C₂H₆), methanol (CH₄O), hydrogen (H₂), hydrogen fluoride (HF) and hydrogen chloride (HCl). Ohsaki et al. [35], identified all these gases emitted from their research i.e. CO₂, CO, C₂H₆, C₂H₄ and H₂.

The burning of any flammable substance generates carbon dioxide (CO₂); CO₂ produces hypoxia which is a reduction in the amount of O₂ available for tissue respiration. 3-6 % intake causes dizziness, headache, and fatigue. 7-10 % cause loss of consciousness within 2mins (10 %) [48].

When carbon monoxide (CO) is inhaled, it forms carboxyhemoglobin (COHb) in the bloodstream. COHb restricts the uptake and conveyance of oxygen to the body's tissues. The quantity of accumulated COHb is measured in percentage. At 10-20%, it leads to headaches, at 30% it causes severe headaches, unconsciousness, nausea, and vomiting. When COHb reaches 50-70%, it can result in death [48].

In a previous experiment carried out by Ouyang et al. [49], the behaviour of the fire for the cylindrical 18650 Li-ion batteries and battery packs under discharge conditions was observed, with a total of eight tests carried out. The trial was conducted employing a cone chamber utilizing a 2-KW electric heater as the primary heat source. The combustion of the lithium-ion batteries was observed in four distinct phases: initial heating, safety vent rupture, battery ignition, and thermal runaway. The experiment recorded

detailed data concerning the timing and temperature at which ignition and thermal runaway occurred.

The data of the time and temperature of ignition and thermal runaway are presented in Table 2.7.

Table 2.7 The fire behaviors of cylindrical 18650 lithium-ion batteries (cathode and graphite anode) under discharge conditions [9]

Test no.	Number of Cells	With Discharging	Time to Ignition (S)	Temperature to Ignition (°C)	Time to Thermal Runaway (S)	Temperature to Thermal Runaway (°C)
1	1	Yes	251	180	295	248
2	2	Yes	225	170	264	247
3	3	Yes	219	172	248	247
4	4	Yes	217	176	242	246
5	1	No	255	180	306	248
6	2	No	234	176	291	239
7	3	No	233	178	283	244
8	4	No	233	175	274	242

Four battery packs, comprising NMC cathode and graphite anode, were employed: a single cell, two cells, three cells, and four cells, all arranged and connected in parallel. Eight experiments were conducted in total, four with 100% state of charge (SOC) subjected to discharge treatment, and four without. Observations revealed that lithium-ion batteries undergoing discharge treatment experienced earlier ignition, material ejection, and stable combustion compared to those without discharge treatment. Notably, the ejection and combustion were notably higher in the former. Moreover, it was found that an increase in the number of cells amplified fire behaviour. However, there was no significant change in the temperature leading to thermal runaway.

It is reported that the state of charge (SOC) i.e., the amount of electrical energy stored in the form of electrochemical potential energy, has a significant effect on Li-ion battery fires. Heating and burning time are directly proportional to SOC, and the fire hazard increases with respect to SOC [30].

2.8 Thermal runaway propagation in multiple cells

Li-ion cells are of different types due to their required power and energy from a battery system, the cells are arranged in series or parallel to increase the capacity and /or the voltage. A battery system consists of several battery packs, which are made up of multiple battery modules, and each battery module contains several cell configurations i.e., arranged in series or parallel [9]. An image description is represented in Figure 2.7.

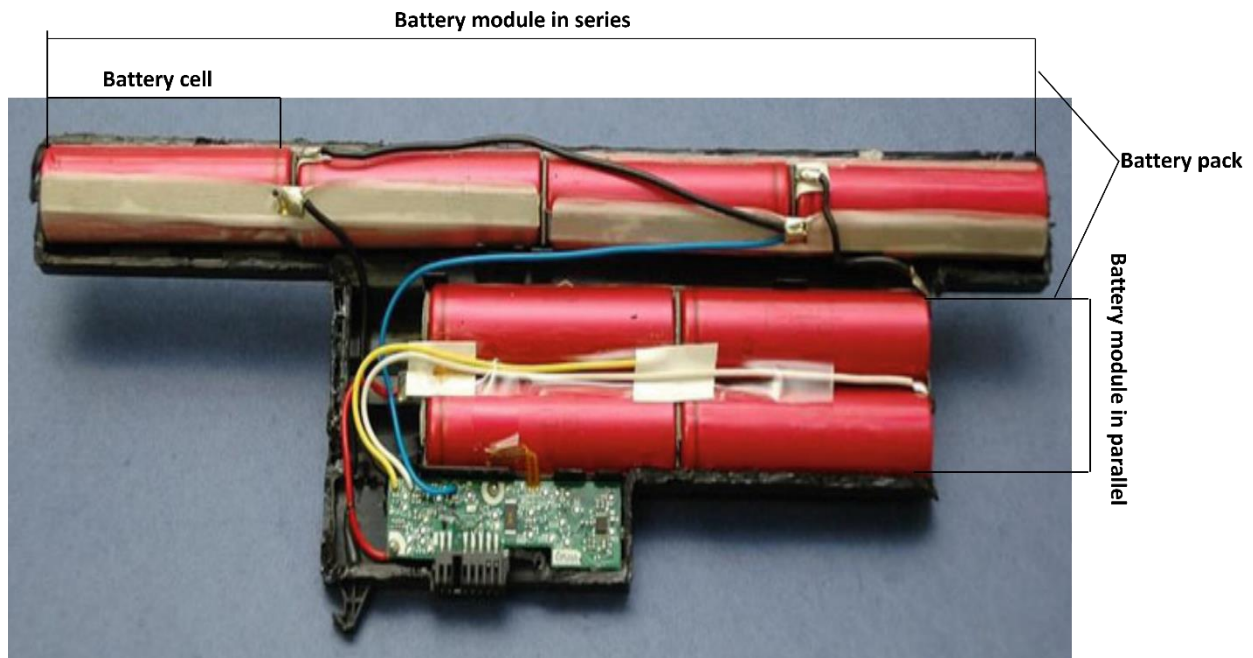


Figure 2.7 Difference between battery cell, module, and pack [15]

The capacity of a battery pack depends on the number of individual batteries it contains, which can vary from a few to several thousand, depending on the intended application.

A single cell within a battery system presents thermal hazards, encompassing high temperatures, safety valve rupture, venting, combustion, explosion, and the emission of toxic gases during thermal runaway. Additionally, there exists a potential for heat to spread to the other batteries. Within the battery pack, this propagation can lead to severe thermal hazards with the potential for catastrophic consequences. However, precautionary measures should be implemented to contain the spread of failure [9].

Once thermal runaway commences in a battery due to any of the abuse mechanisms, it spreads to the remaining battery packs. Understanding the propagation behaviour in various types of Li-ion batteries is crucial to prevent thermal runaway.

Ouyang et al. [32], conducted extensive thermal runaway propagation experiments using cylindrical 18650 packs of various sizes: 2 x 2, 3 x 3, 4 x 4. They reported that the thermal runaway, triggered initially by a cylindrical shaped heater at the corner battery. This propagated throughout the entire battery.

The study also explored various factors such as State of charge (SOC), thermal runaway failure location, spacing, and the number of heaters concerning propagation. Their findings revealed that at higher State

of Charge (SOC), failure propagation increased, indicating earlier thermal runaway, faster propagation, greater mass loss, and higher peak temperatures. Moreover, the intensity of propagation increased in battery packs with a larger number of heaters and when the thermal runaway occurred closer to the pack.

Lopez et al. [4], experimented on thermal runaway and propagation by employing a flexible heating element connected to the battery module (arranged in a 3 x 3 configuration and examined various spacing scenarios. They found out that increasing the distance between cells reduces damage, temperature and voltage on adjacent cells. They also reported that the branched style of tabbing (M-type) enhanced the voltage to hold continuously and further improved the safety of the battery pack compared to the snake-like style of the tab (S-type) as seen in Figure 2.8.

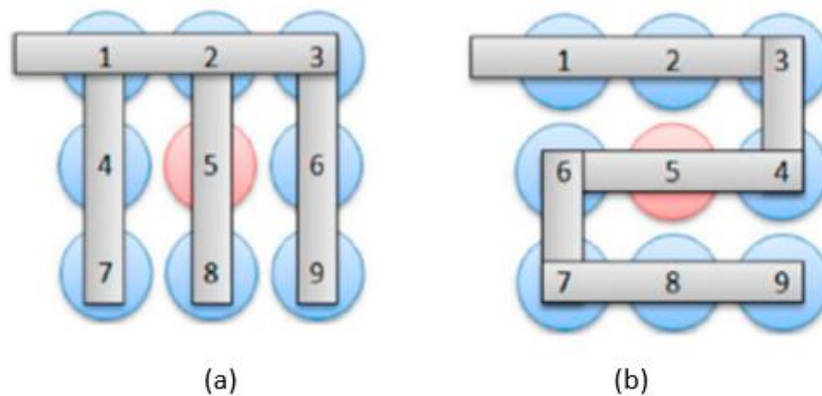


Figure 2.8 Tab configuration of battery pack: (a) branched style (M-type) (b) snake-like style (S-type) [9].

Chen et al, [30], conducted an experiment involving Samsung 18650 Li-ion batteries, each at an 80% State of Charge (SOC), arranged in configurations of 6 x 6 and 10 x 10. They used a heating rod placed near the center of the battery box. Their findings indicated that the initial stage of thermal runaway was initiated by the electrified heating rod, transmitting heat to the cells. Consequently, thermal propagation occurred, extending to adjacent batteries. As a result of continuous heating, the Li-ion batteries ignited, leading to the spread of fire to surrounding batteries.

In addition to the findings, it was noted that the heat transferred through the cell case is greater than that of the thermal runaway and subsequent fire processes. Additionally, it was mentioned that high-speed ejection flames significantly impact thermal and fire propagation. A chain reaction was observed between both sample scenarios. Certain safety measures were suggested to mitigate the risk of thermal and fire propagation.

Lamb et al. [41] experimented to explore the propagation behaviour of two types of batteries, cylindrical and pouch, utilized in battery packs. They employed a mechanical nail penetration method and different circuit connections on the cells. The study revealed that pouch batteries exhibit a higher susceptibility to thermal propagation in comparison to cylindrical batteries. This vulnerability was attributed to the pouch batteries having maximum contact with their surroundings.

Also, previous studies by Zhong et al. [37] performed several experiments to investigate thermal runaway propagation using cylindrical batteries in both 1 x 3 and 3 X 3 configurations, 0 mm (no spacing) and 4 mm spacing. A cylindrical electric-powered heater was used to initiate the thermal runaway process. It was observed that it took 240 to 280 s for thermal runaway to propagate between the battery layers inside the battery pack. Furthermore, batteries with 50 % SOC released larger amounts of combustible gases rather than violent flames. However, once the gases are on fire, extend the combustion due to the increased number of gases.

2.8.1 Heat Transfer in Battery

According to the energy balance equation, the rate of increase of internal energy of the battery is determined by its self-heat generation rate, e (q_r) and the heat transfer intensity. q_r is the heat generated by the chemical reaction inside the battery with an increase in battery temperature [30]. Heat transfer intensity is determined by heat conduction, heat convection q_{Conv} and heat radiation q_{rad} .

$$MCp \frac{dT}{dt} = q_r + q_{Conv} + q_{rad} \quad 2.2$$

$$q_{conv} = h(T_s - T) \quad 2.3$$

$$q_{rad} = \varepsilon\sigma(T_s^4 - T^4) \quad 2.4$$

Where Cp is the specific heat capacity of the component, M is the mass, $\frac{dT}{dt}$ is the temperature rise rate, h is the conduction coefficient and t , T is the surface temperature of the heater. T is the temperature on the boundary of the battery, ε is the emissivity, σ the Stefan-Boltzmann constant $5.67 * 10^{-8} \frac{W}{m^2 K^4}$.

2.8.2 Battery and Safety

Researchers have dedicated significant effort to reducing the risks and consequences linked to thermal runaway by modifying Li-ion battery materials. Most studies have focused on enhancing safety and

reducing hazards by incorporating safety devices and active fire suppression systems. These measures aim to contain thermal runaway deterioration and minimize the impact of fires [9].

The mixture of organic carbonates and lithium salts mostly used in lithium-ion batteries makes the electrolyte highly flammable and this is a major safety concern. Fire retardant (FR) electrolyte additives mixed with the solvents or replacing the flammable solvent could be a solution to mitigate the risk of an unwanted fire scenario. For an additive to be the best option, the following properties are crucial [9].

Good chemical stability, no chemical reaction with battery components, electrochemical inertia, no significant electrochemical reactions within the normal operating voltage range of the Li-ion battery, suitable properties such as conductivity, viscosity, boiling point, density, solubility, etc., low toxicity, good machinability, and appropriate cost. [45].

Presently, the most common FR electrolyte additive include Phosphorus additive, Fluoride additive, Brominated compound, Composite additive, and Ionic liquid.

Details regarding each fire retardant (FR) electrolyte additive can also be found in Ouyang et al, [45]. Another component of lithium-ion batteries that has a very important role in securing battery safety is the separator technology that must be together to improve the safety and efficiency of the Li-ion battery which are fire resistance, mechanical properties, thermomechanical stability, and Ion-transport resistance.

Buddies-Meiwes et al. [14], emphasized the battery safety of hybrid and electric vehicles to enable high customer acceptance. Further emphasis was laid on lithium-ion batteries due to the high energy density they possess, the safety precaution should be both active and passive systems. Further emphasized passive safety is to be implemented at the cell level and system level.

The choice of cell chemistry helps in the safety of comparing (LiFePO₄) as a safer material than lithium-metal-oxide cathode (positive electrode) materials using cobalt. Nickel or manganese. A higher safety level can be attained by using Lithium titanate oxide (Li₄Ti₅O₁₂) as the anode (negative electrode) instead of carbon. The higher the passive safety of a cell, the lower the cell voltage and energy density as seen in Figure 2.9 and the materials used in the cathode and anode are shown. Further safety components such as separators, positive temperature coefficient (PTC) elements to reduce cell current or the use of flame-retardant additive can enhance cell safety. In a battery pack, passive safety can also be achieved, for instance having an overpressure vent to secure the case. 18650 Li-ion battery can emit around 2.5 liters of gas in the event of a thermal runaway [50], which can be compared to the size of a battery pack.

Protection of the battery pack against crush impact by the housing and prevent fuses from being short-circuited.

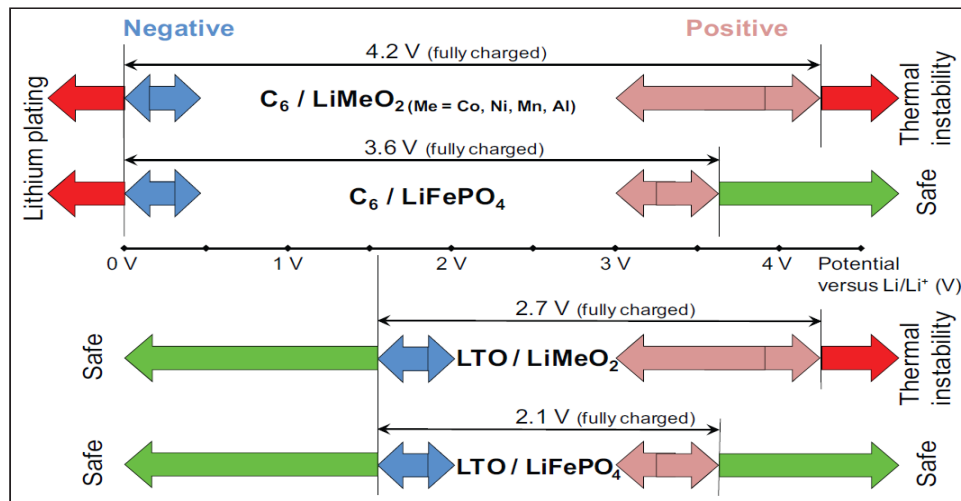


Figure 2.9 Electrode voltages for several material combination with lithium. LTO: lithium titanate ($\text{Li}_4\text{TiO}_{12}$) [14]

For active safety, which includes voltage control of each cell in series connection, exact charge, and discharge control management, as well as temperature control and cooling systems. The measured values should be made reliable and a redundancy for faulty measurements should be given.

Lithium-ion cells or batteries are categorized as Hazardous Materials (HAZMAT) or dangerous goods. They are commonly stored in packs during storage, transportation, and practical applications. If a single battery ignites, the fire can rapidly spread to other batteries in the pack. Therefore, it is vital to thoroughly analyze the thermal properties and the spread of reactions within Li-ion battery packs. [30].

2.8.3 Safety standards and codes for battery

UL 1642, the Safety Standard for Lithium Batteries, was first issued in October 1985. It specifically focuses on ensuring the safety of Li-ion cells for both primary (non-rechargeable such as lithium) and secondary batteries i.e. Li-ion batteries. The most recent edition was released on October 12, 2022. These updated editions have addressed emerging trends, including prismatic and pouch cells. UL 1642 currently includes a range of tests covering electrical, mechanical, environmental, and exposure aspects. These tests involve examining short circuits, abnormal charging, forced discharge, crushing, impact, shock, vibration, heating, temperature cycling, altitude simulation, and projectile tests to ensure safety standards.

Battery safety standards are constantly being updated and optimized because current tests cannot fully guarantee their safety in practical applications. This is still a very serious problem, as there are Li-ion battery fires almost every week around the world. Hence, various international safety organizations

regulate battery safety, and governments of different countries have formulated safety standards by national requirements and conditions, they have gradually improved the safety standards of lithium-ion batteries. Academics and industrial groups have also carried out extensive research on battery safety [10]. UL 9540A test standards (2019) [1] or equivalent full-scale testing states the fire characteristic of a battery energy storage system that undergoes thermal runaway because of fault, physical damage, or exposure hazard. The data generated is used by the large-scale fire tests to be used by manufacturers, system designers, safety professionals, and the applicable authorities in determining the fire and explosion protection required for an energy storage system. The standards comprise;

The cell level defines a repeatable method for abusing a battery into a thermal runaway to get information on the thermal runaway initiation and gas composition. A single cell is heated with an external flexible film heater to cause thermal runaway, other methods can be used such as pressure vessels in atmospheric pressure and limited oxygen volume of less than 1% [1].

The Module level test decides the propagation behaviour in a module. It also determines the HRR and gas composition. The conditioned module is tested with a 100% SOC under an appropriately sized smoke collection hood. Cell(s) in a location where thermal exposure to the other cell is maximized and are forced into thermal runaway like the cell using a film heater to initiate it [1].

2.8.4 Battery management system (BMS)

The BMS is the heart of the battery. The battery management system secures safety aspects as well as long-lasting lifetime [14]. The functions of the BMS include battery monitoring, diagnostics, electrical and thermal management including cell balancing. It provides warnings and initiates shutdown in a system when hazardous conditions are about to happen [9]. The BMS monitors the battery pack SOC and state-of-health (SOH) and updates its power capability. It also provides vehicle management with updates on how to operate the battery to achieve a long-lasting life. It is also important for the lithium-ion cell because it helps to prevent it from any form of overcharge and communicates the estimated time required for full charge [14]. In addition, the SOC of each cell differs over time which is caused by temperature difference and production of the cell, the BMS helps to regulate the temperature when it is critical to mitigate thermal hazard occurrence. The thermal management aids in reducing the temperature within the battery to be as stable as possible at a specified level. For lithium-ion batteries, the maximum charge current must be limited at low temperatures to avoid severe risk in the battery and accelerating aging which is due to lithium plating. Furthermore, safety issues of lithium-ion battery packs arise because of potential

overheating. The three main types of thermal management are; Air cooling systems (ACS), Liquid cooling systems (LCS) and PCM cooling systems (PCM-CS). There are two types of air flow patterns in ACS; natural convection (NC) and forced convection (FC). For the ACS, the rate of airflow is a key factor in improving the efficiency of heat dissipation [45]. In addition, certain factors such as battery arrangement, flow path number, and width also affect the performance. Despite the research to optimize the structure of ACS, it is still a challenge to meet the demand for EVs at present [45].

Compared to LCS, which is a liquid-based cooling system possesses better performance due to a higher heat transfer coefficient. The LCS is divided into two (liquid changing into vapor) kind depending on if a phase change occurs during the process. The phase change may be the driving factor to absorb heat [45]. Consequently, liquids are a huge barrier for an electronic system which requires advanced and complicated design before application, therefore, resulting in high cost.

PCM is made with material that can absorb thermal energy and then release it by a reverse process. It consists of three types: organic, inorganic and eutectic [45]. The organic PCM is made of carbon element with paraffin as the most common compound. The inorganic contains one or more metallic atoms. They also have good thermal conductivity and latent heat [45]. The eutectic PCM is a specific mixture of the previous PCMs which gives PCM properties different from pure materials [45]. A summary of different types of BMS with their merits and demerits is seen in Table 2.8.

Table 2.8 Comparison of different types of battery management systems (BMS) [9].

BMS		Advantages	Disadvantages
ACS	NC	Low; cost; Simple structure; Easy to integrate; Little electricity consumption	Low heat transfer coefficient; Dependent on ambient temperature; Uneven temperature distribution. Low efficiency; Dependent on ambient environment,
	FC	Low cost; Easy to maintain	
LCS	Liquid cooling	Low cost; Easy to maintain	Risk of leakage Higher cost for structural design; high-cost risk of supercooling
	Vapor cooling	Higher efficiency; Low operating cost; Better uniformity.	
		Higher efficiency; Uniform, temperature distribution	Risk of leakage; Volume difference with phase change,

PCM-CS	organic	Appropriate to extreme conditions.	with phase change; Risk of supercooling.
	Inorganic		
	Eutectic		

During normal operating and ambient conditions battery systems can be easily controlled within the range 20-55 °C [51] and Chen et al. [52], stated that the effective cooling control strategy keeps the battery cell temperature between 15-35 °C. During stressful conditions, such as a fast charge at a high cell temperature or a high ambient temperature, heat generation might increase extensively and eventually lead to thermal runaway. This reaction causes heat which propels an exothermic reaction and may eventually lead to explosion and fire therefore, there is a necessity to prevent it from occurring.

Recap

- Cell - it consists of a single-unit device that converts chemical energy to electrical energy.
- Module - it consists of a group of cells arranged in series or parallel.
- Pack - it involves a series of individual modules and protection systems including BMS, cooling systems, etc.

3 Experimental set-up and procedures

This chapter will address the experimental set-up and materials used for the small-scale experiment conducted in this study.

3.1 Purpose and Scenarios

The purpose of this thesis is to study how flame propagates in cells considering various spacing scenarios. All batteries are assumed to be fully charged, meeting the specified voltages as indicated by the manufacturer. In this study, a total of 13 experiments are conducted consisting of six different scenarios as listed below:

- Scenario 1 - Alkaline Single cell (3 experiments)
- Scenario 2 - Li-ion single cell (3 experiments)
- Scenario 3 - Alkaline 3x3 configuration, 0 cm spacing (1 experiment)
- Scenario 3 - Li-ion 3x3 configuration, 0 cm spacing (2 experiments)
- Scenario 3 - Li-ion 3x3 configuration, 0.5 cm spacing (2 experiments)
- Scenario 6 - Li-ion 3x3 configuration, 1 cm spacing (2 experiments)

3.2 Battery types

Two main types of batteries were used:

- Non-rechargeable battery: Alkaline battery (AA)
- Rechargeable battery: Lithium-ion battery (18650 Li-ion cell).

Commercially available non-rechargeable AA alkaline and 18650 Li-ion batteries were used for the experiments. However, there is no information regarding the composition of the battery materials by the manufacturers. Batteries are usually stored and transported under fully charged conditions (90% or greater SOC) [7], the state of charge for the bundled batteries for the experiments is assumed to be 100 % in this current study.

Table 3.1 shows information about the commercial batteries used for the experiment.

INFORMATION OF BATTERY SPECIFICATION		
	18650 Li-ion	Alkaline (AA)
Model	cylindrical	cylindrical
Nominal Capacity (Mah)	2600	2600
Nominal voltage (V)	3.70	1.5
Mass (g)	49.2 ± 2	23.5
Diameter (mm)	18	14.5
Height (mm)	65	50.5

3.3 Set-up

The experimental set-up of all scenarios mentioned earlier in section 3.1 will be addressed in this section.

3.3.1 Single cell (scenario 1 and 2)

The single cell set-up for scenarios 1 and 2 (Alkaline and li-ion) are similar. A single cell was placed in a holder of an insulating board. The cell was heated at a point that was exposed and near the top of the cell, as illustrated in Figure 3.1 and Figure 3.2.



Figure 3.1 (a) shows the AA Alkaline cell placed in the hole in a reversed way with the anode exposed to the butane flame (b) shows the 18650 Li-ion placed in the hole in a normal way.

The experiment involved connecting a K-type thermocouple (1 mm thick) to the cell and securing it with aluminium tape to prevent disconnection. This thermocouple was positioned on the rear side of the cell, to prevent it from being affected directly by the butane flame. The cell and thermocouple were inserted into a pre-drilled hole in the insulating board. A scale was used to measure the weight of the battery. The mass and temperature were recorded every second using a data logger (Agilent 34972A). Additionally, the experiment was recorded using a video camera.

The difference in the setup was the alkaline batteries had their anode (negative) point exposed to the butane burner for heating, while the Li-ion batteries had their cathode (positive) point exposed to heating by the butane burner, see Figure 3.1. The difference in the cell orientation was to witness how the cell reacts when exposed to high temperature butane flame. In both alkaline and Li-ion batteries, the safety vent is at the cathode. The butane torch burner serves as the heat source to generate intense heat within the cell, causing failure at high temperatures. As depicted in Figure 3.1, the butane burner is positioned at the front of the cell, situated 3 cm away from the cell's top, aiming either the cathode terminal for Li-ion or the anode terminal for alkaline batteries.

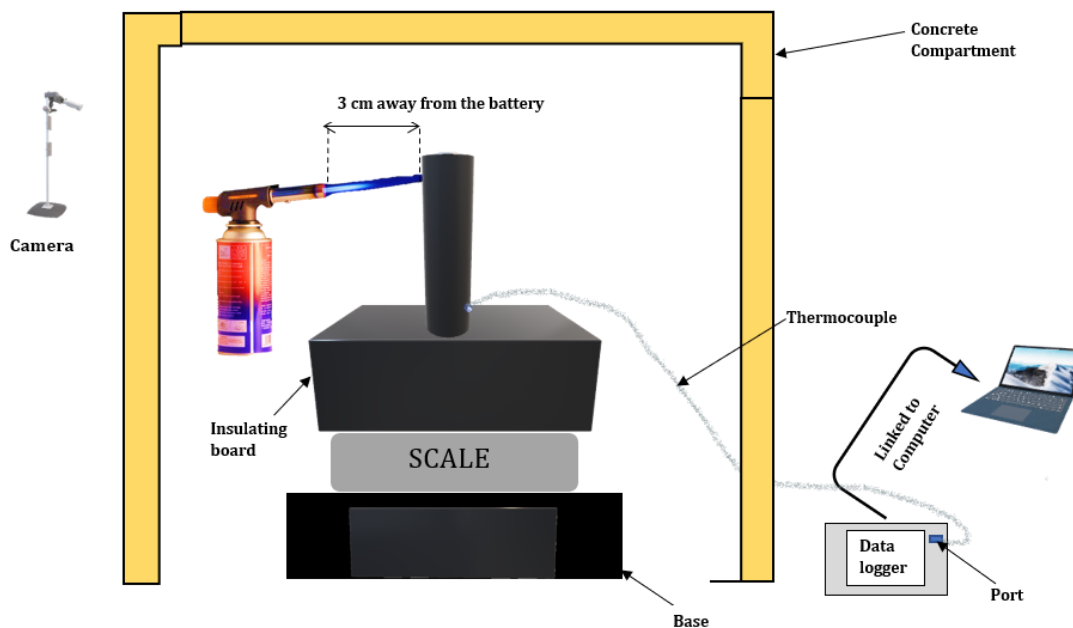


Figure 3.2 Schematic of the set-up of single cells experiment.

3.3.2 3 x 3 Cell Configuration

The alkaline and Li-ion experiments using 3 x 3 configurations have similarities in the setup, as previously stated. The direction of the cell is the same as in the single cell setup as seen in Figure 3.3. With alkaline cells having their anodes facing upwards and Li-ion cells with cathodes facing upward. The following describes the set-up and spacing for all 3 x 3 configurations. It is assumed that each cell has a 100% state of charge (SOC), and the voltage of the cells is approximately 3.7 V each.

The 3 x 3 configuration (module) is set up with different spacings: 1 cm, 0.5 cm and 0 cm intercell spacing. This is done to observe how spacing could affect heat or fire propagation.

The alkaline and Li-ion 3 x 3 cm configuration, 0 cm spacing set up (scenario 3 and scenario 4)

In the alkaline and Li-ion 3 x 3 configuration, a total of 9 cells were used for the experiment. Each cell had a K-type thermocouple secured using aluminium tape and the cell was placed next to each other with no separation and held firmly in place with a wire of 0.5 mm thickness. The alkaline cells are inserted into an insulating board with a drilled 4 cm by 4 cm opening to fit the bonded cells together as seen in Figure 3.3a and the Li-ion cells same is done in an 8 cm by 8 cm opening to fit the bonded cells as seen in Figure 3.3c.

The electronic scale was leveled using a spirit level, connected to a power source, and linked to the computer. The concrete slab is positioned on the scale and reset to raise the cell to the level of the butane burner. Then, the insulating board with the cell is placed on the concrete slab.



Figure 3.3 (a) shows the location of each thermocouple for both Alkaline and Li-ion cells and the direction of the Butane burner (b) shows the set-up of Alkaline 3x3 configuration, 0 cm spacing cells (c) shows the set-up of 3 x 3 configuration, 0 cm spacing cells.

The thermocouple is connected to a channel (1-9) linked to the data logger (Agilent 34972A), which in turn is connected to the computer. The software is initiated, and thermocouples are tested to ensure proper communication.

The Li-ion 3 x 3 configuration, 0.5 cm spacing setup (scenario 5)

This setup was only carried out for 18650 Li-ion cells, all the setup is the same as in section 3.3.2, except for the nine holes on the insulating board, which were spaced 0.5 cm apart. See Figure 3.3.



Figure 3.3 Li-ion 0.5 cm spacing apart with hole diameter in an insulating board.

The li-ion 3x3 configuration, 1 cm spacing set up. (Scenario 6)

The Li-ion 3x3 configuration, 1 cm spacing has a similar setup with 0.5cm except for the spacing of the 9 holes in the insulating board (size of the board) are spaced 1 cm apart from each other as seen in Figure 3.4. The rest of the set-up remains the same as carried out with a 3x3 configuration of 0.5 cm.



Figure 3.4 The photo shows one of the experiments with 3 x 3 configuration and 1 cm spacing.

3.3.3 Location of ignition source

For the 3x3 configurations, the ignition source was placed close to the top of cell 1 (see Figure 3.a), to ensure that most of the heat focused on the cell. The nozzle of the burner which is 3 cm away from the cell prevents the flame from directly affecting the thermocouple at the back of the anode terminal. See Figure 3.3a.

3.3.4 Test compartment

The test compartment was built using a concrete block, to help reduce heat loss from the cell and air entrainment since the experiment is done outdoors at low ambient temperatures ranging from -3 °C to 8 °C throughout the experiment period. The dimensions of the compartment are 1.2 m x 0.8 m x 0.75 m (h x w x l). The compartment's roof is covered with a fire-retardant material made of calcium silicate, ensuring it is non-combustible to mitigate fire spread. Additionally, a slab is positioned on the wooden base to prevent air from entering the compartment from beneath.

3.4 Procedures

The procedures are divided into two: single-cell and 3 x 3 configurations.

3.4.1 Single cell procedure

For single-cell experiments, both Alkaline and Li-ion cells (Scenario 1 and 2). The setup is completed as shown in Figure 3.2:

- The thermocouple was initially checked with a thermometric instrument (Fluke) to ensure good working conditions.
- The datalogger (Agilent 34972A) and the camera are started simultaneously.
- After 60 s of heating the alkaline cell and 120 s of the Li-ion cell the ignition source was removed and turned off.
- Allow the battery to cool after concluding the experiment, waiting until the thermocouple indicates a temperature below 50 °C.
- Power off the camera and datalogger nearly simultaneously.
- Remove the battery, measure its final mass, and disconnect thermocouples from the cell.
- Weigh the cell without the attached thermocouple to determine the mass loss of each cell.

3.4.2 3 x 3 Configuration (0 cm, 0.5 cm, and 1 cm) procedure

After the setup is completed, as described in section 3.2.2, the procedures for the 3 x 3 are as follows:

- The thermocouple was initially checked with a thermometric instrument (Fluke) to ensure good working conditions.
- The initial mass of the cell with attached thermocouple and insulating board was taken together (except for the 3x3 alkaline no spacing).
- The datalogger (Agilent 34972A) and the camera are started simultaneously.
- Heat cell 1 for 60 s for alkaline and 120 s for Li-ion battery and remove ignition source.
- After the experiment is completed, wait until the battery cools off when the thermocouple shows a temperature less than 50 °C.
- Stop the camera and data logger almost simultaneously.
- The final mass of the batteries was taken with the thermocouple and insulating board on it from the data logger reading.
- Finally, weigh each cell without a thermocouple attached, to get the mass loss of each cell.

3.5 Safety considerations before the experiment

Due to the presence of toxic and harmful gases when burning batteries [6], it is essential to consider implementing safety measures. Safety is a top priority, which influenced the choice to conduct the test

outside the 'Hall of Flame'. The climate in western Norway during the winter period is typically cold and windy. The required Personal protective equipment (PPE) will be worn which are;

- Coverall
- Safety goggle
- Safety gloves
- Surface Breathing Respirator
- Safety boot

A distance of 15-20 meters was maintained from the test location throughout the experiment. After the experiment was concluded, approximately 15-25 minutes were allotted to ensure the atmosphere was free from any toxic gases and smoke before approaching the test site. In the event of uncontrolled fire beyond expectation, the 6 kg CO₂ fire extinguisher is available, hence, the Fire hydrant system at RESQ is considered an extra measure.

4 Results

This section presents the results of the experiments obtained in each scenario from Chapter 3. Four main scenarios were considered in the experiment, and a total number of 13 experiments were carried out as seen in Table 4.1.

Table 4.1 Summary of all experiments conducted. Indicating experiment with TR reaction with an explosion resulted in a low peak temperature and high mass loss of the cell and TR reaction without explosion resulted in a high temperature and low mass loss.

S/N	Experiments	TR Reaction ¹ with	TR reactions without	Peak Temperature	Cell(s) with TR	Mass Loss of heated Cell(s) or cell(s) with TR	Propagation case
Scenario 1	Alkaline single cell						
1-1	Alkaline single cell (experiment 1)	No	No		None	1.6 g	
1-2	Alkaline single cell (experiment 2)	No	No		None	3.7 g	
1-3	Alkaline single cell (experiment 3)	No	No		None	1.5 g	
Scenario 2	Li-ion single cell						
2-4	Li-ion single cell (experiment 1)	No	No		None	4.1 g	
2-5	Li-ion single cell (experiment 2)	Yes	-	263 °C	Only cell	25.7 g	
2-6	Li-ion single cell (experiment 3)	Yes ²	-	446 °C	Only cell	29.7 g	
Scenario 3	AA 3X3 configuration, 0 cm spacing						
3-7	AA 3X3 configuration, 0 cm spacing (only experiment) ³	No	No		None	1.8 g	
Scenario 4	Li-ion 3X3 configuration, 0 cm spacing						
4-8	Li-ion 3X3 configuration, 0 cm spacing (experiment 1)	-	Yes	472 °C	1 2	10.2 g 8.5 g	TR on cell 2

¹ Additional reactions such as jet flame, excessive gas emission, or diffusion flame with gas emission, may occur with or without an explosion. More details are seen in section 4.3.

² This experiment resulted in high temperatures with an explosion involved during TR.

³ The 3 X 3 configuration, 0 cm represents 'No spacing configuration' carried out both in Alkaline and Li-ion batteries.

				527 °C			
4-9	Li-ion 3X3 configuration, 0 cm spacing (experiment 2)	-	Yes	445 °C	1	N/A	
Scenario 5	Li-ion 3X3 configuration, 0.5 cm spacing						
5-10	Li-ion 3X3 configuration, 0.5 cm spacing (experiment 1)	-	Yes	525 °C	1	10.3 g	
5-11	Li-ion 3X3 configuration, 0.5 cm spacing (experiment 2)	-	Yes	463 °C	1	9.4 g	
Scenario 6	Li-ion 3X3 configuration, 1 cm spacing						
6-12	Li-ion 3X3 configuration, 1 cm spacing (experiment 1)	Yes	-	278 °C	1	25.8 g	
6-13	Li-ion 3X3 configuration, 1 cm spacing (experiment 2)	Yes	-	260 °C	1	31.9 g	

N/A – The information for the cells was unavailable as the batteries had already been discarded.

4.1 Single cell

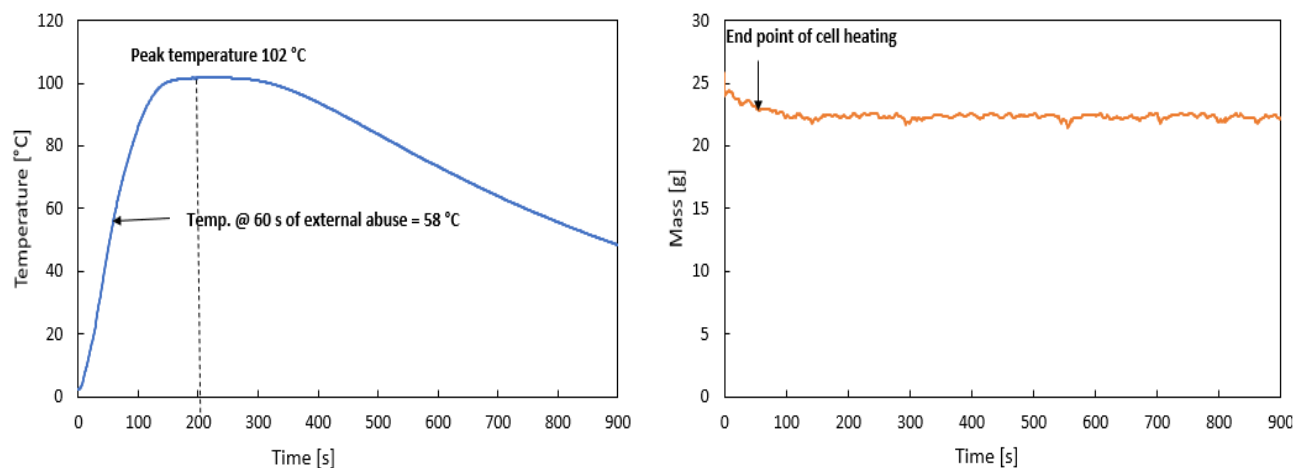


Figure 4.1 shows a typical graphical representation of an alkaline single cell experiment (a) shows the temperature variation with time (b) mass vs time.

When heating single cells, the alkaline batteries in scenario 1 were heated for 60 seconds, while the Li-ion batteries in scenario 2 were heated for 120 s, (see Table 4.1)

There were notable variations in the performance of distinct battery types, and there were differences within each specific type of battery. These distinctions are detailed in the following section.

4.1.1 Alkaline single cell

Following the procedure described in Section 3, the alkaline single cell in experiment 1, (see Table 4.1), was subjected to heating from the anode terminal using a butane burner, at an initial cell surface temperature of 2 °C. After 10 seconds of heating, a small amount of liquid emerged from the cell. There was hardly smoke production during the first 60 seconds of heating. However, after this period, we noticed visible signs of gas being released from the cell.

The temperature reached 58 °C after 60 s of heating, with no signs of combustion observed during this time. This lack of combustion may be attributed to the non-flammable nature of materials in alkaline batteries, unlike in Li-ion batteries. Subsequently, the temperature continued to rise, reaching a peak of 102 °C at 242 s. It remained stable for approximately 120 s before the cooling phase commenced. At the cooling phase, the temperature gradually decreased from 100 °C at 242 s to 49 °C at 900 s, with an average decline rate of 0.1 °C/s. No other interesting reactions were observed, and the cooling process continued until the end of the experiment.

The mass loss observed from the start to the end of the heating period is 1 g. From the end of the heating period to the peak phase at 242 s, the mass loss was 0.3 g. From the cooling phase up to 900 s, an additional 0.3 g mass loss was experienced. In total 1.6 g mass loss was recorded.

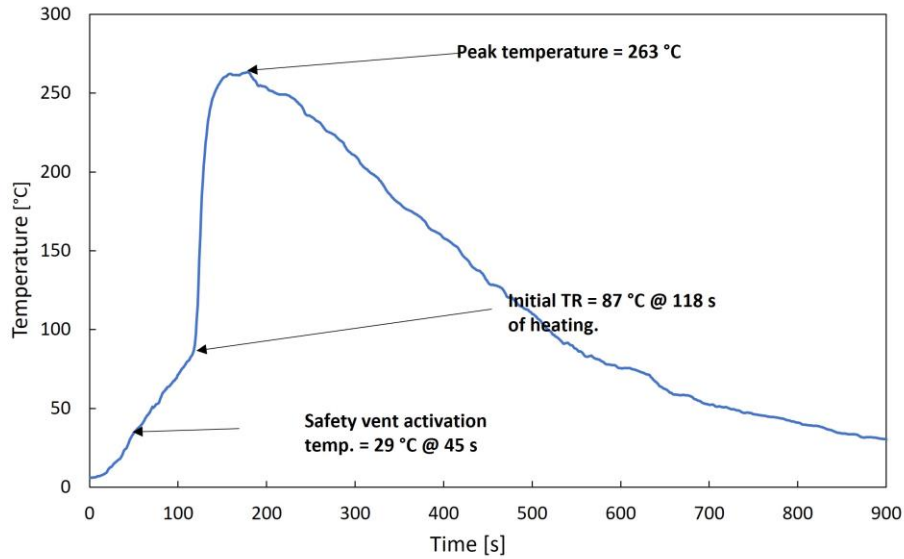
The cell mass moved irregularly due to environmental effects (wind and temperature) on the scale which may affected the data logger reading. Similar trends were observed for the remaining two alkaline single cell experiments in Table 4.1, scenario 1. There was no significant reaction from the cells during the experiments⁴.

4.1.2 Li-ion single cell with thermal runaway

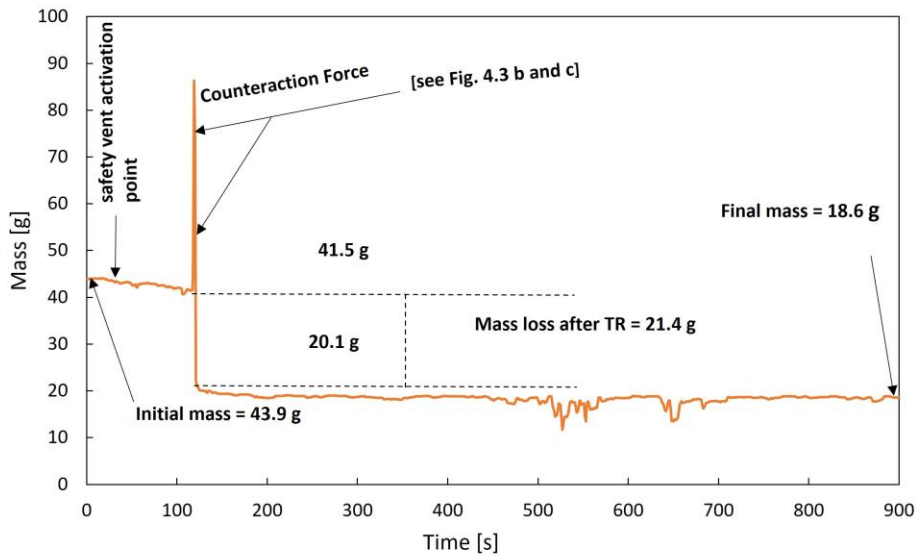
Scenario 2, experiment (2-5) in Table 4.1, conducted for the Li-ion single cell, indicated an exothermic reaction. Figure 4.2a and b show the temperature and mass as a function of time for a typical Li-ion battery that had experienced an uncontrolled reaction or thermal runaway. Similar figures in temperature and mass are seen in the literature reported by Ouyang et al, [32], Chen et al, [7], Zhao et al., [44] and Fredrick Larsson et al [6, 40], Zhong et al. [37].

⁴ Other experiments can be seen in detail in the Appendix section.

The initial surface temperature of the cell was 6 °C, at 45 s of heating, the safety vent activated at 29 °C and released combustible gases that ignited with an initial flash of flame which consumed the released gases while the heating process continued.



a



b

Figure 4.2 shows a typical graphical representation of the mass and temperature of a Li-ion single cell experiment (a) shows the temperature variation with time and (b) mass vs time.

The temperature reached 87 °C at 118 s, which was close to the end of the heating, when TR was initiated with an immediate spark accompanied by an explosion⁵ within a second and some gases were further

⁵ The observation called explosion is due to the violent reaction in the battery (cell) but on a small scale. The observed phenomenon is not a deflagration or detonation kind of explosion.

ejected (see Figure 4.3). The safety vent and TR activation temperatures seem very low. However, this is due to the placement of the thermocouple and slow heat transfer from the heated part of the battery to where the temperature was measured as shown in section 3. Installing an additional thermocouple close to the top or middle could have affected the temperature reading significantly, as the butane flame could engulf the thermocouple which could result in an excess temperature reading.

The side of the cell case walls was still intact, except the cell nylon wrap was burnt off due to the reaction and pressure immediately after the explosion exposing the polymer binders at the surface almost 4 cm long see Figure 4.3d.

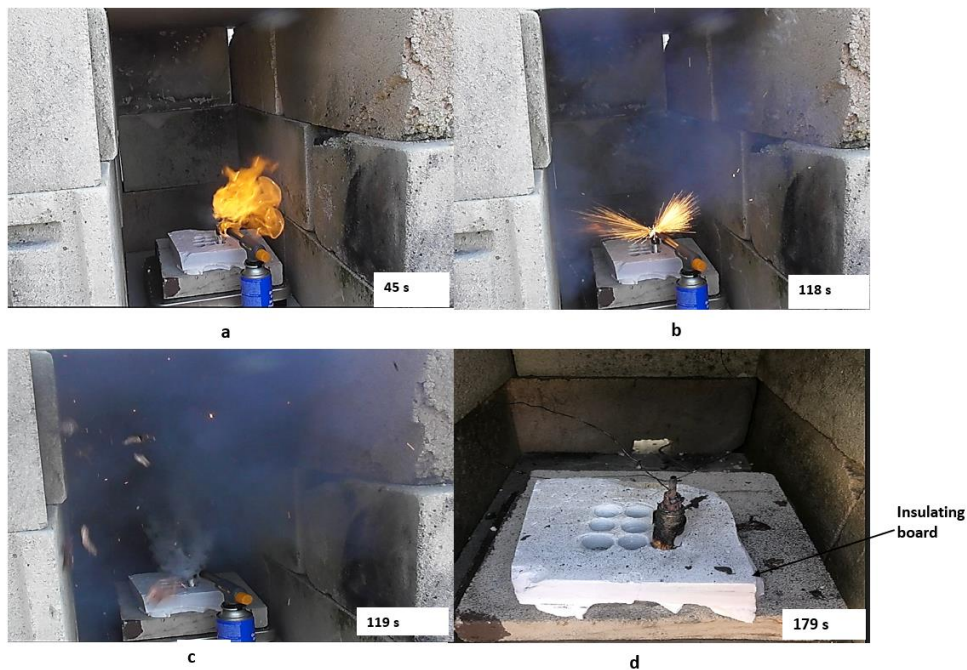


Figure 4.3 The heating process of Li-ion single cell (experiment 2). (a) the safety vent valve activation (b) Activation of TR with rapid sparks (c) explosion with flying debris and slight gas emission afterward (d) Aftermath of TR, protrusion of the inner foil-like material from the cell.

This reaction resulted in an abrupt increase in temperature until the peak temperature of 263 °C was reached at 160 s, see Figure 4.2a.

The cooling phase began immediately after the TR reaction, with a decline rate in temperature of 0.4 °C/s until it approached 75 °C and further declined slowly in temperature at a rate of 0.1 °C/s, till the end of the experiment. At 900 s, the temperature was approximately 31 °C with no more interesting observation but just continuous cooling.

The initiation of the thermal runaway led to violent reactions within the cell, resulting in a sudden increase (up to 85 g) followed by an immediate decline (counter-action) in the mass data, see Figure 4.2b. A similar effect on mass was observed in Chen et al.'s [7], research where the mass increased by up to 80 g. The TR led to a more stable trend in mass during the cooling phase. There was a mass loss of 2.4 g from the start of heating to TR activation at 118 s, followed by a mass loss of 21.4 g at the end of the TR reaction. Additionally, between 160 s and 900 s, further mass loss of 1.5 g was observed, nearing the end of the experiment, resulting in a total mass loss of 25.3 g recorded from the data. After disconnecting the thermocouple, the cell was weighed, resulting in a mass loss of 25.7 g (49.0 g – 23.3 g) and the cell voltage⁶ was affected, reading 0 V.

4.1.3 Li-ion single-cell experiment with no thermal runaway reaction.

The Li-ion single cell experiment (2-4) in Table 4.1, did not undergo TR during the heating process indicating good thermal stability. The initial cell surface temperature was 3 °C before the heating. The safety vent of the cell is activated at a temperature of 33 °C (51 s), with more increased flame because of emitted gases. The photos of the heating process are seen in Figure 4.4.

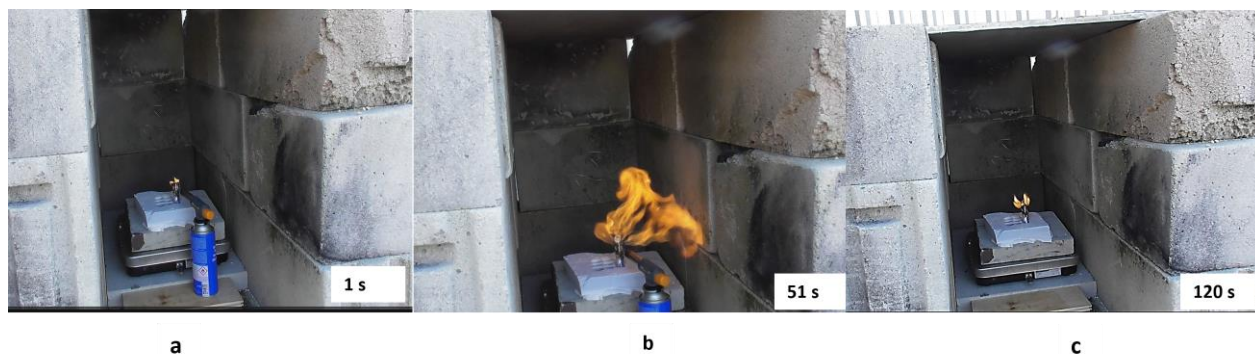


Figure 4.4 The heating process of Li-ion single cell (experiment 1). (a) beginning of cell heating (b) the safety vent valve activation with a flash of flame (c) end of cell heating with a small flame seen on the cell and no further reaction (TR) occurred.

At the end of the heating period, the temperature recorded was 90 °C, see Figure 4.5a. The temperature continued to rise and reached a peak of 139 °C at 259 s, yet no thermal runaway was observed before the cooling phase began. At the cooling phase, the temperature declined at a rate of approximately 0.1 °C/s and approached 72 °C at 900 s. The battery without TR (see Figure 4.5a) cools more slowly than the battery that has experienced TR i.e., uncontrolled self-heating reaction (see Figure 4.2a). This happens likely because when a battery undergoes TR, it generates a substantial amount of heat and releases gases at

⁶ All voltages of each cell heated had drained voltage of 0 V, including other affected cells that undergo either safety venting or TR reaction. Except for Scenario 5(5-11) in Table 4.1, cell 2 safety vent was activated, and the voltage was still intact.

high temperatures due to chemical reactions occurring within the battery. This accelerates the cooling process, as the heat dissipates, and the gases eject rapidly. While cell without TR relies more on the natural cooling mechanism.

From the start point to the end of heating (including safety valve activation) the mass loss observed was 2.4 g. From the end of heating to the peak temperature the mass loss was 1.5 g and from the peak phase to the end of the cooling phase the mass loss of 1 g was observed. A total loss of 4.9 g was recorded by the data logger. After disconnecting the thermocouple, the cell was weighed, resulting in a mass loss of 4.1 g. The post voltage of the cell was 0 V, which means the cell is completely discharged or dead with no electrical energy.

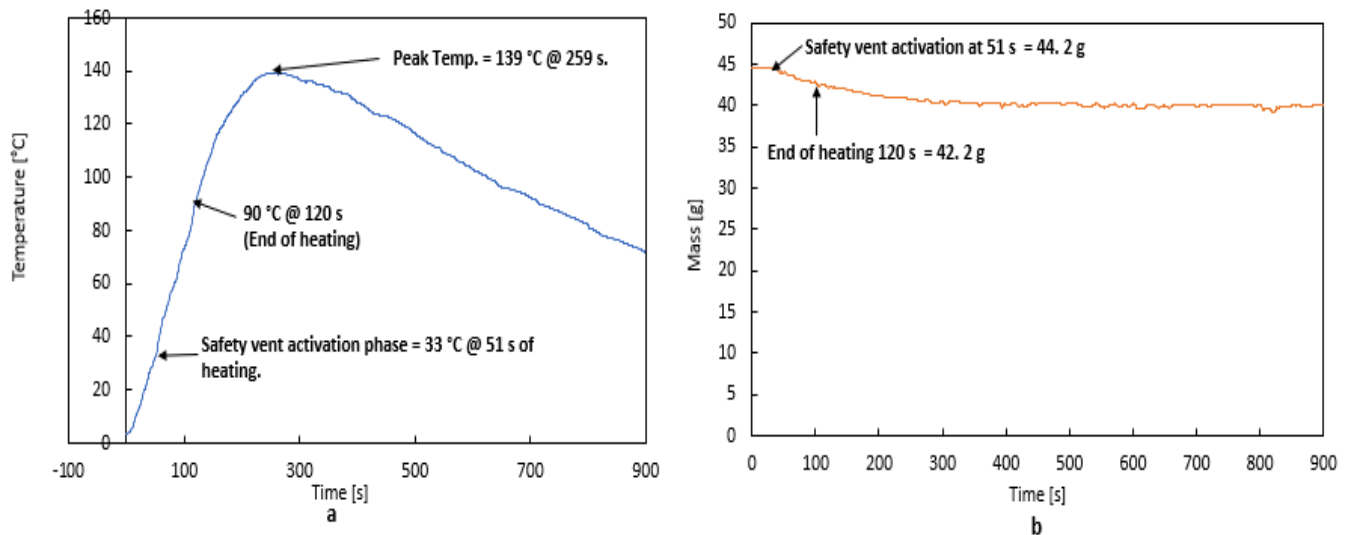


Figure 4.5 Li-ion single cell (experiment 1). (a) Temperature variation with time (b) mass vs time.

4.2 3X3 cell configuration

In this section, four distinct scenarios were examined i.e. 3 to 6 in Table 4.1. To explore both flame and heat propagation behaviours among cells in a 3 x 3 configuration. These experiments involve different spacing: 0 cm for both alkaline and Li-ion batteries, 0.5 cm, and 1 cm only for Li-ion batteries. The heating time for the alkaline batteries was still 60 s and for the Li-ion batteries 120 s. The schematic representation of alkaline and Li-ion 3x3 configuration, 0 cm is seen in Figure 4.6.

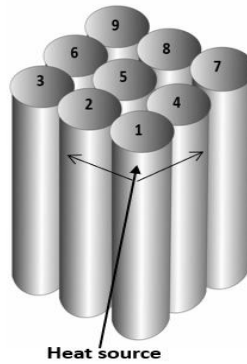


Figure 4.6 Schematic representation of both alkaline and Li-ion 3X3 configurations, 0 cm spacing and location of each cell having the same corresponding thermocouple attached to it, applicable to all 3X3 configuration scenarios.

4.2.1 3 X 3 alkaline configuration, no spacing

For the 3 x 3 alkaline, 0 cm spacing in scenario 3 in Table 4.1, the initial cell surface temperature was approximately 6 °C at 0 s before the heating on cell 1. No combustive reaction occurred in the cell throughout the heating period and the temperature of the cell was 56 °C after 60 s. Little smoke ejection was seen from cell 1 after the heating and the temperature increased steadily to a peak of 81 °C at 162 s. whereas the rest of the cells in the configuration had temperatures below 55 °C.

At the cooling phase seen in Figure 4.7, the temperature rate was observed to decline gradually after the peak temperature of cell 1 at a rate of 0.05 °C/s approximately, and the figure is shown up to 900 s (39 °C) because afterwards nothing interesting was seen happening just continuous cooling cell.

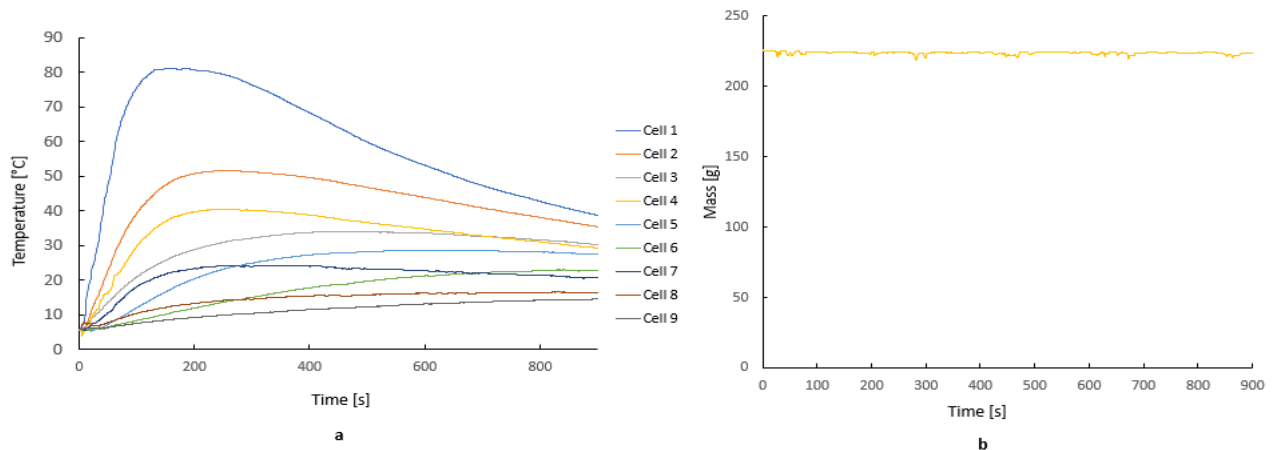


Figure 4.7 Alkaline 3x3 configuration, 0 cm (no spacing). (a) temperature as a function of time (b) mass as a function of time.

Cells 2 and 4 which were in contact with cell 1, were partially affected by the butane flame. Their temperature got to 27 °C and 20 °C at the end of the heating period, which increased and attained a peak

temperature of 52 °C and 40 °C respectively. This increase was due to the time taken for the temperature to be uniform in the cell through the conductive mode of heat transfer from cell 1.

Cells 3 and 5 temperatures also increased which was more associated with the conductive mode of heat transfer from cells 2 and 4 after the heating period. Additionally, the flame radiation from the butane burner initially raised their temperatures to 14 °C and 8 °C at 60 seconds. Eventually, cells 3 and 5 reached peak temperatures of 34 °C and 29 °C, respectively.

The temperature profile of cells 2 and 4 are similar with cell 2 attaining a higher temperature. The rate of decline in temperature for cells 2 and 4 was approximately 0.02 °C/s at 900 s starting from the peak time (271 s) and 0.05 °C/s for cell 1. Cell 6 gradually increased after the heating period from neighbouring cells which sustained the temperature to the end of the 900 s. Cell 9 attained the lowest temperature in the experiment due to the distance and abused cell.

The mass data in Figure 4.7b exhibits a consistent horizontal pattern. This is attributed to the absence of combustion or exothermic reactions during the heating process. The observed fluctuations could potentially be influenced by environmental conditions affecting the scale and the cell.

4.2.2 3X3 Li-ion configuration, 0 cm (no spacing)

The 3 x 3 Li-ion configuration, 0 cm experiment 4-8 in Table 4.1, the timeline and image of the heating process for this experiment can be seen in Figure 4.8. The initial surface temperature of cell 1 was -1 °C before heating. Cells 2 and 4 were partly affected by the heating process due to the direct contact with cell 1. At 37 s, the pressure relief mechanism (safety vent) activated on cell 1 at a temperature of 54 °C, and the ignited gases and flammable materials increased flame and radiation (see Figure 4.8b) to the point of TR.

At 71 s, TR for cell 1 occurred at a temperature of 88 °C which was initiated with sparks and flares (see Figure 4.8c) and accompanied by a diffusion flame (see Figure 4.8d). The flame from cell 1 affected cells 2 and 4 in addition to the direct contact with the cells increased their temperature significantly (see Figure 4.9a). Cell 2 and 4 safety vents triggered at a temperature of 62 °C (83 s) and 57 °C (94 s) respectively sustaining the flame on cell 1 until TR.

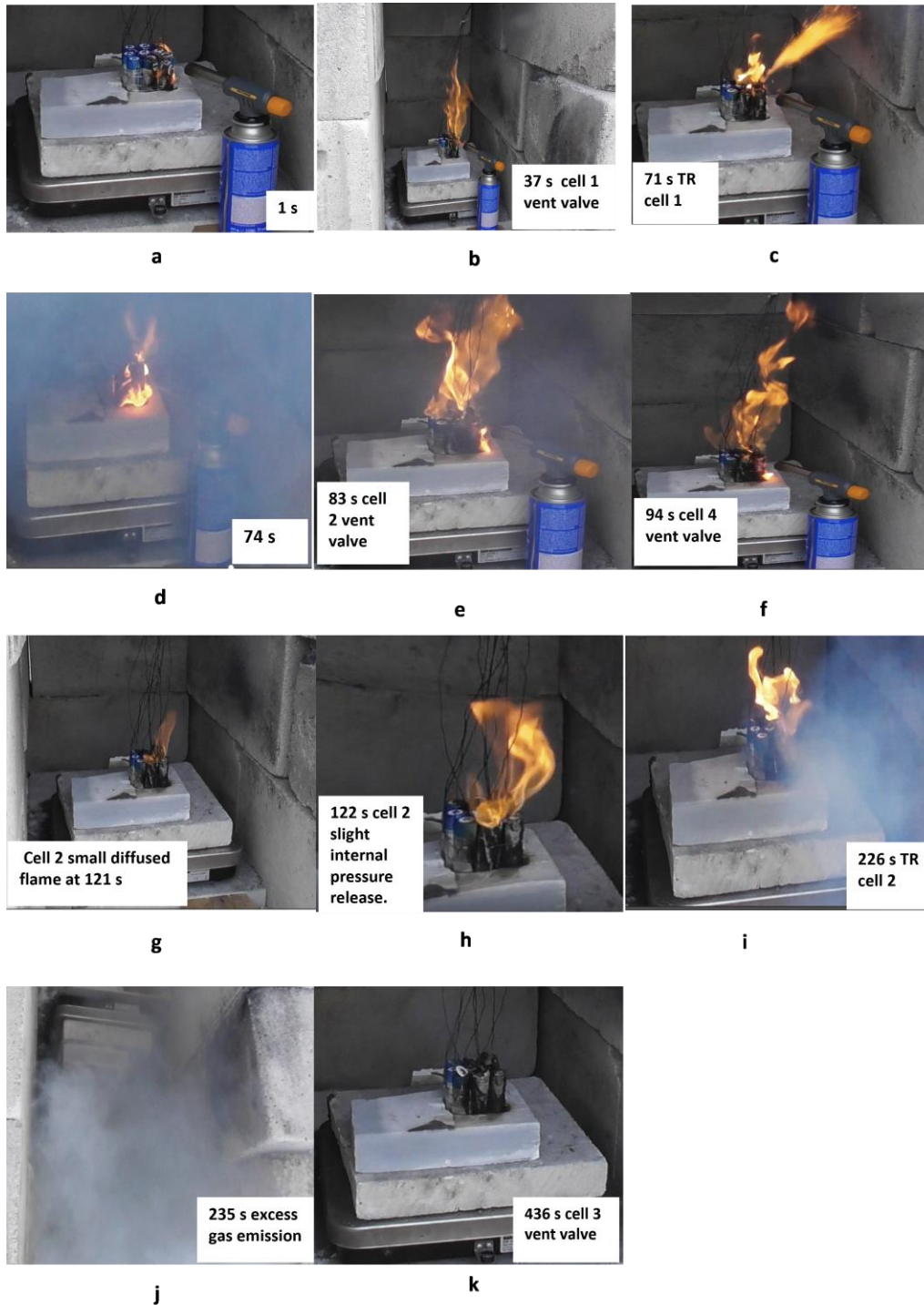


Figure 4.8 The heating process of Li-ion 3x3 configuration with no spacing (experiment 1). (a) beginning of igniting cell 1 (b) pressure build-up in cell activates safety vent valve in cell 1 with increased flame due to vented gas (c) initiation point of TR on cell 1 with sparks (d) TR ejected gas and fire engulfed cell 1 and partly on cell 2 and 4 (e) cell 2 safety vent valve activated during the TR process on cell 1 and increased flame (f) cell 4 safety vent valve activates during the heating process and emitted gases sustained flame (g) butane burner removed at 120 s and small diffused flame spotted on cell 2 (h) Cell 2 slight internal pressure release increased flame (i) flame and heat propagation on cell 2 through conduction, and radiation triggered Thermal runaway on cell 2 with flare and spark (j) excessive whitish gas/smoke ejection from cell 2, extinguished flame (k) heat propagation activated cell 3 safety vent valve.

Cell 1 TR attained a peak temperature of 472 °C at 103 s before it started declining. At 120 s the butane burner was removed, and shortly after 122 s, cell 2 released slight internal pressure with ignited gases within 2 s as seen in Figure 4.8h. This had a slight effect on the temperature of cell 1 from 438 - 440 °C which can be observed in cell 1 temperature (see Figure 4.9a) close to the start of the cooling phase after attaining a peak temperature of 472 °C. The mass data displayed a counteraction observed when TR was displayed, see Figure 4.9b.

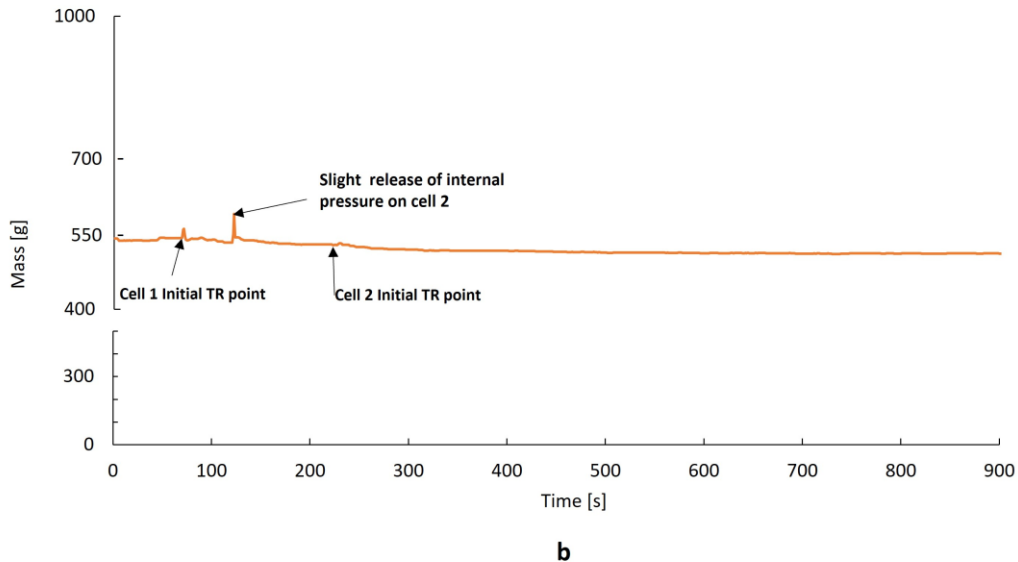
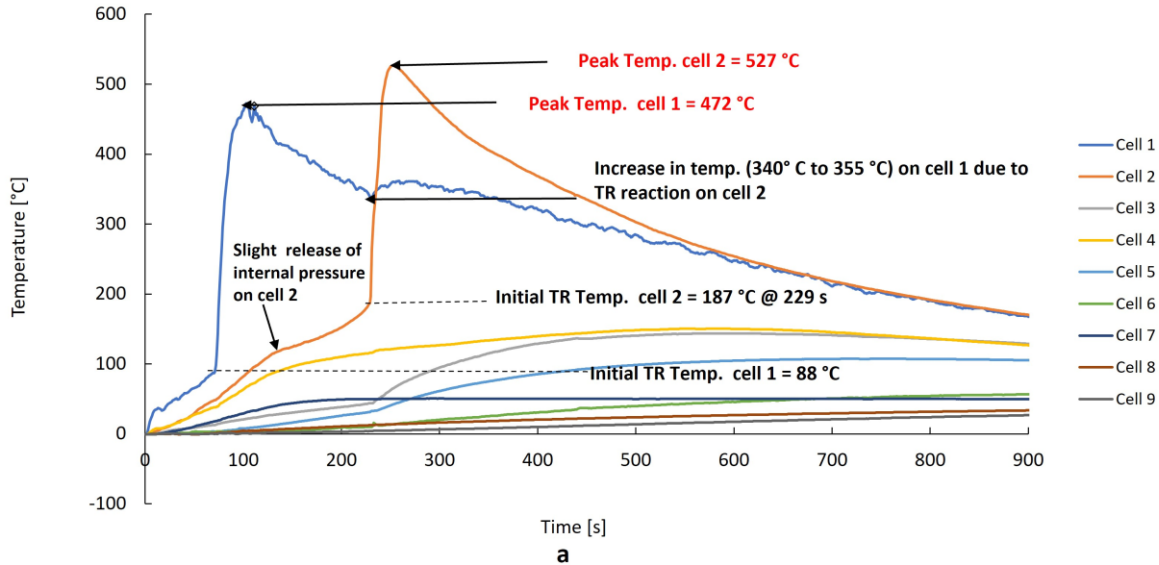


Figure 4.9 Results of Li-ion 3x3 cell configuration with no spacing (experiment 1). (a) Temperature variation with time (b) mass vs time for Li-ion cell.

Cell 2 was still in contact with cell 1 and with a low diffused flame resting on cell 2, which is sustained by the slight gas ejection with the flammable materials in the cell. This flame lasted for 104 s. At 229 s, cell 2 TR triggered at a temperature of 187 °C as seen in Figure 4.9a). The TR reaction released excessive gas with no combustion which put off the flame (see Figure 4.8i). Cell 2 reached a higher peak temperature of 527 °C than cell 1 from all the experiments conducted in this study despite no further combustion was seen. Figure 4.6 indicates the location of cell 2, to have direct contact with cells 1, 3, and 5. This TR reaction on cell 2 had a significant effect on the temperature of cells (1, 3, and 5) via the conduction mode of heat transfer since there was no combustion during or after the TR reaction. At 235 s on cell 1, the temperature increased from 335 °C to 360 °C, see Figure 4.9a, which prolonged the cooling phase.

On cell 3 at 238 s, the temperature significantly increased from 50 °C to 144 °C. Finally, on cell 5 at 235 s, the temperature increased from 33 °C to 107 °C. The heat released during this reaction was slightly felt by cells 6, 8 and 9 as observed a few seconds from the point of TR initiation on cell 2.

Table 4.2 Summary of Li-ion 3x3 configuration, 0 cm spacing, experiment 1.

Cells	Initial Voltage (V)	Final voltage (V)	Initial Mass (g)	Final Mass (g)	Safety vent activation time/temp. (s) / (°C)	Initial TR activation time/temp. (s) / (°C)	Peak cell surface temp. (°C)	Peak cell surface time. (s)
1	3.702	0.00	49.0	38.8	37/54	67/ 84.7	472	103
2	3.696	0.00	49.1	40.6	83/54	286/181	527	253
3	3.684	0.00	49.2	46.5	436/136	-	144	572
4	3.690	0.00	49.1	45.5	94/ 57	-	151	585
5	3.693	3.685	49.3	49.3	-	-	107	24.1
6	3.686	3.687	49.5	49.5	-	-	59	1139
7	3.677	3.77	49.3	49.3	-	-	51	301
8	3.685	3.684	49.1	49.1	-	-	37	1347
9	3.669	3.669	49.4	49.4	-	-	35	1581

Significant mass loss was observed on cells 1 and 2 (see Figure 4.9b). The initiation of TR in cell 1 indicated a sudden increase (at 71 s) with an immediate reversal (decrease) in mass followed by a gradual decline with a total mass loss of 10.2 g. At approximately 120 s, another sudden increase is recorded by the mass

data at 120 s, which cannot be reckoned with any form of visible reaction except that the slab and thermocouple on the scale were shaken when removing the ignition source.

At 229 s as seen in Figure 4.9, TR on cell 2 registered a small increase with an immediate and gradual decrease in mass with a gradual decline which is indicated in Figure 4.9b. Finally, the mass remained constant in almost a linear (horizontal) pattern.

The total mass loss from each cell i.e. 1, 2, 3 and 4 from Table 4.2 resulted in 34.2 g and from the data logger reading. The total mass of approximately 32 g was obtained, with a difference of 2.2 g (34.2- 32). The total mass loss in cell 2 is 8.5 g in Table 4.1. Cells 3 and 4 had temperatures of 144 °C and 151 °C which is close to the maximum TR activation temperature (181 °C) attained from these experiments conducted and for all scenarios. The experiment displayed propagation on cell 2 of which there was a high possibility for more propagation to occur on cells 3 and 4 due to their current temperature which can be prone to TR activation if more radiation or heat occurred. Other cell temperature and mass information can be seen in Table 4.2.

4.2.3 Li-ion 3x3 configuration, 0.5 cm spacing.

Experiment 5-10 from Table 4.1, the schematic representation of the cells is seen in Figure 4.10. The initial cell surface temperature was 1 °C before the heating process. Part of the flame affected adjacent cells 2 and 4. The butane flame also scorched the top of Cell 5. The spacing effect among cells also made room for convective heat which had more influence on cell 5.

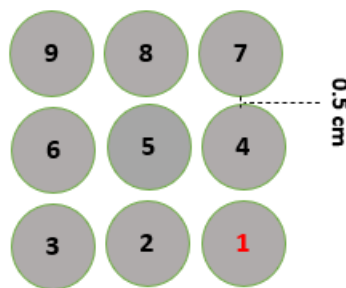


Figure 4.10 Schematic representation of cells on Li-ion 3x3 configuration, 0.5 cm spacing.

The temperature got to 25 °C at 41 s when the safety vent⁷ of cell 1 activated. The ignited gases released increased flame radiation and temperature of cell 1 at a range of 2.5 - 3 °C in each time step.

⁷ Most of the safety vent temperatures are low due to the location of the thermocouple on the cell and the time for heat to transfer from the heated point to where the thermocouple is located as described in Chapter 3.

The ignited gases and flammable cell material sustained the flame to the point of uncontrolled reaction with a high rise in temperature (TR), which was initiated at 102 °C (96 s). This TR resulted in sparks accompanied by gas emission and diffused flame (with no explosion) see

Figure 4.11c, d, f and g.

The diffused flame on cell 1 radiated towards cells around especially cells 2 and 4 and reached a peak temperature of 525 °C (108 s) as shown in Figure 4.12. The peak temperature of cell 2 was 75 °C with no safety vent. The temperature, mass and voltage information of all the cells can be seen in Table 4.3.

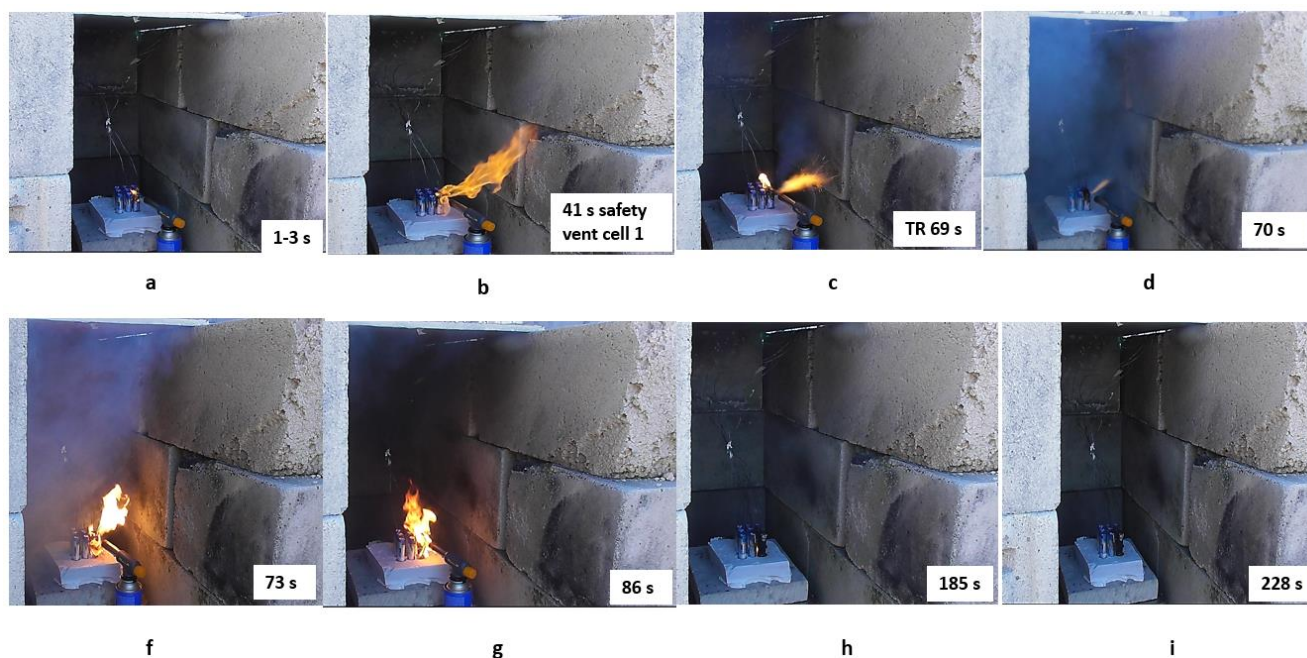
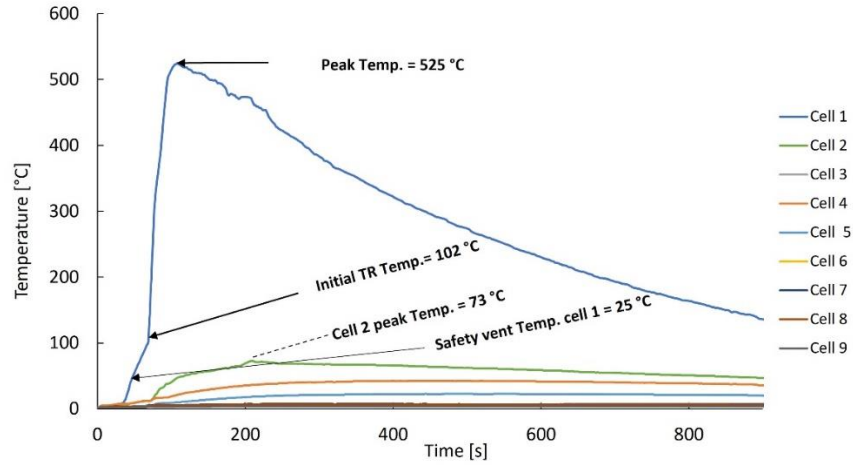


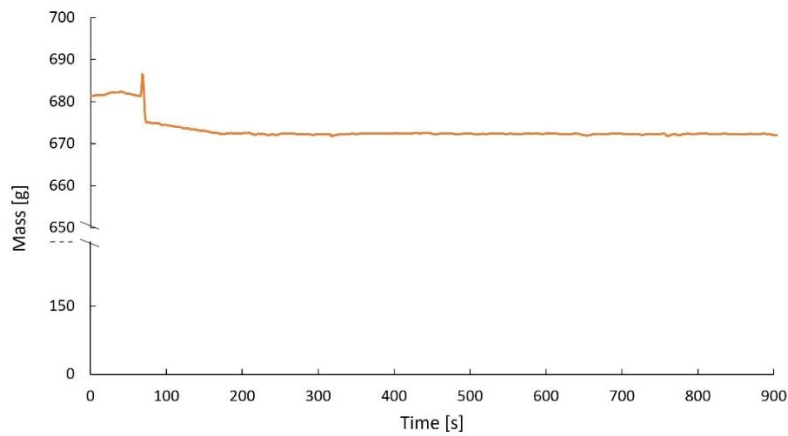
Figure 4.11 The heating process of li-ion cell 3x3 configuration, 0.5 cm spacing (experiment 1). (a) initiation of butane torch burner to cell 1(b) safety vent valve cell 1 activates with wind effect on ignited gas (c) initiation of TR on cell 1 (d) visible smoke emission during TR (e) safety vent activates (f) safety vent activates with increased flame (h) butane torch burner removed at 120 s and flame decays drastically with little flame spotted on cell 1 (i) current situation of cells after the experimental abuse with cell 1 fully burnt.

The mass data recorded a total mass loss of 9.2 g for the experiment, in which the rest of the cells were intact as seen in Table 4.3 and only the heated cell was reweighed the mass loss was 10.3 g.

Cell 1 temperature in this experiment has shown almost the same kind of temperature development as in Figure 4.2 and Figure 4.8a. Cells 3,6,7,8 and 9 in this experiment had a very low temperature increase ranging from 3-8 °C. See Table 4.3.



a



b

Figure 4.12 Li-ion 3x3 configuration, 0.5 cm spacing (experiment 1). (a) Temperature variation with time (b) mass loss with time

Experiment 5-11 in Table 4.1, Li-ion 3x3 configuration, 0.5 cm spacing, similar cells (3,6,7,8, and 9) experienced low temperatures ranging from 4 – 20 °C. This experiment experienced more safety vent activation on cells 2 and 4 at a temperature of 65 °C and 25 °C (Figure 4.13) after TR activation which had a more intense diffused flame (see appendix section). This event also contributed to the increased radiation and temperature in the cells. Cell 1 TR activated at 100 °C (53 s) and reached 463 °C before the thermocouple disconnection.

Table 4.3 Summary of Li-ion 3x3 configuration, 0.5 cm spacing, experiment 1.

Cells	Initial Voltage (v)	Final voltage (v)	Initial Mass (g)	Final Mass (g)	Safety vent activation time/temp. (s) / (°C)	Initial TR activation time/temp. (s) / (°C)	Peak cell Surface temp. °C	Peak cell Surface time. (s)
1	3.701	0.00	49.0	38.7	41/ 25	69/ 102	525	108
2	3.708	3.70	49.0	49.0	-	-	73	209
3	3.70	3.70	49.0	49.0	-	-	8	1122
4	3.699	3.706	49.0	49.0	-	-	43	470
5	3.701	3.699	49.1	49.1	-	-	23	480
6	3.692	3.689	49.3	49.3	-	-	6	832
7	3.702	3.70	49.2	49.2	-	-	7	251
8	3.68	3.68	49.0	49.0	-	-	7	398
9	3.70	3.70	49.0	49.0	-	-	3	167

Therefore, the peak temperature was not achieved by the data logger reading including the mass data. Cell 1 gave a mass loss of 9.4 g and the summary of other cells, and their masses, voltage, and temperatures are recorded in Table 4.4

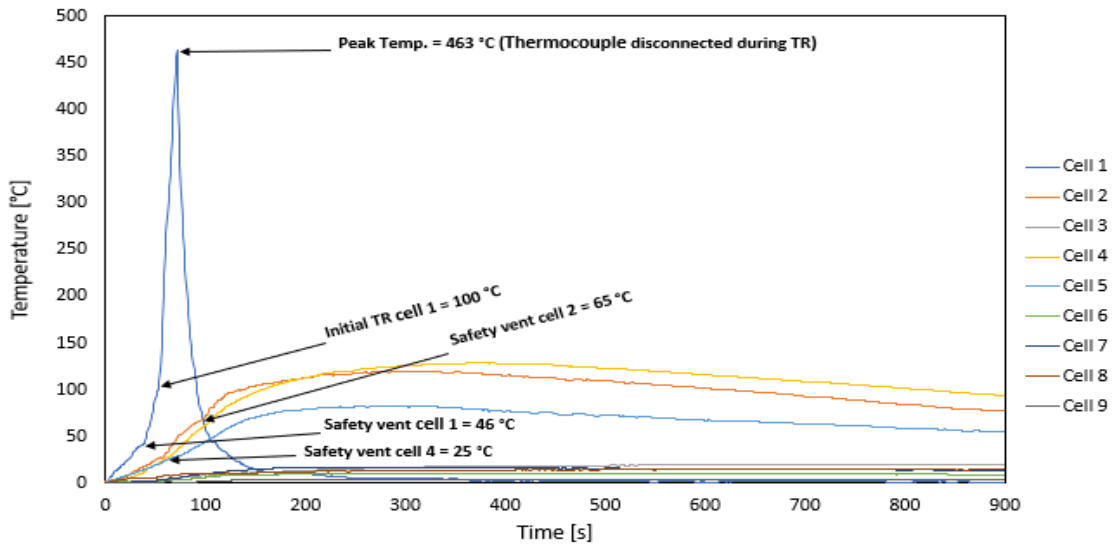


Figure 4.13 Li-ion 3x3 configuration 0.5cm spacing (experiment 2). Temperature variation with time, indicating the points of occurrence of events.

Table 4.4 Summary of Li-ion 3x3 configuration 0.5 cm spacing, experiment 2.

Cells	Initial Voltage (v)	Final voltage (v)	Initial Mass (g)	Final Mass (g)	Safety vent activation time/temp. (s) / (°C)	Initial TR activation time/temp. (s) / (°C)	Peak cell surface Temperature (°C)	Peak cell surface time. (s)
1	3.693	0.00	49.3	39.9	35/ 39.3	53/ 100	464	72
2	3.705	3.698	49.1	46.2	92/65	-	120	327
3	3.621	3.621	49.4	49.4	-	-	20	828
4	3.696	0.00	49.0	49.0	59/25	-	129	376
5	3.696	3.696	49.5	49.5	-	-	58	59
6	3.697	3.695	49.2	49.2	-	-	10	326
7	3.70	3.70	49.2	49.3	-	-	17	324
8	3.684	3.684	49.4	49.5	-	-	14	417
9	3.697	3.797	49.4	49.4	-	-	4	318.1

4.2.4 Li-ion 3x3 configuration, 1 cm spacing.

Experiment 6-12 in Table 4.1, Li-ion 3x3 configuration, 1cm spacing, was conducted and Figure 4.14 indicates the position of each cell.

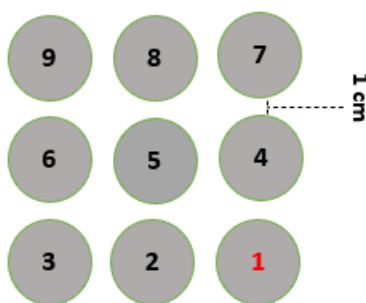


Figure 4.14 Location of cell and thermocouple.

The initial cell surface temperature was 1 °C and during the heating process, the flame surrounded cell 1 from the side of the walls and top which radiated toward cell 5 due to the spacing and wind effect (Figure 4.15a). This affected the temperature of cell 5 significantly.

At 39 °C (41 s) safety vent was activated on cell 1. When the temperature reached 93 °C (98 s), TR initiated with sparks/flares, and emitted gases were accompanied by a jet flame as seen in Figure 4.15c, d and e.

Cell 1 peak temperature reached 278 °C at 146 s (see Figure 4.16) and the TR elevated the temperature of cells 2,4 and 5. Cell 2 observed a slight increase from 25 - 40 °C before the temperature declined.

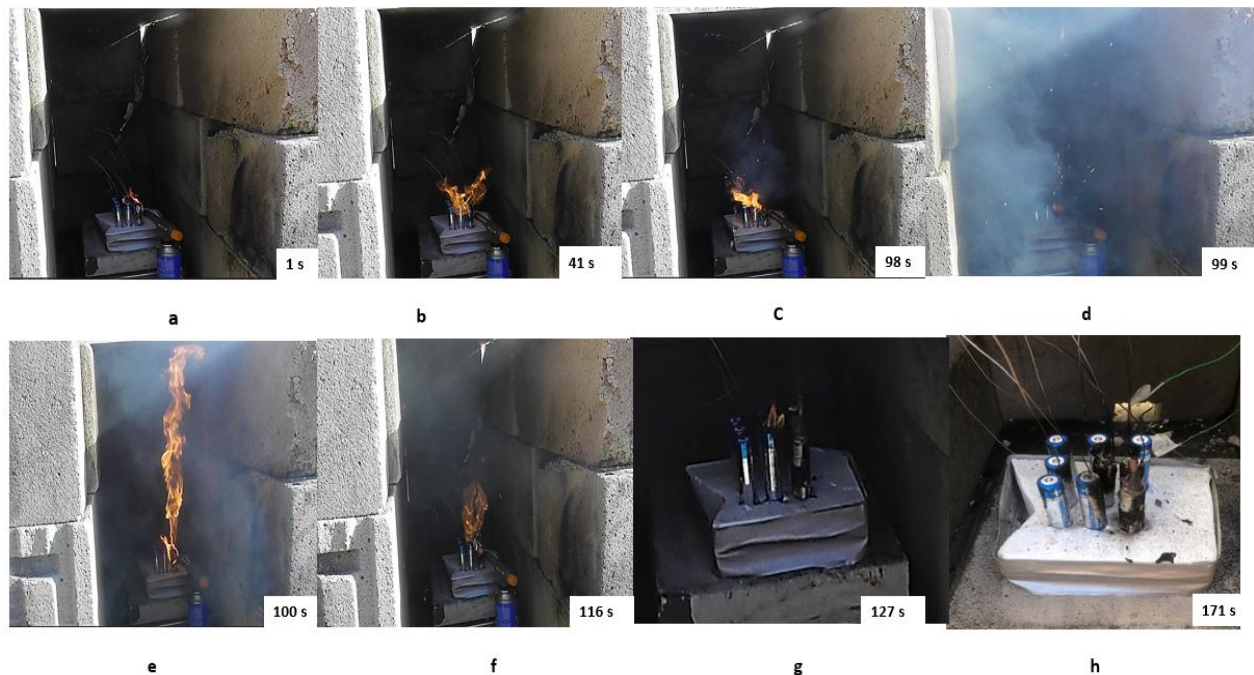


Figure 4.15 shows a timeline of several events in Li-ion 3x3 cell configuration 1cm spacing, experiment 1 (a) An initial burning process on cell 1 and cell 5 partly affected by the flame and radiation (b) cell 1 safety vent activation with gas ignition on cell 1 (c) initiation of TR with sparks/flare on cell 1 (d) rapid gas ejection with little sparks on cell 1 (e) jet fire ejection from cell 1 touching the roof of the compartment (f) cell 5 safety vent activation with ignition (g) reduction of the flame on cell 5 after removing heat source (h) cooling of the cells.

Cell 1 mass loss displayed a sharp decline as anticipated due to TR, (see Figure 4.16b). Only the TR reaction on cell 1 resulted in a mass loss above 20 g and the total mass loss on cell 1 was 25.8 g indicating a downward trend in Figure 4.16b. No other cell encountered a safety vent or TR activation.

However, the temperature development of cells 3,6,7,8, and 9 was very low ranging from 10-18 °C (see Figure 4.16a) as a result of the ambient temperature and spacing effect. Similarly, in experiments 6-13, Li-ion 3 x 3 configuration with 1 cm spacing the temperature of cells 3,6,7,8 and 9 ranged from 7-12 °C.

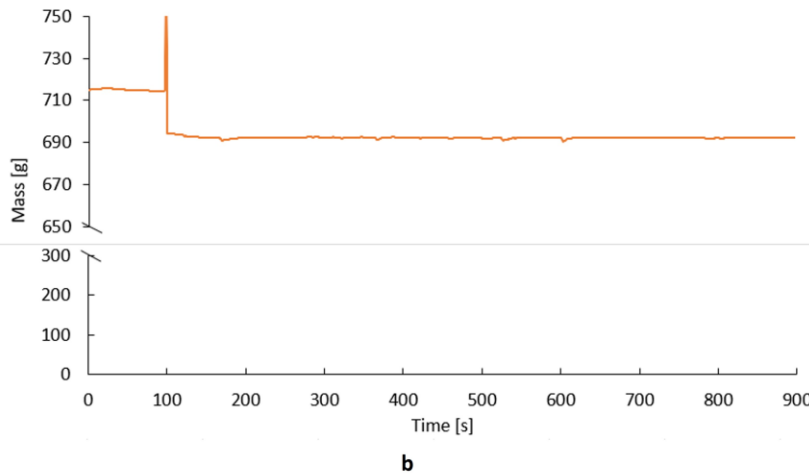
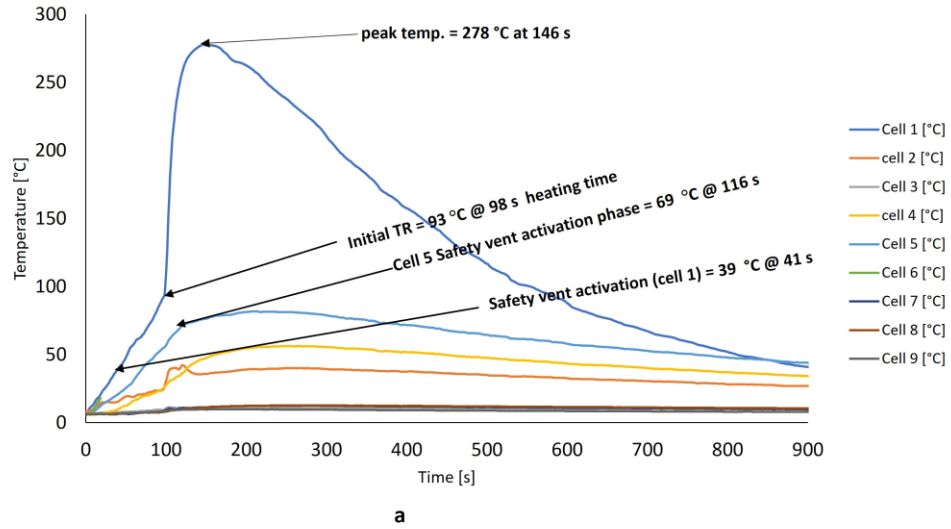


Figure 4.16 Li-ion 3x3 cell configuration 1cm spacing, experiment 1 (a) temperature variation with time (b) mass loss vs time.

Cell 2 in scenario 6 (6-13) was more affected by the flame spread with a peak temperature of 71 °C, however, no safety vent was activated at this temperature. More information on all cell temperature mass and voltages can be seen in Table 4.5.

Table 4.5 Summary of Li-ion 3x3 configuration 1 cm spacing, experiment 1

Cells	Initial Voltage (v)	Final voltage (v)	Initial Mass (g)	Final Mass (g)	Safety vent activation time/temp. (s) / (°C)	Initial TR activation time/temp. (s) / (°C)	Peak cell surface temp. °C	Peak cell surface time. (s)
1	3.68	0.00	49.0	23.2	41/ 40	98/ 93	278	146
2	3.70	3.70	49.3	49.3	-	-	40	259
3	3.70	3.70	49.3	49.3	-	-	11	104
4	3.696	0.00	49.3	49.3	-	-	56	248
5	3.70	0.00	49.2	48.5	116 / 59	-	82	213
6	3.692	3.692	49.3	49.3	-	-	18	232
7	3.651	3.651	49.3	49.3	-	-	13	235
8	3.678	3.68	49.1	49.1	-	-	13	261
9	3.70	3.70	49.0	49.0	-	-	10	170

4.2 Thermal runaway behaviours

TR is the major hazard of Li-ion batteries [30], resulting in propagation escalating the hazard of Li-ion battery modules/packs [53]. From the experiments in this study, TR reaction is easily identified when it starts in a cell but from the observation in this work, they have displayed to behave in five (5) several ways listed below.

From these five identified reactions in this study, some can pose a high risk to propagation which will be discussed in section 5. The images below identified these different five behaviours experienced in this study during TR.

1. Explosion without further combustion (see Figure 4.17). From Experiment 2-5, the cell displayed this reaction during thermal runaway, more information on the experiment is seen in section 4.1.2



Figure 4.17 (a) Activation of TR with rapid sparks (b) explosion with flying debris and slight gas emission afterward. Also seen in Figure 4.3 b and c.

2. Excessive gas emission without combustion or explosion (see Figure 4.18). From experiment 4-8, the cell displayed this reaction and can contain toxic substances in such a volume during TR, more information on the experiment is seen in section 4.2.1.



Figure 4.18 TR propagation on cell 2 initiates with flare and sparks (i) excessive whitish gas/smoke ejection from cell 2, extinguished flame. Also seen in Figure 4.8 i and j.

3. Explosion accompanied by jet flame (see Figure B.1 and Figure 4.15). High-speed jet flame was observed from the heated cell, releasing energy during TR. This occurred in two different experiments i.e. 2-6 and 6-12 in Table 4.1. More information about the experiments is seen in the appendix section and section 4.2.4



Figure 4.19 Li-ion single cell experiment 3. (a) Initiation of TR with flare/sparks with whitish gas emission (b) explosion accompanied by a flame jet touched the ceiling. See appendix.

4. Explosion accompanied with diffused flame and gas emission (see Figure 4.20). More details about the experiment 6-13 in Table 4.1 can be seen in the appendix section.



Figure 4.20 Li-ion 3x3 configuration 1cm spacing (experiment 2). (a) flare with sparks (b) explosion with flying debris accompanied by gas emission with radiation flame engulfed cell 1

5. Diffused flame with gas emission and no explosion (see Figure 4.21). more details of this reaction can be seen in the appendix section. Experiment 5-10 had similar reaction seen in section 4.2.3 and 5-11 which more details can be seen in the appendix.



Figure 4.21 Li-ion 3x3 configuration 0.5 cm spacing (experiment 2). (a) initiation of TR with flare /sparks (b) Diffused flame engulfed cell with gas/smoke ejected during TR without explosion

NB: The focus is on the last photos with reactions taking place in only Li-ion batteries.

4.3 Thermal runaway and temperature

Following the result obtained from the experiment conducted, TR is seen to have initiated from the range of 74 °C - 102 °C for heated cells, and 181 °C for cell 2 due to the propagation effect in experiment 4-8 in Table 4.1. However, some studies experienced TR above this range. As earlier stated, the point of the heating source and the rate of heat transfer from the top of the heated point of the cell to where the thermocouple is located at the back. This can be factored into the low temperature ranges experienced in this study. TR has shown to be uncontrolled when it gets to the initiating temperature from all the cells that experienced the reaction.

The peak temperature attained after TR has ranged from 260 - 527 °C seen in Table 4.1. Some literature from Ouyang et al [32], Larsson et al [6], Zhao et al. [44], Zhong et al [37] and Lopez et al [4]. have shown peak temperature results within this range and above 600 °C [44, 4]. SOC and cell material can influence the increased temperature.

The cooling phase starts immediately after much energy is released from the battery by all of the ways mentioned in section 4.3 and peak temperature is reached. The cell starts to cool by a decrease in temperature and since the experiment is not fully confined and there is air entrainment, the cooling process is faster.

Temperature plots for all TR reactions in cells affected in this study are represented in Figure 4.22. from the 5 ways mentioned in section 4.3, the reactions involving explosion (except for experiment 2-6) resulted in higher temperature ranges. Similarly, other TR reactions with no sign of explosions resulted in lower temperature ranges see Figure 4.22 and Table 4.1.

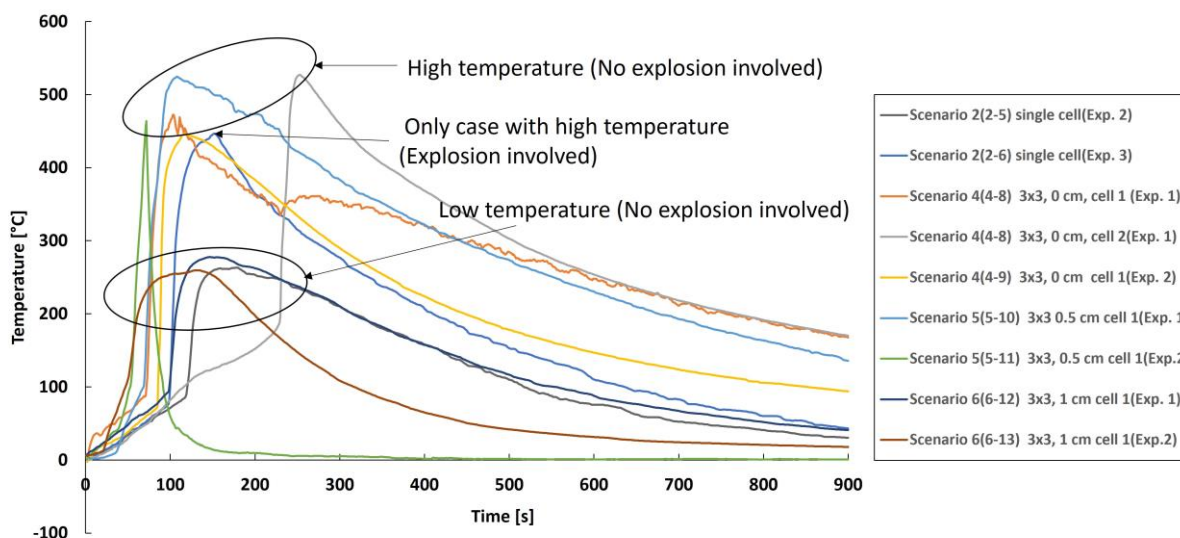


Figure 4.22 Temperature variation with time for all cells with TR in all experiments conducted.

4.4 Thermal runaway and mass loss

Low mass loss is experienced in the alkaline scenarios (single cell and 3 x 3 configuration with no spacing) because no significant uncontrolled self-heating reaction was experienced resulting in the ignition, TR and ejection of the material from the cell. Moreover, their material is not as flammable as the Li-ion batteries, including their low energy densities. The maximum mass loss obtained for all alkaline experiments is approximately 4 g (experiment 1-2). The mass loss variation with time for all alkaline experiments has shown more of a stable and horizontal trend with some fluctuations which can be because of environmental conditions on the scale due to their small mass. A similar mass loss result is also observed in a Li-ion experiment conducted in experiment 2-4 where no TR was observed. See section 4.1.3.

Figure 4.2b shows a typical graphical representation of individual cell behaviour with mass loss rate with a counter-action display when represented in a li-ion single-cell or 3 x 3 configuration. The total mass loss for each cell that went through the uncontrolled self-heating reaction from all conducted experiments has ranged from 8.5 – 31.9 g.

Figure 4.2b indicated an increase in mass from 43 - 86 g within 2 s, quickly followed by a reversal (decline) in mass in less than 1 s and further declined below its initial mass until it maintained a stable trend like a straight-line pattern. Similar counteraction occurred in Figure 4.12 and Figure 4.16. This can be described with Newton's 3rd law of motion (for every action there is an equal and opposite reaction). The rapid and forceful ejection of gases and materials out of the cell is an action, that resulted in the same reaction inside

the cell with some thermal shock since the cell is placed on the insulation board that was resting on the scale. The scale senses the reaction and records a sudden upward movement followed by a reversed decline in mass.

The weight reduction solely attributable to thermal runaway (TR) is about 21.4 grams. Similar experiments with comparable patterns have shown a similar mass loss related to TR for both the heated cell (Cell 1) and other cells engaged in the TR reaction. The Li-ion 3x3 configuration, Scenario (6-13) has the highest mass loss (31.9 g) with a final mass of 17.4 g.

Also, Li-ion single cell experiment 3, scenario (2-6) resulted in a total mass loss of 29.7 g. some part of the inner material was displaced by the explosion from the cell, this is attributed to the higher mass loss of the cell.

With the different observations on Li-ion with TR reaction as stated in section 4.3, further observation is noticed in their mass loss and peak temperature results. Most cells with TR reaction with explosion and/or additional reaction such as jet flame, excessive smoke, diffused flame, have resulted in low peak temperatures after TR (260 °C, 263 °C and 278 °C) except for experiment (2-6), where a high peak temperature reached of 446 °C was reached with higher mass loss, refer Figure 4.22 and see Table 4.1.

In addition, another observation from the experiment has shown that all cells with TR reactions not involving explosion reaction as stated in section 4.3 gave a high peak temperature ranging from (445 °C, 462 °C, 463 °C, 525 °C and 527 °C) with a low mass loss, typically in the range 8.5 – 10.2 g. see Table 4.1.

5. Discussion

For this study, experiments have been conducted, to determine flame propagation between unprotected batteries. Different scenarios were tested considering the spacing effect of the batteries to investigate the propagation effect on the module (involving two or more cells together). The result has shown how spacing can affect flame and heat propagation in cells (18650 cylindrical Li-ion). The term “18650” is known for the dimension of the cell i.e., 18 mm diameter and 65 mm length. Also, it was seen that various behaviours of cells during TR reactions have a high tendency to influence propagation and the peak temperature. This will be discussed in detail in the chapter.

5.1 Different effects of battery behaviours on fire and heat

Li-ion batteries and alkaline batteries are two different types of batteries with distinct chemistries and properties. Alkaline batteries are constructed with materials that are less prone to combustion and do not contain highly flammable components. The electrolyte inside an alkaline battery is typically water-based such as potassium hydroxide solution [16]. This affects the battery volatility or flammability unlike the flammable electrolytes seen in lithium-ion batteries, used in this experiment. The alkaline separators can be thicker and protected which improves their protection from short circuit or damage. They are designed to be more stable and less reactive coupled with their low energy densities, as was observed in this study in scenarios 1 and 3 (alkaline) for this experiment. After heating for 60 s using a butane burner, there was no combustion reaction observed, except for a slight release of gas, and no thermal runaway occurred. They are designed to be more stable and less reactive. For example, in Figure 4.1, the temperature profile increased steadily during the heating phase and at the cooling phase, it decreased slowly without any obvious reactions. Only the outer skin of the cell was affected visibly with soot in the experiment conducted in scenario 1.

On the other hand, Li-ion batteries are seen to contain flammable materials. The experiment from this study with an 18650 cylindrical Li-ion battery (see Fig 4.2a), has shown to react violently when exposed to fire and heat. One of the challenges of the Li-ion battery is the flammable electrolyte. The electrolyte reacts with active electrode materials to release a significant amount of heat and gases at elevated temperatures. Firstly, the cells experience increases in temperature resulting in some liquid or organic materials going to the vapor phase causing expansion and increased internal pressure in the cell. This

emerging situation results in safety venting at the top of the cell by opening the safety cap and creating a passage for the gases to be released. All the vented gases during the heating process ignited when exposed to flame and sufficient oxygen. All heated cells were able to display this safety feature to be functional and effective in this study. Finally, TR has always initiated with rapid ejection of sparks and flares with gas emissions and in some cases led to cell explosions releasing jet flame or diffused flame or excessive smoke resulting in peak temperatures that ranged from 260 – 527 °C before the cooling phase as seen from the results in section 4. Mass loss may vary in the cell depending on the TR reaction experienced in section 4.3 and voltage hereafter is drained or discharged in almost all cases.

In summary, the major stages experienced using a butane burner in this study are; cell venting and gas ignition, TR, and cooling. Chen et al. [7] experienced “*self-heating, rupture and ignition, violent ejection or explosion, peaceful combustion, flame reduction, and extinguishing*”. In their research, they provided detailed descriptions of these major stages, noting the presence of a high-speed jet flame accompanied by whitish smoke and sparks. Ouyang et al., [32] experienced similar reactions in 18650 Li-ion batteries such as heating, venting, gas release, ignition, combustion, and finally, abate and extinguishment. Yan et al., [2], and Larsson et al. [6] also experienced heating, venting, TR, and cooling. Most of the experiments experienced first (venting) and second combustion (TR).

The high energy density of the cell contributes to the escalation of rapid release of energy observed during TR. Li-ion battery has a thin separator that keeps the anode and cathode apart from contacting each other. However, this thin separator can make the battery more vulnerable to short circuits at high temperatures, which can result in thermal runaway. This is one of the challenges with Li-ion.

In Table 4.1, among nine Li-ion experiments conducted, one did not result in TR (only safety venting) after 120 seconds, see Figure 4.4. As a result of this, the cell displayed good thermal stability by not exhibiting any uncontrolled self-heating reaction (TR). Thus, the voltage was affected after the heating process. The temperature profile of the single cell Li-ion battery experiment without TR and the single cell alkaline experiment are similar when heated, see Figure 4.1 and Figure 4.5.

5.2 Effect of distance between cells on thermal runaway propagation

Fire and heat are critical concerns in battery modules, packs, and systems. In this study, the propagation effect has been observed on alkaline and li-ion batteries considering different spacing scenarios 0 cm, 0.5 cm, and 1 cm. Previous research has been carried out to investigate propagation using different means to cause failure in cells, such as heaters/ heating rod, oven (thermal abuse); external short-circuit (electrical);

nail penetration (mechanical abuse), etc. For this current study, the propagation effect was investigated using a butane burner as the heating source. This accelerates the process of heating the cell with radiative and convective forms of heat to cause short circuit and TR thereafter. The alkaline result did not combust from the heated process with no flame propagation see Figure 4.7. In addition, there is no prior research on flame propagation in alkaline cells. Alkaline materials have been seen to withstand heat without combusting, which makes them a source of ignition.

The result for the Li-ion 3 x 3, 0 cm spacing, is shown in Figure 4.8 and Figure 4.9. The flame and heat from the heated cell resulted in propagation in only cell 2, through different modes of heat transfer. The cell (2) only released excessive gas and smoke during TR that eventually put off the existing flame, see Figure 4.8j. The mode of heat transfer was significantly effective with conduction. If cell 2 experienced diffused flame as cell 1, this would have posed more risk to cells 3 and 4 by elevating the temperature more.

Even though the highest temperatures of cells 3, 4, and 5 were 144 °C, 151 °C, and 107 °C, respectively, this indicates that certain processes or reactions took place between the anode/electrolyte solvent [4]. After the experiment, a voltage of 0 V indicates that the cells were dead and had no electrical energy.

Similarly, Ouyang et al. [32], experimented with different configurations, 2 x 2, 3 x 3, 4 x 4 (0 cm spacing). The result obtained from the 3 x 3 configuration with 0 cm spacing from the same experiment, using a cylindrical heater from the same location (refer to Figure 5.1a). This has a similar setup as seen in Figure 5.1d of the current study except from their heating source. The experiment resulted in propagation throughout the battery pack. The result indicates that the location of failure can also delay propagation.

Similarly, Lopez et al. [4], conducted a 3 x 3 configuration experiment with 0.1 cm interspacing, and used flexible heating element to heat the center cell (refer to Figure 5.1b). From their result, no propagation was experienced in their experiment. However, four neighbouring cells reached temperatures in the range of approximately 100 to 125 °C with decreased voltages.

Chen et al. [30], experimented with 6 x 6 and 10 x 10 battery configurations with the cardboard separating the cells Figure 5.1 g (only the 10 x 10 is presented in the photo). The thickness of the cardboard for each cell separation cannot be found in this work but it is assumed to be in the range of ± 1 mm (± 0.1 cm) and the cells were induced with a 500 W heating rod from the centre of the packs. The result shows that thermal and fire propagation between multiple batteries can spread continuously after igniting, further stating that in the later stage of fire, 5 batteries ignited at the same time in a 6 x 6 configuration and 32

batteries can be burning together simultaneously in a 10 x 10 configuration, leading to a large heat release rate.

Lamb et al, [41] conducted an experiment that involved testing various circuit connections on both 18650 cylindrical Li-ion batteries and pouch batteries. They evaluated these batteries with no spacing (0 cm) to assess the thermal hazards and propagation within a module arranged in a triangular configuration. A mechanical nail penetration from the centre cell to investigate propagation (see Figure 5.1i). The result for the cylindrical cell indicated propagation to neighbouring cells. However, it is more prone to occur in pouch cells. Zhong et al. [37], some experiments conducted on a 3 x 3 configuration with 0 cm spacing and different SOC, using a cylindrical-shaped electric heater. The increased SOC led to increased propagation within the module. Generally, the 3 x 3 configuration with 0 cm spacing is seen to result in a major propagation, from previous research. In this current study, only one cell experienced flame propagation, with the likelihood that more cells may be affected.

The two conducted experiments on a 3 x 3 configuration with 0.5 cm spacing (see Figure 5.1e) from this current study, did not result in any propagation. However, in one of the experiments, the safety vent of two cells was activated. These cells, specifically cell 2 and cell 4, exhibited elevated temperatures of 120 °C and 129 °C, respectively (see Figure 4.13). It is conceivable that at this temperature, decomposition will be initiated in the anode and possibly in the cathode materials. This assumption is drawn from the literature by Lopez et al. [4] and RISE [33] and others. Notably, for the post-test voltage, cell 2 had a full voltage of 3.7 V which indicates the cell is still active, while cell 4 showed no electrical energy with a voltage of 0 V.

In contrast with one of the experiments conducted by Lopez et al. [4], with a 3 x 3 configuration with 0.4 cm interspacing, connected in parallel with a flexible connector for schematic set up, refer to Figure 5.1c. The cell at the center was heated while surrounded by four cells. The outcome indicated no propagation to the adjacent cells, although one adjacent cell reached a peak temperature of 100 °C. This is consistent with the findings obtained in the present study involving a 3 x 3 configuration with 0.5 cm spacing, where adjacent cells reached peak temperatures within a similar range. Possibly anode decomposition is initiated at this temperature according to literature by Lopez et al. [4] and RISE [33] and others.

In a similar experiment to Zhong et al. [37], they also conducted an experiment using a 3 x 3 configuration with 0.4 cm cell spacing with a heater of 200 W. The cell that was heated was positioned between three cells, see Figure 5.1j. This led to the propagation of three cells experiencing thermal runaway.

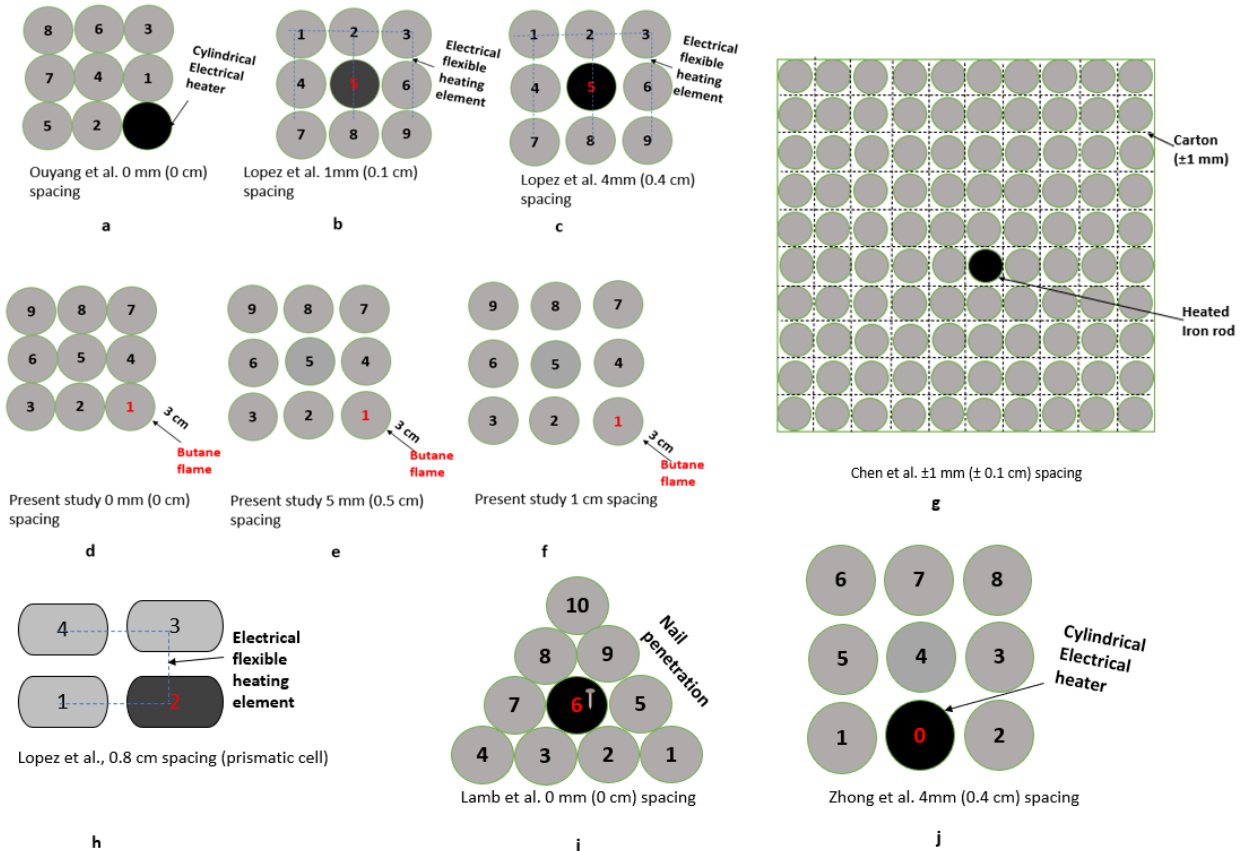


Figure 5.1 Schematic representation of some experiments from previous and present studies.

The results obtained by Ouyang et al. [32], and Chen et al. [30] in comparison to the 3x3 0 cm spacing of the current experiment, were influenced by the amount of cells in contact with their heat source(s) using a heater and heated rod. From Figure 5.1a and g, the heating sources made contact with two or more cells, possibly increasing their temperatures almost simultaneously in both experiments. This circumstance can potentially trigger TR in two cells simultaneously or cause a cell TR reaction to immediately trigger the other, as the temperature of the adjacent cell has already been raised near its thermal limit. Similarly, in Zhong et al. [37] experiment, the heating source (cylindrical shaped heater) was in contact with three cells simultaneously, raising their temperatures at the same time. Consequently, the first cell to initiate TR triggered another immediately and so on.

Ouyang et al. [32], Chen et al. [30] and Zhong et al. [37] heat sources were powered throughout the experiments, and it was not mentioned that their heat sources were turned off at a specific time. As this current study stopped heating after 120 s and Lopez et al. [4] turned off the heating sources when the heated cell got to TR. But for this current study, the butane torch burner was focused on a single cell, in which only one cell experienced propagation.

Furthermore, according to the study, the cardboard material contributed to the fire, increased the heat release rate (HRR), and facilitated easier ignition.

In addition, Ouyang et al. [32], Chen et al. [26], Lopez et al [4], Zhong et al [37] experiments were done in a calm environment with controlled wind and temperature. Chen et al. [26] used a laboratory from the calorimeter equipment to analyze several parameters and gas measurements. Also, Chen et al. [26], the initial surface temperature of the cell was around 20-25 °C. Ouyang et al. [28], the initial surface temperature ranged between 22 ± 5 °C. Zhong et al. [37], the initial cell surface temperature stated was 20 °C. Lamb et al. [41], the initial surface temperature of the cell during the experiment varied around 24 ± 1 °C, as indicated from their experimental graphs since the ambient temperature was not stated. These readings suggest a relatively warmer environmental temperature at the experiment's location, but this present study was done in a more extreme environmental condition i.e. cold, humid, and windy, during the winter which ranged between - 3 to 8 °C, at the location RESQ. This represents a worst-case scenario that could have influenced the outcome. However, flame propagation still occurred in a cell, which may have extended further to more cells if another combustion reaction involving any diffused flame or jet flame from section 4.3 had occurred in cell 2 during TR instead, the reaction with excessive gas release without combustion occurred in the 3 x 3 configuration with 0 cm spacing in this present study.

The heat loss as a result of natural airflow into the fire compartment and the ambient temperature in the environment impact how surrounding cells increase in temperature and the duration it takes for the cells to exceed their thermal stability limit and lead to TR. In an environment with less windy conditions and an ambient temperature of 20 °C or above, similar to Ouyang et al. [32] and Chen et al. [26] and Lopez et al. [4], heat loss from the cell will be reduced. This will possibly impact the outcomes of this experiment which can potentially cause flame propagation in multiple cells.

The results for the 3 x 3 configuration with 1 cm cell spacing in this study, had no propagation, see Figure 4.15. The highest cell temperature of the neighbouring cell (5) was 82 °C with the post-voltage reading 0 V indicating the battery was drained due to the existing reaction occurring inside.

A literature study specifically addressing propagation of 3 x 3 configuration with 1 cm spacing using 18650 cylindrical cells was not found. However, in the same study by Lopez et al. [4], an experiment was conducted using a 2 x 2 configuration with 0.8 cm cell spacing and an M-type connection (see Figure 5.1h). A prismatic cell with 50 % and 100 % SOC was used and correlated with the 3 x 3 configuration with 1 cm

spacing in this present study. Lopez et al. [4] result led to propagation in one cell for a 2 x 2 configuration with 0.8 cm spacing with 50 % SOC with the voltages of other cells drained. Moreover, in the same research conducted for the 2 x 2 configuration with 0.8 cm spacing at 100% SOC by Lopez et al. [4], no propagation occurred with the voltages of other batteries remaining fully intact.

This study revealed that when a Li-ion cell is heated using a butane burner in unfavorable environmental conditions i.e. windy and low temperatures, the safety vent gases released will ignite. This ignition can escalate into a thermal runaway, causing various reactions mentioned in section 4.3. This reaction poses a significant risk of propagation when cells are not spaced or protected. However, there's a decreased risk of propagation when cells are appropriately spaced, and additional safety measures are implemented.

5.3 Different behaviours during thermal runaway

Thermal runaway with propagation to other battery cells is the major hazard of Li-ion batteries [30] and TR resulting in propagation is the major hazard of Li-ion battery modules/packs. As described in section 4.3, different behaviours of thermal runaways have been observed during the current experiments. Some of these TR reactions are of higher risk and can impact propagation. All scenarios have been performed in this present study accordingly and there are several observations from the cell's behaviours during TR as stated in section 4.3.

An explosion with no further combustion occurred in one of the single cell experiments. The explosion had a substantial impact, evidenced by the flying debris that was observed exiting the compartment. Figure 4.3a. In a no spacing scenario, it can only result in a conductive heat transfer to cells in contact with it, but not attaining a very high temperature (more than 263 °C) may not pose a risk to any cell close to it. Hence, the gases released immediately after the explosion which can be flammable and toxic [6] as a result of electrolyte decomposition can be an issue in a more confined setting.

In a situation where the module is cased and confined as seen in some of the e-motocycles, with little air entrainment, the gases and heat released when the cell fails(TR) can pose a risk of ignition of the gases which can influence flame propagation in more cells.

In addition, when a cell experiences an explosion during TR, it causes more mass loss in the cell and exposes more internal materials of the cell which will fuel the combustion. If connected with a flexible connector (either in series or parallel), and one of the cells fails and experiences an explosion during TR, this can affect the cathode terminal electrical connection. In addition, it may further result in issues that may contribute to flame propagation.



Figure 5.2 Different behaviours experienced during TR, are presented from Figure 4.17b to Figure 4.21b.

Explosion with jet flame, this reaction was experienced in two experiments, single cell Figure 5.2b and 3 x 3 configuration with 1 cm spacing (scenario 6) for propagation in Figure 4.15. The jet flame is one of the behaviour often experienced in studies by Chen et al. [7], RISE [33] and Zhang et al. [54]. In the 3x3 configuration with 1 cm spacing where it was seen that the jet flame did not last more than 2 s before it decayed and became a normal diffused flame. Hence, this did not lead to propagation which is because of several factors such as the battery spacing, compartment opening resulting in heat loss and height of the compartment. Jet flame may influence propagation possibly if the compartment is lower and confined. The jet flame transfers heat through radiation and convection to the batteries around and to the ceiling and can spread in length to increase the temperatures of other cells.

Another risk involved in a jet flame is that it can cause the ignition of any flammable materials up to the roof of the compartment, (see Figure 5.2b) and further when the cells are exposed without cell casing. The roof of the compartment may be exposed to fire if is not insulated or fire retardant. The closer the roof compartment, the more risk of exposure to jet flame fire, from the experiment by Zhang et al, [54]. Substantial energy was released within 2 s of the jet flame (from Figure 5.2b and another in Figure 4.15e). Zhang et al, [54] indicated that the highest heat flux within a confined space is approximately four times

greater than that in an open space. Chen et al. [30] observed that high-speed ejection flame influences thermal and flame propagation.

Excessive gas and smoke emission without combustion or explosion, were observed during two experiments in the current study. Research has shown that 18650 li-ion cells can emit around 2.5 liters of gas in the event of a thermal runaway [50]. Similarly, RISE [33] stated *“When the thermal event was limited to a single battery cell, 3.6 liters of flammable gas were formed”*. These gases from previous research indicate more flammable chemical compositions. During the initiation of TR beginning with sparks, gas emission and smoke which extinguished the butane flame, there was no explosion observed during the TR reaction and neither the cell nor the butane torch burner ignited or underwent further combustion. This scenario has not been observed or discussed in previous studies. This reaction took place in the propagated cell i.e. cell 2. This event transferred additional heat through conduction, which raised the temperature of cell 3 to the point where the safety vent was activated after 200 s.

The gases released consist of organic electrolyte solvents (DMC, DEC, CE) and decomposition of products of the electrolyte and cathode around 155- 285 °C [4]. The gases ejected were not tested during this study but several studies have observed the presence of either of these flammable and toxic gases such as CO, H₂, CH₄, C₂H₄, HF, SO₂ and more [6] [34][42]. RISE [33], presented the quantity and composition of some of these gases in the event of a thermal runaway in a battery and stated that *“degassing contains many different gases: carbon dioxide, flammable components such as carbon monoxide, various hydrocarbons, methanol and hydrogen, as well as toxic components such as hydrogen fluoride, hydrogen chloride and hydrogen cyanide. The degassing also poses an explosion hazard due to the large proportion of flammable gases (such as approx. 30 % volume fraction hydrogen)”*.

The situation may have escalated more if the gases released ignited, this could result in more heat transfer which will eventually cause more propagation to cell(s). Larsson [6] observed that released gases with delayed ignition could result in a risk of gas explosion posing more consequences, in a confined or semi-confined environment. On the contrary, one of the results from this experiment (scenario 4-9, see appendix) extinguish the flame from the butane burner during TR resulting in a low mass loss in cell 1. See Table 4.2. A similar reaction occurred, (see Scenario 4-9, details in Appendix), the internal pressure released sparks and gases which extinguished the butane flame during TR initiation, and the butane gas burner could not ignite further.

Explosion accompanied by diffused flame, gas and smoke emission (Figure 5.2d) was experienced in one experiment, see scenario 4-12, see appendix). The explosion led to an immediate ignition of flammable

gas and materials in the cell at 108 °C (48 s). The explosion impact with flying debris is seen almost as the same as the one experienced in the reaction with only explosion (see Figure 5.2 a and d). The immediate ignition of the diffused flame with thick visible gas and smoke radiated to cells around it while decaying. In the experiment, the reaction did not result in propagation. However, this type of TR reaction can pose a high risk of propagation when the cells are closer or the ambient temperature of other cells is from 20 °C. Diffused flame with no explosion, was experienced in 3 of the current experiment scenarios (0 cm and 0.5 cm). This type of TR reaction resulted in a higher influence on propagation, and it occurred more in the current study.

In the case of the 3 x 3 configuration with 0.5 cm spacing from the present study, both experiments conducted in this setting encountered a comparable reaction without any propagation. This outcome could be influenced by the spacing effect and ambient temperature. However, it could pose a risk at higher ambient temperatures, potentially leading to an increase in the initial cell surface temperature. This reaction results in higher peak temperatures ranging from 463 – 525 °C and low mass loss ranging from 9.4- 10.3 g, as most of the internal materials from the cells are not ejected and exposed to ignition.

In 0 cm spacing, there was heat transfer through conduction, radiation, and convection during this TR reaction to cells in contact with the heated cell, see Fig 4.8(d-h). The photo shows how the flame from one cell engulfed some of the neighbouring cells for almost 12 seconds. This posed a high risk to surrounding cells which were affected by the diffused flame from the heated cell. The gases ejected from two adjacent cells during venting sustained the flame. This type of TR reaction influenced propagation in one cell despite the environmental condition which tends to impede propagation. This shows how TR with diffused flame or fire represents hazards for the battery modules and battery pack.

5.4 Safety concerns, prevention, and control.

Li-ion batteries are known to be flammable, which poses a high risk depending on the quantity of cells within the module or pack and their location. Cell spacing helps to reduce the risk of flame propagation in batteries, but this precaution might not be entirely effective. Certain reactions occurring during TR can still lead to flames or fires despite cell spacing measures. It is possible for individuals or companies not certified by UL to construct their batteries and devices like e-scooters, e-bikes etc [55], with the intent of reducing production costs. However, in doing so, they might overlook essential safety measures and fail to adhere to regulatory guidelines, by UL. Neglecting these safety measures and standards increases the risk of safety hazards, including fire, explosion, or other safety-related incidents associated with the use of batteries.

Following established safety protocols and regulatory guidelines, such as those provided by UL standards, is crucial to ensure the safe design, assembly, and usage of battery modules in electronic devices. In some cases, cells are clustered closely together rather than being adequately spaced. This practice can compromise safety measures intended to prevent fires or thermal incidents in battery assemblies. Some laptops, e-bikes, e-scooters [36], and EVs utilize 18650 cylindrical cells, comprising the battery module or pack. In many cases, these cells lack proper spacing inside, posing a significant risk in the event of a cell failure.

Most of these electric motorcycle batteries such as e-bikes or e-scooter and balance boards may be kept and charged indoors to prevent theft not considering the risk of fire [36]. Reports have indicated instances where e-bikes and e-scooters caused fires in residential homes and buildings due to failures in their Li-ion batteries. [36]. When cells are overcharged or discharged (external short circuit) can trigger TR resulting in an explosion or fire. It can also be a result of a fault from the battery or charger or manufacturing defect or the battery has been previously damaged [22]. It can also be a result of low-quality separators, material contamination and improperly arranged constituents [45]. Another issue can be because the battery management system (BMS) that is supposed to monitor the voltage, current, temperature, etc., does not have very good reliability and does not function properly [33].

RISE [36] stated that *“Bergen fire brigade has registered 22 incidents of fire in electric scooter batteries and electric scooters in the period from November 2019 to September 2022, of which there was one incident at the end of 2019, 3 incidents in 2020, 11 incidents in 2021 and 7 incidents until September 2022”*. In the United States, one can find several examples of fires that have started in an electric scooter where lives have been lost, and according to CBS News, the American authorities reported 19 deaths in 2022 [36].

NFPA stated, *“In 2022 alone, the Fire Department of the City of New York (FDNY) has reported investigating 130 fires related to lithium-ion batteries regularly used to power e-bikes—fires that have resulted in five deaths and dozens of injuries”*. In October 2022, the Consumer Product Safety Commission (CPSC) recalled about 22,000 e-bikes whose lithium-ion batteries can ignite, explode, or spark, posing fire, explosion, and burn hazards to consumers [56].

Research from RISE publication observed for electrical scooters, failure leading to TR can occur when charging the battery, and this can be a result of the battery previously damaged or a manufacturing issue [36]. Jersey Fire Rescue Services also warns that wrong charging of e-bikes and e-scooters can lead to fire. Advised users to follow guidelines and avoid prolonged charging all through the night, always inspect

chargers and cables for signs of damage and finally, it should not be kept in escape routes of shared spaces or buildings with many occupants [57] and other transport means [57].

As much as the desire for green or clean energies is needed, safety measures are paramount and thorough regulatory implementation should be reviewed from time to time. FSRI [55] according to their survey stated “44 % of the people know nothing about Li-ion batteries”. Battery safety awareness is vital to ensure people know signs to look out for and take precautions when using Li-ion battery-powered products and ensure following authorized manufacturer’s guidelines, to help mitigate the risk of accidents to humans, properties, and the environment [55]. Some level of enforcement can be considered for manufacturers not complying with regulatory laws.

Some toxic gases observed such as hydrogen fluoride (HF), and carbon monoxide (CO) etc. have been researched by several studies [6, 33, 47]. They are dangerous to human health as they can result in asphyxiation [6] or death when inhaled in high concentration [33] and could affect evacuation [36, 55]. This safety reason was why the experiment was done outdoors with more air concentration in this study.

In the case of landfills, some waste materials decompose and emit gases such as methane, or they contain flammable materials capable of combustion. Li-ion cells can be a source of ignition. However, alkaline cells may pose a lower risk of causing ignition than Li-ion batteries. If Li-ion cells are mechanically deformed or heated, could cause an uncontrolled increase in temperature and can pose a high risk of ignition of flammable materials or lead to a gas explosion. Research from RISE [33] also stated, “*Common sources of ignition have been found to be composing (self-ignition), thermal runaway in batteries, heat friction by grinding, human activity and unknown cause*”. Toys could be sometimes discarded without removing the batteries. Some of these toys are made of flammable materials, both alkaline and Li-ion batteries found in them could act as a potential ignition source, leading to a fire. The alkaline batteries contain heavy metals and corrosive improper disposal can impact negatively to the environment and cause health issues and contaminate soils etc. [16]. Therefore, proper sorting and safe disposal of the batteries are necessary. Also where it is packed and stored after production or for sale and possibly encounters an impact of the cell which may lead to cell failure and produce one of the high-risk reactions involving flames may pose a high-risk impact to propagation on other cells.

Research is evolving in the battery space to seek more ways to make the battery safer and last longer, such as the use of silicon materials in the anode due to it can withstand higher energy density instead of convectional anode material and the use of self-healing materials with silicon materials will help reinstate silicon particles degrading during the charging and discharging cycles and make it last longer and safer

[21]. This will help the future battery generation safer and make more communities embrace the energy transition.

6 Conclusion

In this work, a series of experiments were conducted for alkaline and Li-ion cells to determine flame propagation using a 3 X 3 configuration with the effect of distance (0 cm, 0.5 cm and 1 cm). A butane torch burner was the external heating source used in an extreme climatic condition during the winter period in the Western Part of Norway. The temperature ranged from -3 to 8 °C with a high windy condition. Photos showed different stages during the heating process also with the TR behaviours in various forms to see how flame and heat can cause propagation between cells.

The major finding for this thesis signifies propagation will occur to at least one cell and may pose a risk of spreading to other cells in a close configuration (0 cm). In addition, more spacing between cells reduces the likelihood and impact of propagation and damage to neighbouring cells. Nevertheless, some behaviours during the TR reaction such as diffused flame with or without explosion, and jet flame, are a high contributor to influence propagation.

Another interesting finding from this study is that thermal runaways are often assumed to result in explosion or produce fire or flames, but surprisingly they can also emit only excessive smoke during TR without explosion, or fire and further extinguish existing fire from the butane burner. This happens rarely and requires more findings.

A recommendation of 0.5 cm (5 mm) spacing should be implemented for modules using 18650 Li-ion batteries under similar temperate conditions observed in this work. Due to various behaviour displayed during TR such as jet flames, diffused flame with or without explosion, can further transfer heat in close cells and elevate their temperature to exceed the thermal limit which can result in propagation and can have severe consequences in a more confined space. Consequently, the spacing recommendation can impact the weight of the module case, but safety is prioritized.

7 Further work

This study looked at the flame propagation between cells considering the effect of distance between cells. This was done in a low-temperature and windy atmosphere. It is interesting to see how the effect of distance affected flame propagation. Also, the types of reactions experienced during TR and how they can influence propagation.

Further studies can be carried out using the same spacing scenarios but in a more confined environment with a high temperature and less windy conditions to ascertain how these cells react during TR and flame propagation on spacing using the same heat source.

8 References

- [1] J. Conzen, S. Lakshimipathy, A. Kaphi, S. Kraft and M. Didomizio, "Lithium-ion battery energy storage systems (BESS) hazards," *Journal of Loss Prevention in the Process Industries*, p. 104932, 14 November 2022.
- [2] H. Yan, K. C. Marr and O. A. Ezeokoye, "Thermal runaway behaviour of nickel-manganese-cobalt 18650 lithium-ion cells induced by internal and external heating failures.," *Journal of Energy Storage*, p. 103640, 2022.
- [3] M. Arumugam, Yu Xingwen and Wang Shaofei, "Lithium battery chemistries enabled by solid-state electrolytes," *Natures Reviews | Materials*, vol. 2, p. 16, 14 February 2017.
- [4] C. Lopez, J. Jeevarajen and P. Mukherjee, "Experimental Analysis of Thermal Runaway and Propagation," *Journal of the Electrochemical Society*, pp. A1905-A1915, 2015.
- [5] R. Aalund and M. Pecht, "The Use of UL 1642 Impact Testing for Li-ion Pouch Cells," *IEEE Access*, vol. 7, p. 1176711, December 2019.
- [6] F. Larsson, "Lithium-Ions - Assessment Abuse Testing, Fluoride Gas Emissions and Fire Propagation," Fredrik Larsson, Goteborg, 2017.
- [7] M. Chen, J. Liu, Y. He, R. Yuen and J. Wang, "Study of the fire hazards of lithium-ion batteries at different pressures," *Applied Thermal Engineering*, pp. 1061-1074, 2017.
- [8] S. W. Kim, S. G. Park and J. E. Lee, "Assessment of explosion risk during lithium-ion battery fires," *Journal of Loss Prevention in the process industries*, p. 104851, 2022.
- [9] M. Ghiji, S. Edmonds and K. Moinuddin, "A Review of Experimental and Numerical Studies of Lithium Ion Battery Fires.," *Applied Sciences*, p. 29, 29 January 2021.
- [10] Y. Chen, Y. Kang, Y. Zhao, L. Wang, J. Liu, Y. Li, Z. Liang, X. He, X. Li, N. Tavajohi and B. Li, "A review of Lithium battery safety concerns: the issues, strategies and testing standards," *Journal of Energy Chemistry*, pp. 83-99, 2021.
- [11] Circuit Globe, 2022. [Online]. Available: <https://circuitglobe.com/difference-between-cell-and-battery.html#:~:text=The%20cell%20and%20battery%20both%20store%20the%20chemical,the m%20are%20explained%20below%20in%20the%20comparison%20chart..>
- [12] Abu-Lebdeh, Yaser, "Nanotechnology for Lithium-ion Batteries," Springer Science+ Business Media, Ontario, 2013.
- [13] A. Roy, R. B. Patil and R. Sen, *Journal of Energy Storage*, p. 105841, 2022.

- [14] H. Budde-Meiwes, J. Drillkens, B. Lunz, J. Muennix, S. Rothgang, J. Kowal and D. U. Sauer, "A review of current automotive battery technology and future prospects," *Journal of automobile engineering*, pp. 761-776, 2013.
- [15] C. Mikolajczak, M. Kahn, K. White and R. T. Long, "Introduction to Lithium-Ion Cells," in *Lithium-Ion Batteries Hazard and Use Assessment*, Springer, 2011, pp. 1-24.
- [16] [Online]. Available: https://en.wikipedia.org/wiki/Alkaline_battery.
- [17] "The Engineering toolbox," [Online]. Available: https://www.engineeringtoolbox.com/electrode-potential-d_482.html.
- [18] "Nobel Prize," [Online]. Available: <https://www.nobelprize.org/prizes/chemistry/2019/press-release/>. [Accessed 2023].
- [19] F. Larsson, S. Bertilsson, F. Maurizio, I. Albinsson and B.-E. Mellander, "Gas explosions and thermal runaways during external heating abuse of commercial lithium-ion graphite-LiCoO₂ cells at different levels of ageing.," pp. 220-231, 2017.
- [20] A. El Kharbachi, O. Zavorotyńska, M. Latroche, F. Cuevas, V. Yartys and M. Fichtner, "Exploits, advances and challenges benefiting beyond Li-ion battery technologies," *Journal of alloys and compounds*, p. 153261, 2019.
- [21] R. Narayan, C. Laberty-Robert, J. Pelta, J.-M. Tarascon and R. Dominko, "Self healing: An Emerging Technology for Next-Generation smart batteries," *Advanced Energy Materials*, p. 2102652, 2021.
- [22] C. Mikolajczak, M. Kahn, K. White and R. T. Long, "Lithium-Ion Batteries Failures," in *Lithium-ion Batteries Hazard and Use Assessment*, Springer, 2011, pp. 43-69.
- [23] Y. Wang and W.-H. Zhong, "Development of Electrolytes towards Achieving Safe and high-performance energy-Storage Devices:A Review," *ChemElectroChem*, pp. 22-36, 2015.
- [24] C. X. He, Q. L. Yue and T. S. Zhao, "Modeling thermal runaway of lithium-ion batteries with a venting process," *Applied Energy*, p. 1211110, 2022.
- [25] W. Lu, I. Belharouak, J. Liu and K. Amine, "Thermal properties of Li₄/3Ti₅/3O₄/LiMn₂O₄ cell," *Journal of Power Sources*, vol. 174, no. 2, pp. 673-677, 2007.
- [26] K. Amine, I. Belharouak, Z. Chei, T. Tran, H. Yumoto, N. Ota, S.-T. Myung and Y.-K. Sun, "Nanostructured Anode Material for High-Power Battery," *Advanced Materials*, pp. 3052-3057, 2010.
- [27] Y. Inui, Y. Kobayashi, Y. Watanabe and Y. Kitamura, "Simulation of temperature distribution in cylindrical and prismatic Lithium ion secondary battery," *Energy Conversion and Management*, pp. 2103-2109, 20 February 2007.

- [28] "Wikipedia," [Online]. Available: https://en.wikipedia.org/wiki/List_of_battery_sizes. [Accessed 6 November 2022].
- [29] I. Buchmann, "Battery University," Cadex Electronics Inc, 1985. [Online]. Available: <https://batteryuniversity.com/article/bu-410-charging-at-high-and-low-temperatures>.
- [30] M. Chen, D. Ouyang, J. Liu and J. Wang, "Investigation on thermal and fire propagation behaviors of multiple lithium-ion batteries within the packages.," *Applied Thermal Engineering*, p. 113750, 2019.
- [31] S. Shahid and M. A. Chaab, "A review of thermal runaway prevention and mitigation strategies for lithium-ion batteries," *Energy Conversion and Management: X*, p. 100310, 2022.
- [32] D. Ouyang, J. Liu, M. Chen and J. Wang, "An experimental study on the thermal failure propagation in lithium-ion battery pack," *The Journal of Electrochemical Society*, vol. 165, pp. A2184-A2193, 2018.
- [33] C. Meraner, T. Li and . C. . S. Meli, "Degassing from lithium-ion batteries in the home," RISE, 2021.
- [34] L. Yuan, . T. Dubaniewicz, . I. Zlochowe, R. Thoma and N. Rayya, "Experimental study on thermal runaway and vented gases of lithium-ion cells," *Process Safety and Environmental Protection*, pp. 186-192, 17 July 2020.
- [35] T. Ohsaki, T. Kishi, T. Kuboki, N. Takami, N. Shimura, Y. Sato, M. Sekino and A. Satoh, "Overcharge reaction of lithium-ion batteries," *Journal of Power Source*, pp. 97-100, 2005.
- [36] J. S. Fjærestad, . F. R. Mikalsen and C. Meraner, "Escape in case of fire in lithium-ion battery," RISE, 2023.
- [37] G. Zhong, H. Li, C. Wang, K. Xu and Q. Wang, "Experimental Analysis of Thermal Runaway Propagation Risk within 18650 Lithium-Ion Battery Modules," *Journal of the Electrochemical Society*, p. A1925, 2018.
- [38] FFI Norwegian Defence Research Establishment, "FFI Norwegian Defence Research Establishment," [Online]. Available: <https://www.ffi.no/en/news/li-ion-batteries--hazards-and-mitigation>. [Accessed 1 June 2017].
- [39] D. Belov and M. H. Yang, "Failure mechanism of Li-ion battery at overcharge conditions," *Journal of Solid State Electrochemistry*, pp. 885-894, 2008.
- [40] F. Larsson and B. Mellander, "Abuse by External Heating, Overcharge and Short Circuiting of Commercial Lithium-Ion Battery Cells," *Journal of the Electrochemical Society*, pp. A1611-A1617, 2014.
- [41] J. Lamb, C. J. Orendff and L. A. M, "Failure propagation in multi-cell lithium ion batteries," *Journal of Power Source*, pp. `517-523, 2015.

- [42] F. Larsson, P. Andersson and B.-E. Mellander, "Lithium-Ion Battery Aspects on Fires in Electrified Vehicles on the Basis of Experimental Abuse Test.," *Batteries*, p. 13, 11 April 2016.
- [43] F. Larsson and B.-E. Mellander, "Abuse by External Heating, Overcharge and Short circuiting of Lithium-ion Battery Cells," *Journal of The Electrochemical Society*, p. A1611, 2014.
- [44] C. Zhao, J. Sun and Q. Wang, "Thermal runaway hazards investigation on 18650 lithium-ion battery using extended volume accelerating rate calorimeter," *Journal of Energy Storage*, vol. 28, p. 101232, 2022.
- [45] D. Ouyang, C. Mingyi, Q. Huang, J. Weng, Z. Wang and J. Wang, "A Review on the Thermal Hazards of the Lithium-Ion Battery and the Corresponding Countermeasures," *Energy Science and Technology*, p. 2483, June 2019.
- [46] A. W. Golubkov, D. Fuchs, J. Wagner, H. Wiltsche, C. Stangl, G. Fauler, G. Voitic, A. Thaler and V. Hacker, "Thermal-runaway experiments on consumer Li-ion batteries with metal-oxide and olivin-type," *Royal Society of Chemistry*, pp. 3633-3642, 2014.
- [47] P. Ribière, S. Grugeon, M. Morcrett, S. Boyanov, S. Laruellea and G. Marlair, "Investigation on the fire-induced hazards of Li-ion battery cells by fire calorimetry," *Energy & Environmental science*, 2012.
- [48] D. . A. Purser and J. . L. McAllister, "Assessment of Hazards to Occupants from Smoke,," in *SFPE Handbook of Fire Protection Engineering (Fifth Edition)*, Springer, 2016, pp. 2308-2428.
- [49] D. Ouyang, M. Chen, R. Wei, Z. Wang and J. Wang, "A study on the fire behaviors of 18650 battery and batteries pack under discharge," *Journal of Thermal Analysis of Calorimetry*, pp. 1915-1926, 27 October 2018.
- [50] C. J. Orendorff, "Mitigating Critical Safety Concerns in Lithium-ion Batteries," *Sandia National Laboratories*, 2011.
- [51] R. Kizilel, R. Sabbah, J. R. Selman and S. Al-Hallaj, "An alternative cooling system to enhance the safety of Li-ion battery Packs.," *Journal of Power Source*, pp. 1105-1112, 2009.
- [52] D. Chen, J. Jiang , G.-H. Kim, C. Yang and A. Pesaran, "Comparison of different cooling methods for lithium ion battery cells," *Applied Thermal Engineering*, pp. 846-854, 2016.
- [53] Y. Jia, M. Uddin, Y. Li and J. Xu, "Thermal runaway propagation behaviour within 18650 lithium-ion battery packs; A model study," *Journal of Energy Storage*, p. 101668, 2020.
- [54] Y. Zhang, D. Kong, P. Ping, H. Zhao, X. Dai and X. Chen, "Effect of plate obstacle on fire behavior of 18650 lithium ion battery: An experimental study," *Elsevier*, p. 105283, 2022.
- [55] Fire Safety Research Institute , "Fire Safety Research Institute (FSRI)," [Online]. Available: <https://batteryfiresafety.org/#section-8>.

- [56] National Fire Protection Association (NFPA), "The National Fire Protection Association," [Online]. Available: <https://www.nfpa.org/news-blogs-and-articles/blogs/2022/10/20/electrical-safety-tips-for-users-of-e-bikes-and-e-scooters>.
- [57] "Fire warning on charging e-bikes and e-scooters," BBC, 2023.
- [58] IREVOLUTION 4.0, "Li-Ion battery types | Lithium Ion Battery tutorial | LI Ion Cells Types By Size," [Online]. Available: <https://www.youtube.com/watch?v=fUDEhyJKwbo>. [Accessed 19 June 2021].
- [59] "https://www.youtube.com/watch?v=_65GwUliX-w," WFMY News 2, 1 April 2023. [Online].
- [60] E. M. Valeriote and D. M. Jochim, "Very fast charging of low resistance lead/acid batteries," *Journal of Power Source*, pp. 93-104, 1992.
- [61] B. Bose, A. Garg, B. K. Panigrahi and J. Kim, "Study on Li-on battery fast charging strategies, Review, challenges and proposed charging framework.," *Journal of Energy Storage*, p. 105507, 2022.
- [62] T. M. Chang, E. M. Vaeriote and D. M. Jochim, "Effects of fast charging on hybrid lead/acid battery temperature," *Journal of Power Source*, pp. 163-175, 19 February 1994.
- [63] S. Barcellona, S. Colnago, G. Dotelli, S. Latorrata and L. Piegari, "Aging effect on the variation of Li-ion battery resistance as a function of temperature and state of charge.," *Journal of Energy Storage*, p. 104658, 2022.
- [64] L. L. Hu, Z. W. Zhang, M. Z. Zhou and H. J. Zhang, "Crushing behaviors and failure of packed batteries," *International Journal of Impact Engineering*, p. 103618, 2020.
- [65] T. Wu, H. Chen, Q. Wang and J. Sun, "Comparison analysis on the thermal runaway of lithium-ion battery under two heating modes," *Journal of Hazardous Materials*, pp. 733-741, 2018.
- [66] A. Lecocq, G. Grbresilassie, G. Sylve, M. Nelly, L. Stephanie and M. Guy, "Scenario-based prediction of Li-ion batteries fire-induced toxicity," *Journal of Power Source*, pp. 197-206, 2016.
- [67] X. Li, J. He, D. Wu, M. Zhang, J. Meng and P. Ni, "Development of plasma-treated polypropylene nonwoven-based composites for high-performance lithium-ion battery separators," *Electrochimica Acta*, pp. 396-403, 2015.
- [68] L. Kong, Wnag Yu, H. Yu, B. Liu, c. Qi, D. Wu, Tian Guofeng and J. Wang, "A Robust, High-Wettability, and Fire-Resistant Hybrid Separator for Advanced and Safe Batteries," *Journal of Physical Chemistry C*, 2019.

9. Appendix

Appendix A

Alkaline single cell experiment, Scenario (1-2 and 1-3)

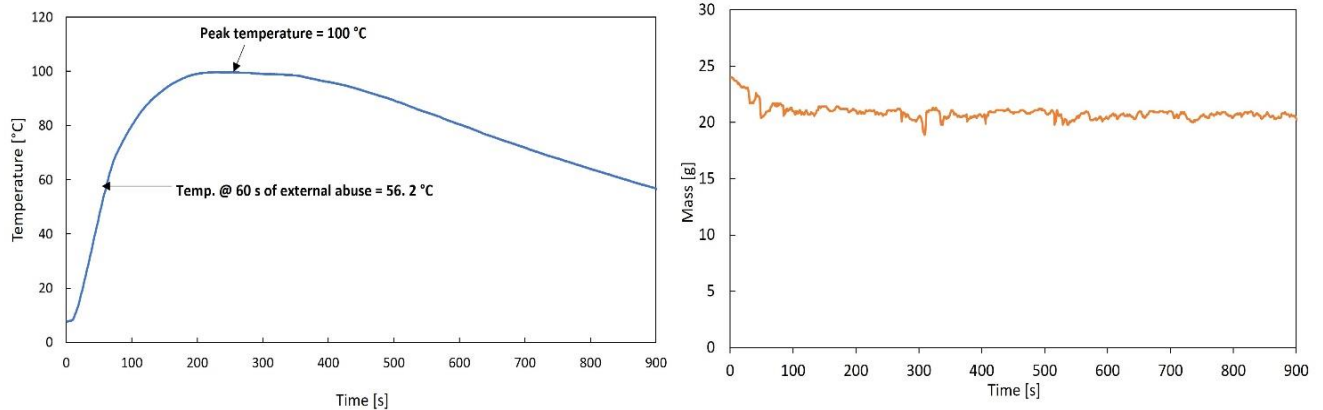


Figure A1 Alkaline single cell experiment (experiment 2). (a) shows temperature variation with time (b) mass loss vs time.

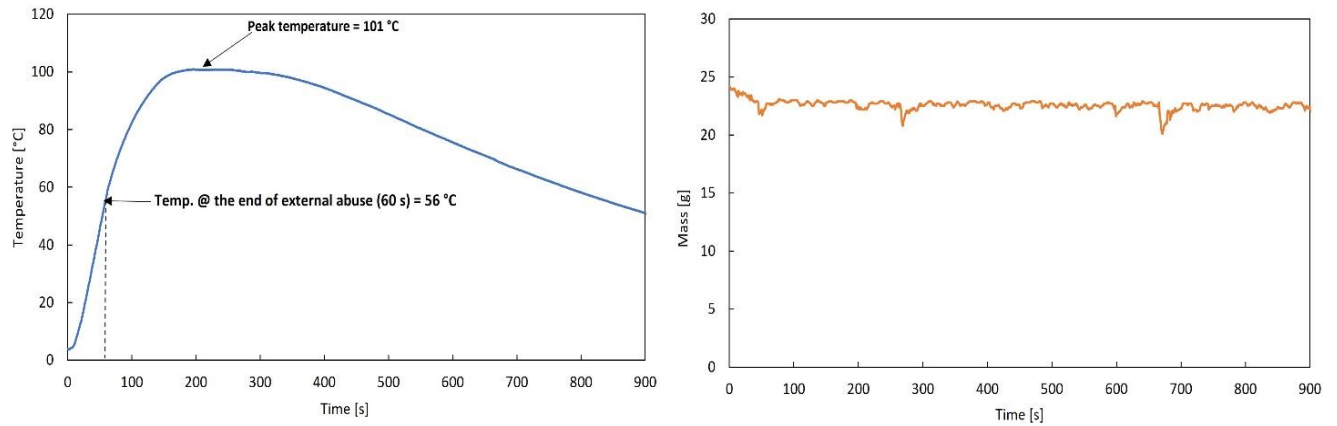


Figure A2 Alkaline single cell experiment (experiment 3). (a) shows temperature variation with time (b) mass loss vs time.

For the alkaline single cell experiments, the remaining two experiments were conducted, the cell was heated for 60 s in a low ambient temperature condition and the two different experiments (1- 2 & 1-3) behaved similarly with the same trends as seen in Figure A1 and Figure A2. Melting of the materials at the anode produced a liquid substance that came out of the cell within 10 s during the heating process. At the end of heating for 60 s, no specific exothermic reaction was seen in either experiment. Neither safety venting nor TR was observed. The cell temperature for experiments 2 and 3 at the end of the heating was 56 °C and 56 °C respectively. The temperature of the cells increased, and they got to a peak of 100 °C, and 101 °C, corresponding time of 228 s, and 196 s. The temperature profiles for all the alkaline single cell are

similar. Each cell's initial and final mass reading was weighed before and at the end of the experiment see Table A1.

Table A1 result summary from the experiment performed on AA Alkaline single cells. Scenario 1

	Experiment (1-1)	Experiment (1-2)	Experiment (1-3)
Initial mass [g]	24	24	24
Final mass [g]	21.6	20.1	21.2
Ambient Temperature [°C]	4	4	3
Initial surface temperature [°C]	6	8	4
Surface @ 60 s of temperature [°C]	58	56	56
Peak Temperature [°C]	102	100	101
Safety vent activation temperature [°C]	No	No	No
TR activation temperature [°C]	No	No	No
Total mass loss [g]	1.6	3.7	1.5

NB: Scenario (1-1) was emphasized in section 4.1.1 to generalize alkaline cells.

Appendix B

Li-ion Single cell experiment, Scenario (2-6)

During the heating of the cell, the safety vent activated at 28 °C (42 s), with ignited gases released. Shortly, at a temperature of 75 °C (97 s), TR was initiated, releasing sparks, gases and smoke emission, explosion accompanied by a jet flame due to internal increase pressure. Summary of the heating process and cell failure is seen in Figure B1. The release of the jet fire came in contact with the roof of the compartment in a second which is up to 8 m in height. The impact of the reaction resulted in the safety vent cover disengaged from the cell, see Figure B1 (g), and displaced about 4.2 m Figure B1(h) away from the point source.



Figure B1 Initial external abuse process (b) safety vent activation with ignition of ejected gas (c) initiation of TR with rapid gas ejection with sparks (d) sparks with little gas ejection (e) ejection of flame touching the roof of the compartment (f) outcome of TR caused cell material displacement with the hollow opening on the cell and cathode current collector damaged (g) vent cover displaced (h) distance at which the vent cover was displaced from the experiment point.

In addition, the top of the cell with some of the inner foil-like material was displaced which created a hollow opening with a depth of up to 25 mm, with the current collector of the cathode affected. This

resulted in a peak temperature of approximately 446 °C as seen in Figure B2 which was higher than all previously performed experiments for scenario 2.

The mass loss for the cell was weighed on a scale before and after, then it was compared with the mass loss obtained from the data logger, the initial and final readings gave a mass loss of 29.7 g (49.3-19.3). Reading from the data logger gave a mass loss of 29.6 g (47.9 -18.3). Only the TR resulted in a mass loss of 25.2 g which is higher than the mass loss obtained in tests 1 and 2 and this was due to some of the materials which were displaced from the cell during TR.

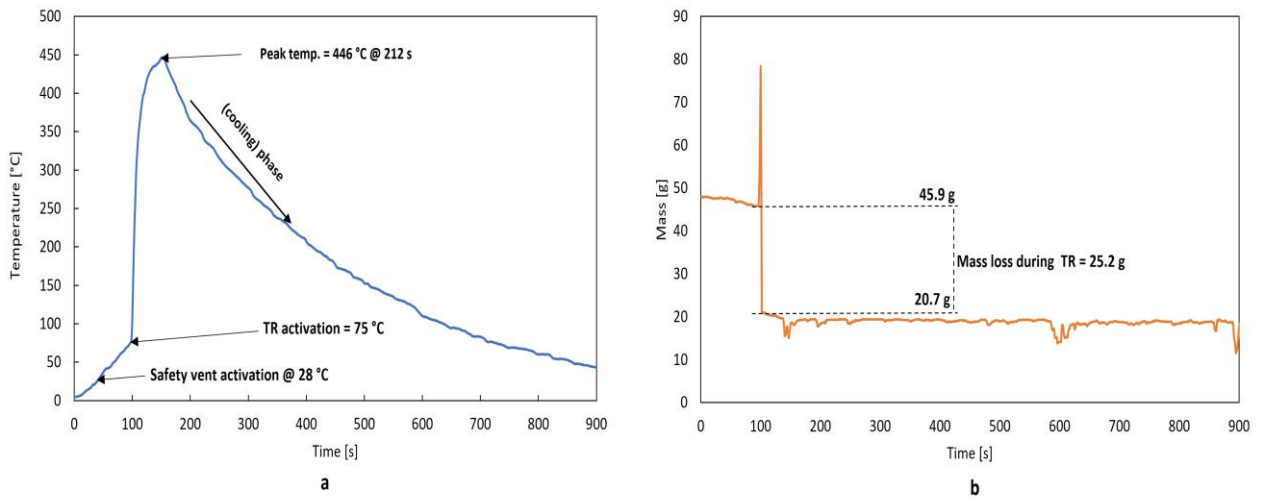


Figure B2 Li-ion single cell experiment 3 (a) temperature vs time (b) Mass vs time.

Appendix C

Li-ion 3 x 3 cell configurations 1cm spacing. Scenario (6-13)

The heating process is shown in Figure C1, At 0 s the butane burner was turned on and the heating commenced. it was observed cells 2 and 4 were partly affected by the flame radiation during the heating process.

Cell 1 safety vent was activated at 32 °C (26 s) and the released gases were ignited increasing the flame radiation of the cell to the point of TR Figure C1 (b). There was no obvious sign to point out the start of TR initiation because the flame was continuously sustained by the ejected gas when the safety vent activated without reduction until TR initiated and got to a peak temperature of 260 °C (192 s) see Figure C2.

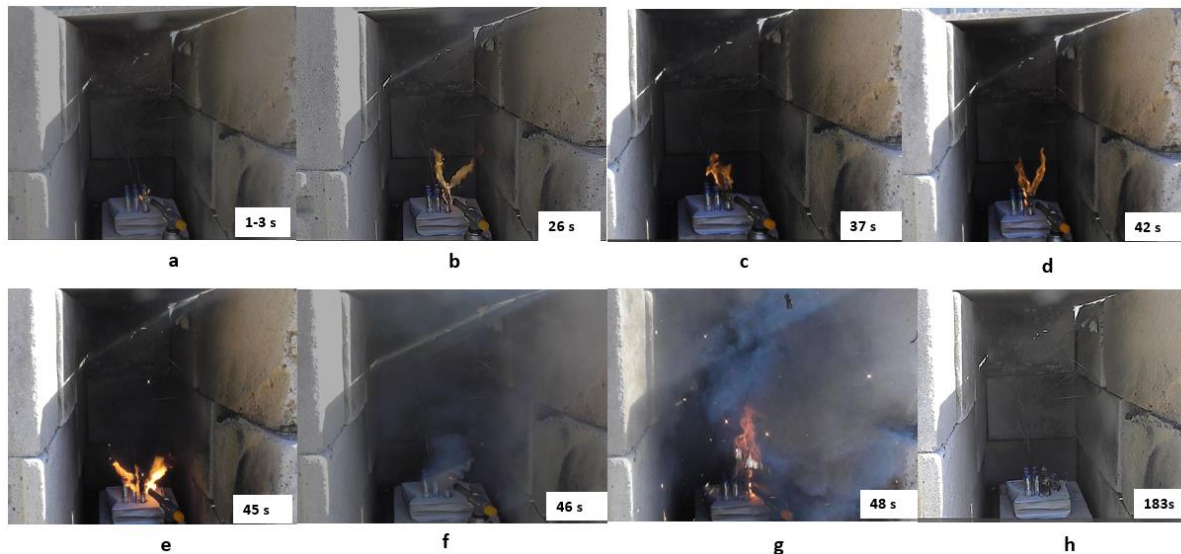
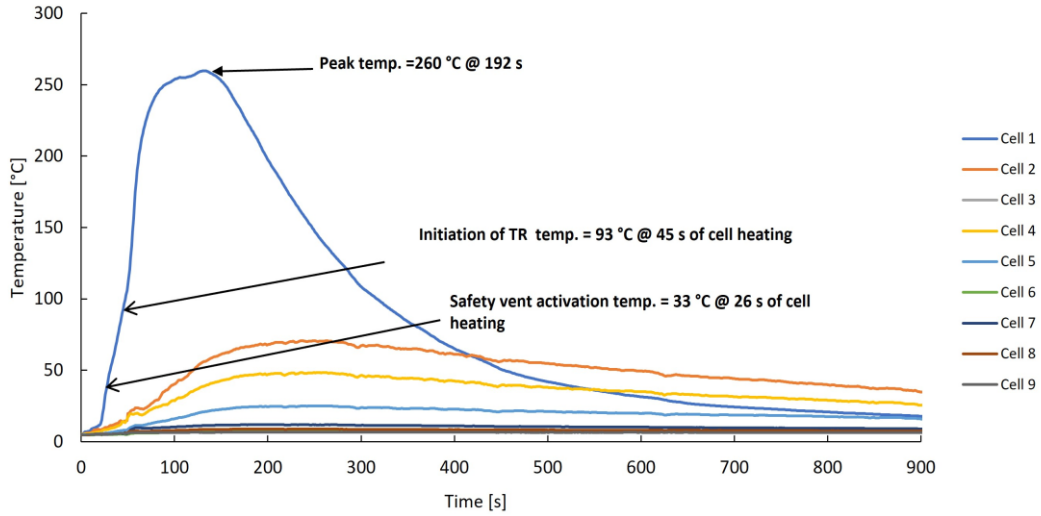
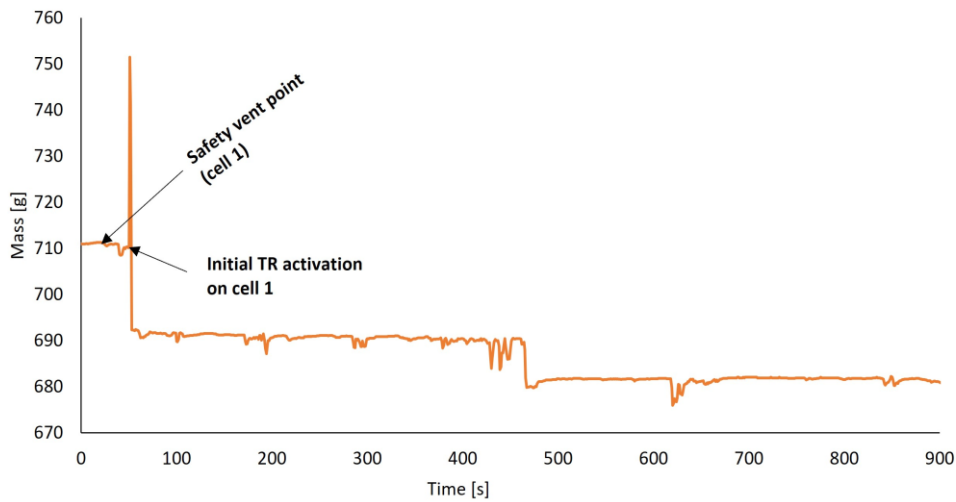


Figure C1 The heating process of Li-ion 3x3 configuration 1cm, experiment 2 (a) initiation of butane torch burner to cell 1 (b) safety vent valve cell 1 activates with increased flame due to relieved gas (c) flame still sustained by the combustible gases emitted from cell 1 (d) flame still sustained at 42 s of heating (e) TR initiation with sparks and flares (f) initiating smoke ejection (g) explosion (with flying debris) accompanied with flames and more gas/smoke ejection.

This also increased the heat radiation on cells 1 and other neighbouring cells i.e. 2, 4, and 5. The TR was activated at 45 s at a temperature of 93 °C, resulting in sparks accompanied by an explosion with some flying debris noticed on the image caption, seen in Figure C1 (g) and the cell was fully consumed with fire. This is the earliest TR activation time experienced, compared to all other experiments conducted in Figure C1.



a



b

Figure C2 Li-ion 3x3 configuration 1cm spacing (experiment 2). (a) Temperature vs time (b) Mass vs time.

The mass loss reading scaling initial and final mass of the cell 1(heated cell) resulted in 31.9 g (49.3 – 17.4), as the rest of the cell information is seen in Table A2. The total mass loss of the whole cells i.e. (cells + insulated drilled slab) obtained scaling the initial and final mass of the cell is 27.6 g (710 – 682 g) and the corresponding result obtained from the data logger is 31.9 g (710- 678.9) with a difference of 4 g.

Table A2 Summary of Li-ion 3x3 configuration 1cm spacing experiment 2. Scenario (6-13)

Cells	Initial Voltage (V)	Final voltage (V)	Initial Mass (g)	Final Mass (g)	Safety vent activation time/temp. (s) / (°C)	Initial TR activation time/temp. (s) / (°C)	Peak cell surface temp. °C	Peak cell surface time. (s)
1	3.694	0.00	49.3	17.4	26/ 32	105/ 93	260	132
2	3.688	0.00	49.4	49.3	-	-	71	238
3*	3.70	3.70	49.0	49.0	-	-	9	453
4	3.699	3.706	49.0	49.0	-	-	48	262
5	3.679	3.686	49.5	49.4	-	-	25	262
6*	3.692	3.692	49.3	49.3	-	-	8	237
7	3.692	3.70	49.0	49.0	-	-	12	212
8*	3.68	3.68	49.1	49.1	-	-	9	210
9*	3.70	3.70	49.0	49.0	-	-	7	210

Appendix D

Li-ion 3x3 cell configuration 0.5cm spacing experiment 2. Scenario (5-11)

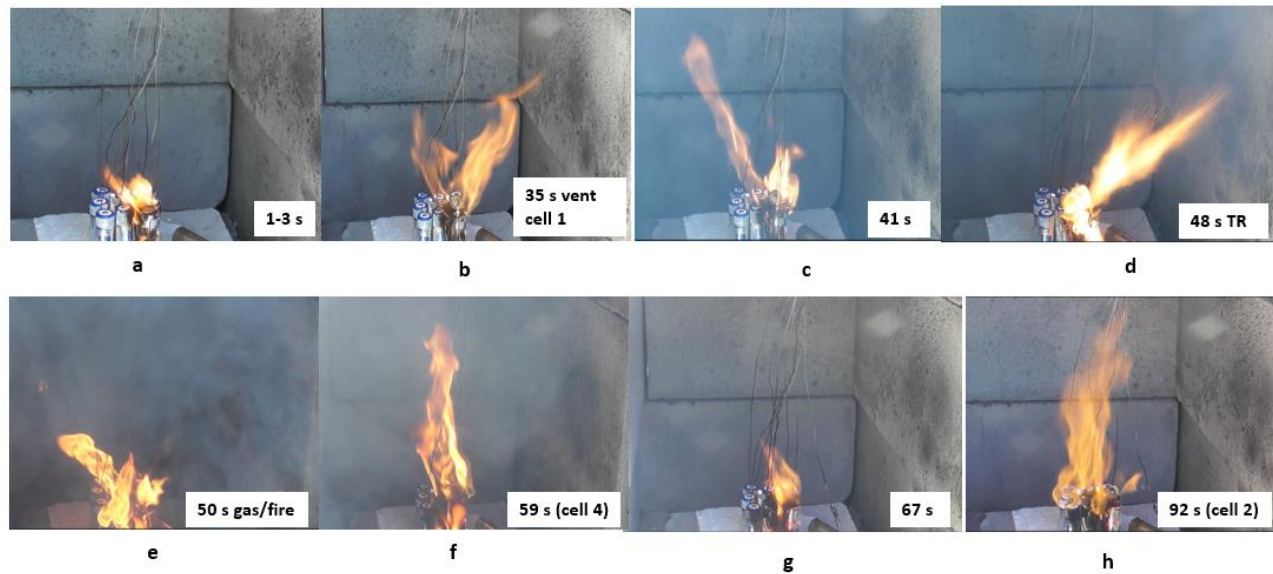


Figure D1 The heating process of li-ion cell 3x3 configuration 0.5 cm spacing (experiment 2). (a) initiation of butane torch burner to cell 1(b) safety vent valve cell 1 activates with wind effect on ignited gas (c) initiation of TR on cell 1 (d) visible smoke emission during TR (e) safety vent activates (f) safety vent activates with increased flame (h)butane torch burner removed at 120 s and flame decays drastically with little flame spotted on cell 1 (i) current situation of cells after the experimental abuse with cell 1 fully burnt.

Appendix E

Li-ion 3x3 cell configuration 0cm spacing experiment 2. Scenario (6-13)

The images of the external abuse process/stages are shown in Figure E1. During the heating, at a low ambient temperature (-3°C), the flame partly radiated and was scorching on spread cells 2 and 4 as seen in the photo (a). The safety vent valve of cell 1 was activated at 51 s with ignited gas at a temperature of 39.3°C , see photo (b).

At 85 seconds, TR initiated at 74°C with sparks/flare, see photo (c). The rapid gas and whitish gas ejection from the cell extinguish the butane flame from heating cell 1 at 87 s as seen in photo (d) and the peak temperature for cell 1 got to a peak of 446°C , see Figure E2.

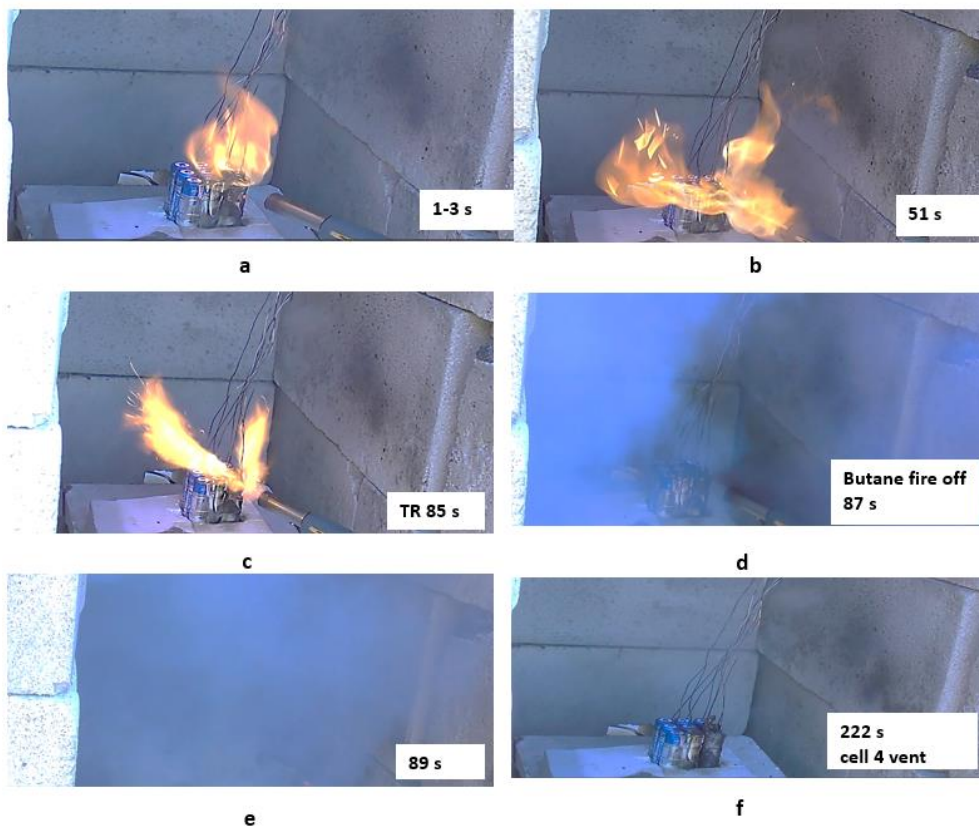


Figure E1 The heating process of Li-ion cell 3x3 configuration with no spacing test 02 (a) shows the initial external abuse (b) safety vent valve activation (c) initial TR activation with sparks (d) flame from butane torch burner was put off by the reaction of TR approximately 87 s (e) excess gas emission by the cell during TR process (f) cell 4 safety Vent valve activates due to heat transfer by conduction.

The cooling phase started at immediately after the peak temperature was reached at 118 s. An observation was cell 2 got to 138°C with no safety vent activation, only cell 4 activated at a temperature of 133°C

(162 s). No mass reading available for this result error from data logger and cells were not weighed before disposal.

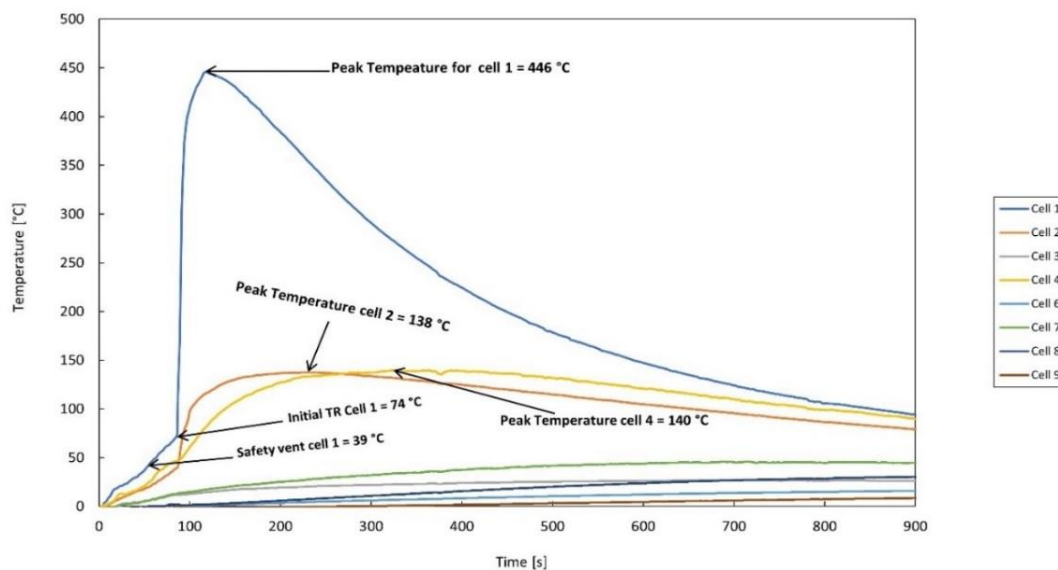


Figure E2 Li-ion 3x3 configuration no spacing, experiment 2. Temperature vs time.

Table B1 Summary of Li-ion 3x3 configuration 0 cm spacing experiment 2. Scenario (6-13)

Cells	Initial Voltage (V)	Final voltage (V)	Initial Mass (g)	Final Mass (g)	Safety vent activation time/temp. (s) / (°C)	Initial TR activation time/temp. (s) / (°C)	Peak cell surface temp. °C	Peak cell surface time. (s)
1	3.70	0.00	49.0	-	51/39	85/73.8	446	116
2	3.684	0.00	49.1	-	-	-	138	234
3	3.70	3.668	49.2	-	-	-	26	834
4	3.669	0.00	49.1	-	162/133	-	140	327
5	3.686	3.678	49.3	-	-	-	53	726
6	3.680	3.670	49.5	-	-	-	18	1482
7	3.702	3.695	49.3	-	-	-	46	712
8	3.707	3.697	49.1	-	-	-	32	1185
9	3.709	3.696	49.4	-	-	-	14	1696